Master's Thesis

Master's Degree in Industrial Engineering (MUEI)

Experimental investigation on the detection of fatigue failures in hydraulic turbines

REPORT

April 18, 2022

Author: Adolfo de la Torre Suárez

Director: Francesc Xavier Escaler Puigoriol

Delivery: 09/2021

Escola Tècnica Superior d'Enginyeria
Industrial de Barcelona

Abstract

Hydroelectric power stations are nowadays one of the most important ways to obtain a clean and sustainable electricity supply. Actually, hydroelectric energy is the most renewable energy used in the world. Even so, there still exists a very important potential of development in many areas in these kinds of stations. These plants use mainly 3 types of turbines, called Francis, Kaplan, and Pelton, to obtain electricity due to the flow of water through its blades. We will focus our project on the Kaplan turbines.

For doing so, the core of this project was the use of a flat disk of six blades linked with a shaft, which is a simplification of a Kaplan turbine. After installing it in a test rig of reduced scale in a laboratory, some experimental analysis were carried out.

The project intention was to investigate the feasibility of detecting fatigue cracks in submerged structures such as Kaplan turbine blades by means of adequate sensors, measurement techniques and signal processing tools. For that, a series of experiments have been carried out in a laboratory with a simplified structure where a fatigue failure has been artificially provoked, which keeps similarity with the cracks observed in actual hydraulic turbines. Various detection techniques have been tested and evaluated to determine their capability to achieve the expected objective.

To define a representative crack, before the experiments in the laboratory, some numerical simulations have been carried out to better understand the fracture mechanisms involved, and those simulations have been used to select the best experimental set up in the laboratory machines. Software like SolidWorks or Ansys have been used to simulate the appearance and spread of a crack in the disk until the failure of the structure.

To analyze the effect of fatigue in the simplified structure used, a modal analysis has been carried out using instrumentation like accelerometers, software like Labview and theory about vibrations in machines. During this project, thus, the concepts of vibrational behavior and fatigue phenomena have gone hand in hand.

Results obtained were really similar between the experiments and the numerical simulations. For the most destructive frequencies, the way that our structure vibrated with a crack practically matched between the numerical simulation and the experiments. Regarding some other frequencies of higher value, results were even closer. Moreover, the variation of frequency as the crack spreads presents a characteristic shape, similar to other machines. Due to the results obtained, I can confirm that it is possible to detect fatigue cracks that appear in the blades of a turbine and identify, by the vibration of the structure, the length of that crack.

Linking the brands of studies mentioned (both numerical and experimental), the results obtained, the path we have followed to obtain these results, and with further studies, the future work will try to develop predictive maintenance techniques in actual hydraulic machines in order to avoid failures in the hydroelectric power stations due to the effect of fatigue.

Contents

Glossary and Acronyms

➔ Glossary:

- **Ansys**: It is a general-purpose, finite-element modeling package for numerically solving a wide variety of mechanical problems. These problems include static/dynamic, structural analysis, heat transfer, and fluid problems, as well as acoustic and electromagnetic problems.
- **LabView**: It is a graphical programming environment that engineers use to develop automated research, validation, and production test systems.
- **SolidWorks**: It is a 3D CAD (computer-aided design) design software for modeling parts and assemblies in 3D and drawings in 2D.
- **Predictive maintenance:** Predictive maintenance is the maintenance that evaluates the state of the machinery and recommends intervening or not depending on its state, which produces great savings, using techniques and tools to detect failures and defects in the machines.
- **Test rig**: It is a piece of machinery that is primarily used to test and assess the capability and performance of components for industrial use.
- **Strain**: It is the change in size or shape of a body due to internal stresses produced by one or more forces applied to it.
- **Natural frequency:** It is the frequency at which a body vibrates after giving it an external excitation (energy).
- **Mode Shape:** It is the deformation that the structure/body would show when vibrating at the natural frequency.
- **Frequency response function:** It is a function used to quantify the response of a system to an excitation, normalized by the magnitude of this excitation, in the frequency domain.

➔ Acronyms:

- **L_{Crack}**: Crack length
- **L_{crit}**: Critical crack length
- **F_n**: Natural frequency
- **FRF**: Frequency response function
- **ND**: Nodal diameter
- **NC**: Nodal circle
- **FEM**: Finite Element Method
- **FT**: Fourier transform
- **NI**: National Instruments

List of figures

List of tables

1. Preface

1.1 Origin of the project

The origin of the project is based on the idea of improving the tools and methods that society nowadays has for obtaining renewable energy in a better way. As we know, maintenance is a key factor for all the machines and processes, and, in this case, we will consider this fact as the main motivation of the study, as maintenance and prevention are basics in today's industry.

Over the years that I have been studying in the university, maintenance has become a primary topic of very different subjects that I have studied (such as Management or even Chemical technology), and I thought that, in some way, all things I have learned there could be applied for hydraulic machines such as hydraulic turbines. Once I told the idea to the director of this project, Xavier Escaler, we considered that an investigation for improving the maintenance of the Kaplan turbines should be carried out.

In this study, I will have the possibility to apply all concepts I have been taught over the years, and extrapolate them to the Kaplan turbines. For carrying out this project, the concepts and topics learned in the subjects *Machines Technology* and *Hydraulic Machines* (i.e fatigue failures basics or Kaplan turbine design) will be key factors for trying to have a successful result, or, at least, for trying to set a base for future studies in this field, the predictive maintenance of Kaplan turbines.

1.2 Previous knowledge

Regarding the previous knowledge for this study, things learned in the subjects mentioned in the previous paragraph will be necessary. Moreover, as I mentioned before, 2 types of studies will be carried out in this project.

Firstly, a numerical simulation will be executed in the computers of the department of Fluid Mechanics for analyzing the behaviour of the simplified turbine. Therefore, for this first study it will be necessary to gain some knowledge about specific software such as SolidWorks and Ansys. It will be necessary to create the geometry of the turbine and the successives cracks that will appear on it in SolidWorks, so It will be necessary to refresh the concepts we learnt of SolidWorks in the university degree. Then, I will have to simulate the performance of the model of turbine we have in different scenarios because of the crack and its expansion in Ansys by carrying out a Modal Analysis, so I will need to learn how to do a modal analysis in Ansys and how to obtain the results.

Secondly, to enlarge the study, an experiment will be carried out in the laboratory. I will measure different ways of vibration of a simplified model of a Kaplan turbine and I will analyse the results. Thus, it will be necessary to learn about how to do an experimental analysis in a laboratory, how to proceed to measure with very sensitive sensors, and how to obtain the results with software provided by the department of Fluid Mechanics like Labview. For analyzing the results, I will need to know first how to measure different parameters such as displacement or acceleration of the points of a turbine, and then, I will need to know how to obtain the results and show them.

Finally, I will try to relate the results obtained in both models with the concepts of predictive maintenance and failure due to fatigue, so it will be necessary to have some knowledge about these two fields of engineering too.

2. Introduction to the project

2.1 Objectives of the project

The main objective of this project is to identify the effects of the appearance and expansion of cracks on the dynamic response of a hydraulic machine similar to a Kaplan turbine. Having the reference of the main goal mentioned, other specific objectives in this project would be the following:

- Knowing about the situation of the Kaplan turbines and their performance in today's society: We will try to understand how important this kind of turbine is for society in order to obtain electricity, and we will try to describe its uses and its current situation.

- Try to understand how the vibrations affect the integrity of a structure: By some numerical simulations, we will try to identify how vibrations affect the integrity of a body (in our case, the body to study will be a simplification of a Kaplan turbine) and we will try to understand the effect of the vibrations of a body in different environments (at first in air, and, if time permits, we will study the vibrations in water).

- Know how to apply simulation softwares like Ansys into reality: With the Ansys software we will try to obtain the different vibrations modes of the blades to see when the hydraulic machine we are using should stop working because of a crack apparition and spread. Different modal analysis will help us to identify different vibratory behaviors of the model of the turbine.

- Learn how to measure different parameters of a real model in a laboratory: One of the objectives of this project was also to begin to familiarize myself with the environment of experimentation of real models in a laboratory. In addition, the idea is also to learn how to use measurement elements such as sensors, or even measurement softwares that could provide results of different parameters of a real model studied in a laboratory.

- Develop a methodology to carry out a project from its beginning, and know how to link a numerical model and a real model: As the project has two different parts (experimental and numerical analysis), it will be necessary to create a path or methodology that could relate these two parts in order to carry out this project as successfully as possible.

- Identify techniques and methods to improve the predictive maintenance in Kaplan turbines: Gathering all the previous objectives explained, the idea is to set and discover a new method of predictive maintenance by a vibration analysis in the hydraulic machines, using our simplification of Kaplan turbine as reference. The idea is to identify a certain vibration response in different phases of fatigue in a structure, and to see how that vibration affects the model we have in different stages depending on the length of the crack.

2.2 Scope of the project

In this project, a simulation over a simplification of a Kaplan turbine will be done in the laboratory. We will study and force the appearance of 'bad performance' in the turbine by doing a crack in a point in the blade that we will define as the critical point. Once we have identified the critical point, which is the point where the crack will likely appear, we will do a vibration analysis to identify until which situation our simplified Kaplan turbine can be working in optimal conditions with the crack evolution.

Comparing these studies (both numerical and experimental), the idea is to describe the response of a simplified Kaplan turbine with the appearance of cracks due to fatigue, and we will try to define values to improve the maintenance of these kinds of turbines. The ideal end of this project is to create a measurement system in turbines to detect possible appearances of cracks due to the effect of fatigue. As it would take years to analyse behaviors of turbines in different environments and loads, a modal analysis (what is a vibration analysis in air) will be done experimentally and will be constantly supported by numerical simulations.

3. Basic concepts

3.1 Importance of Hydroelectric energy in the society

3.1.1 Introduction to Hydroelectric Energy

Hydroelectric energy, also called hydroelectric power or hydroelectricity, is a form of energy that uses the power of water in motion -such as water flowing over a waterfall- to generate electricity. People have used this force for thousands of years. Over two thousand years ago, people in Greece used flowing water to turn the wheel of their mill to ground wheat into flour, for example [1].

Thus, the origin of this energy is the natural water cycle. Actually, and it's not known at all, the source of the hydroelectric energy is the sun, because water acquires potential energy under the action of the energy received from the sun.

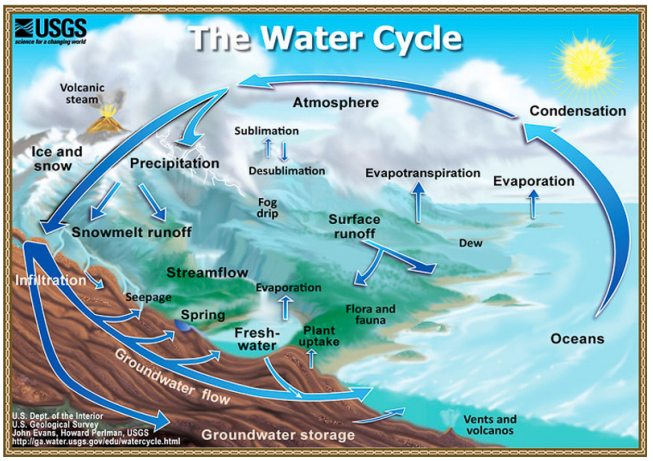

Figure 1: Water Cycle [2]

Hydroelectric energy is mainly obtained from rivers, waterfalls and water reservoirs, and year after year, due to climate change, the consumption of this renewable source is increasing. The fact that water is considered an inexhaustible resource on Earth for all generations, responds why it has always been used for producing energy. Actually, 20 years ago, hydroelectric energy represented almost the 98% of the renewable energy generated in the world [3], as we can see in Figure 2, that represents the evolution of consumption of electricity from different renewable energies throughout the years:

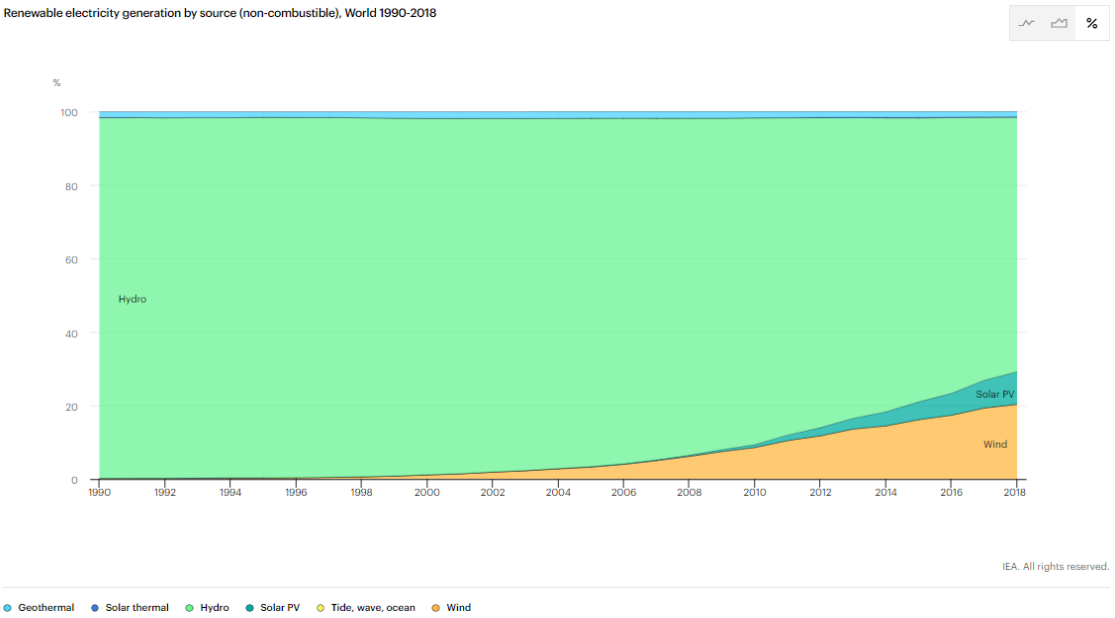

Figure 2: Renewable electricity generation by source [3]

Nowadays, renewable energy has become a crucial element of our lives. As the world is changing due to global warming, new methods and technologies for obtaining clean energies are becoming more and more important in society. That's why, as we can see in Figure 3, the hydropower generation is increasing year after year, and today, the world is consuming 4 times more hydroelectric power than 40 years ago, especially thanks to the contribution of Asia, which has tripled its consumption in the lasts 20 years [4].

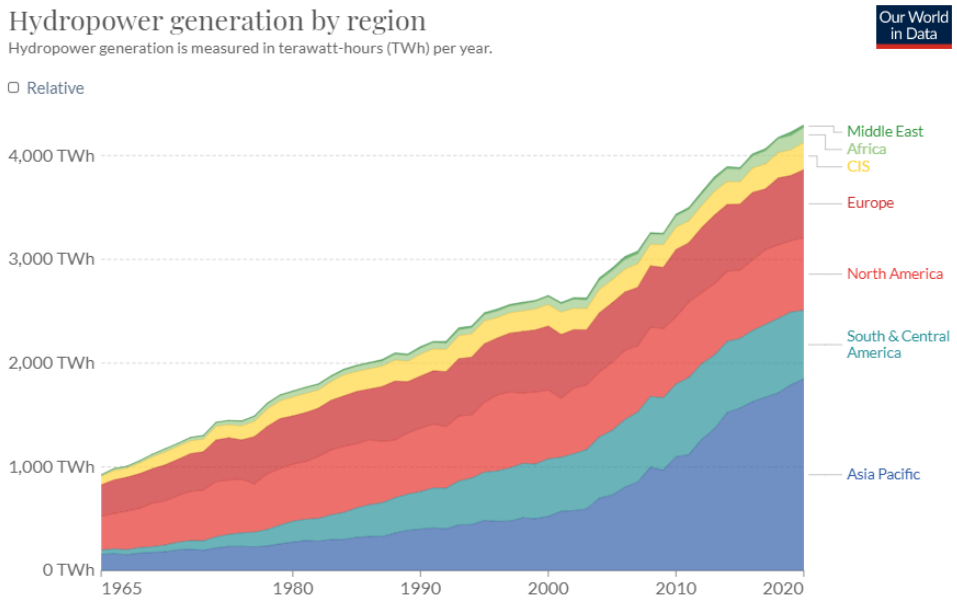

Figure 3: Evolution of hydropower generation [4]

3.1.2 Types of Hydroelectric Plants

There are mainly two groups of Hydropower plants. In both of them, water is the most important element of the generation system, and a turbine or groups of turbines are used for generating electricity due to the flow of water through that hydraulic machine. The first group is the one which uses the water as it flows through the river and it's called Run-of-the-river plants (ROR). The second group is the one which uses water stored in a reservoir when it is more convenient to use that water. This second group is called Reservoir hydroelectric power plants (RP).

- **Run-of-the-river plants (ROR):**

  The ROR are hydroelectric systems that harvest the energy from flowing water to generate electricity in the absence of a large dam reservoir. We can see an basic scheme of them in Figure 4 below:

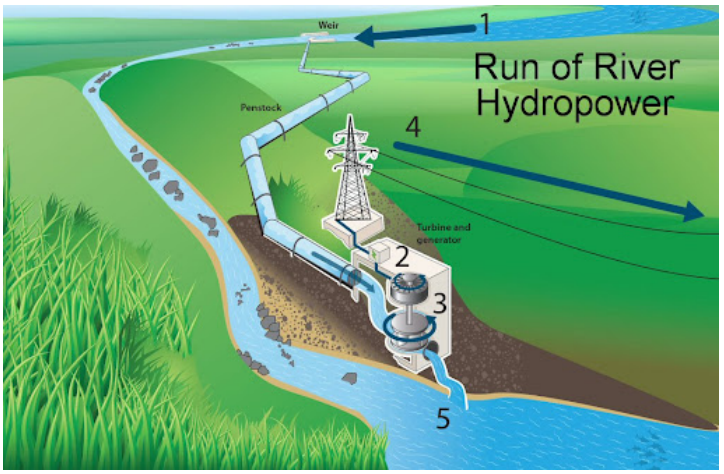

Figure 4: Scheme of a ROR plant [5]

The powerhouse is composed of, at least, a turbine and a generator that will send the electricity generated to the power grid. As a main characteristic of this kind of plant, it should be mentioned firstly that water is used when it is available. Depending on the season of the year or the quantity of rains in the place, there will be different levels of water flowing in the river. Thus, the turbines of the powerhouse will work in different regimens of work. Another important fact is that these stations do not use large water reservoirs, but small dams are usually built on the river to try to maintain the level difference constant, and that allows a small storage and provides constant power for a short period of time.

- **Reservoir plants (RP):**

  The reservoir plants are stations that use water from natural lakes or artificial reservoirs created by dams. The main characteristic of these kinds of plants is that the generation of electricity is used on demand. There are also two kinds of reservoir plants, the Regulation plants and the Pumped-Storage plants:

  ❖ **Regulation plants:**

  A regulation plant is a power station that allows storage of large volumes of water, and can be used as a water reservoir during times of drought. The main characteristics of these plants is that they are very adaptable to the supply of electricity on high demand hours, because they have a short startup time (they just need to allow the flow of water through the dam).

  ❖ **Pumped-Storage plants:**

  The pumped storage plants are a particular type of Regulation plants with the peculiarity that includes a pumping group in its powerhouse. This pumping group allows the plant to send water to the upper reservoir from the lower reservoir while there are cheap electricity hours, and this water can be used to generate electricity in high hours demand later. This kind of plant helps to keep the production/consumption balance in the electric system. In Figure 5 below we can see the classical scheme of a Pumped-Storage power plant:

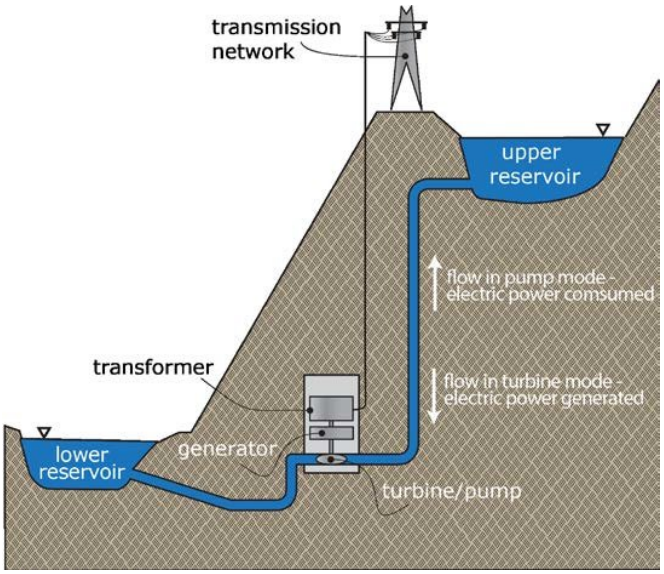

Figure 5: Main parts of a Pumped Storage power plant [6]

3.1.3 Hydropower in the electric system generation

In every single electricity system, the demand of electricity must be equal to the production at that moment (including losses due to transportation), otherwise, the electric system could collapse. Therefore, these kinds of plants must adapt themselves to the electric system, and they must be available for every moment in the day to supply electricity to the grid.

Hydraulic turbines have an important characteristic, which is that they don't usually work in constant regim (especially in the Reservoir plants, that adapt themselves to the electricity demand). An electric system is composed of two main groups of power plants related to its supply of energy to any electric system. Those are the base load power plants and the peak load power plants.

On the one hand, a base load power plant [7] is a power station that usually provides a continuous supply of electricity throughout the year with some minimum power generation requirement. Base load power plants will only be turned off during periodic maintenance, upgrading, or overhaul. Examples of base load power plants are the nuclear power plants or the thermal power plants.

On the other hand, a peak load power plant is a power plant that generally runs only when there is a high demand of electricity, known as peak demand. Due to the fact that they supply power only occasionally, the power supplied commands a much higher price per kilowatt hour than base load power. Here is the fact that highlights the importance of the proper functioning of hydraulic turbines in the world. Below in Figure 6 we can see the distribution of electricity generated depending on the way to generate it:

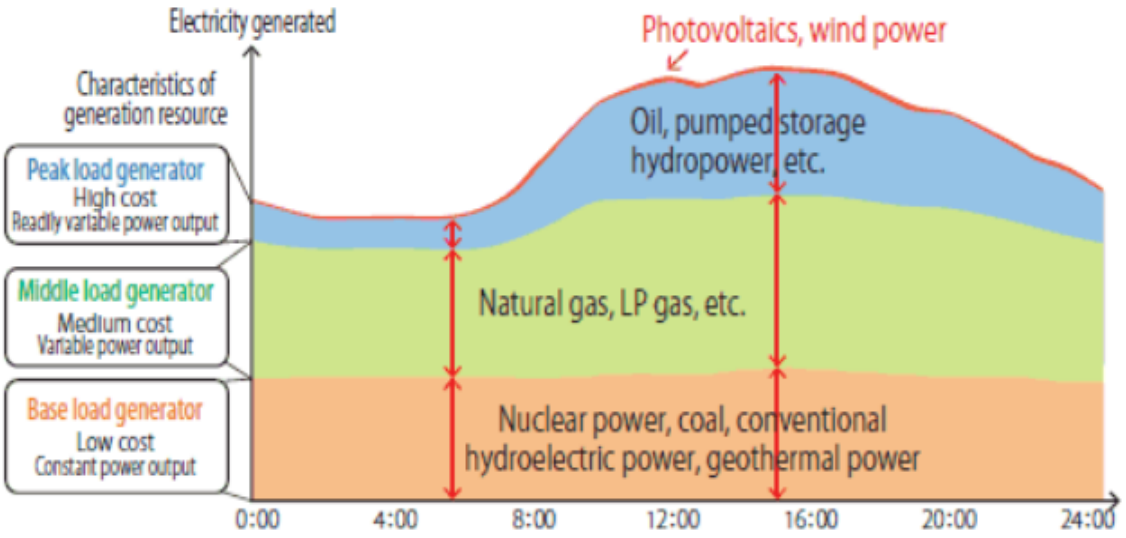

Figure 6: Electricity generated per kind of energy source [8]

As we can see, pumped-storage hydropower plants are the most important peak load plants in terms of contribution, because they send electricity when it's needed and the revenue generated with these kinds of plants is higher because the generation of electricity is done in the expensive hours of electricity.

Due to this fact, we can highlight the importance of the good maintenance of the turbines, and we can say that hydraulic turbines are a very important element in the generation of electricity in an electrical system, because they have to provide energy when it is more demanded. Thus, research in the field of hydraulic turbines sounds good as a challenge to improve the operation of electricity supply and, therefore, the day-to-day life of people who need electricity as a basic resource in their lives. In future subjects, we will analyse the performance of different types of hydraulic machines, and we will understand their functioning and how those machines can contribute to the generation of electricity.

3.2 Hydraulic machines

In this topic we will see the importance of hydraulic machines in society and how they work for producing energy, for using it or for storing it depending on the machine. We will also describe differences between similar types of machines, and we will see how they work in different regimes of work and their efficiency depending on how they work.

3.2.1 Introduction to hydraulic machines

Basically, a hydraulic machine is a mechanical system that exchanges mechanical energy with the fluid that is contained on it, or that circulates through it, considering that the fluid mentioned is incompressible [9]. Hydraulic machines have been used for thousands of years. For example, water mills and the Archimedes' screws have been used for several centuries even before the Roman Empire.

More recently, Hydraulic machines were one of the engines of the Industrial Revolution. The contributions of engineers such as Burdin, Fourneyron, Sablukow, Pelton, Francis or Kaplan, especially throughout the 19th and 20th centuries, were decisive for the manufacture of high-performance hydraulic machines. Some of them have given their names to different types of hydraulic turbines (that we will discuss later). Some examples are the Pelton, Kaplan and Francis turbines. In recent years, considerable improvements have been made in the study of hydraulic machines. For example, the three-dimensional effects, even assuming ideal flows or trying to evaluate the effects of losses due to the effects of friction and turbulence have made important contributions to the hydroelectric industry.

In this particular work we will talk more about turbomachines, since they are the hydraulic machines most used, and, mainly, because the Kaplan turbine (actually a turbomachine) is the element which our study is focused on. The hydraulic volumetric machines, also called machines of positive displacement (such as a simply acting cylinder) are other kinds of hydraulic machines of which we will not give many details, although they also have their importance in the industry.

3.2.2 Classification of hydraulic machines

There are many possible ways to classify hydraulic machines. Two different ways are the most used in order to understand them and differentiate them clearly.

- **According to the direction of the energy transmission:**

  - Generating machines: These machines are characterized by giving mechanical energy to the fluid they are working with. An engine is responsible for generating that mechanical energy. Examples of these machines are fans and pumps.

  - Motor machines: These machines extract mechanical energy from the fluid. Examples are hydraulic turbines, steam turbines or gas turbines.

  - Reversible machines: This kind of machines have a design that allows them to work alternately as generating machines or as motor machines. The main examples are the turbine-pump groups of the pumped-storage power plants mentioned in chapter 3.1.2.

  - Transmitting machines: They transmit energy between two mechanical systems or two fluids, combining a motor and a generating machine. The main function of these machines is the change of torque, or the change of a rotating speed, avoiding the vibration transmission and other mechanical connection problems. An example could be a Föttinger converter, used in vehicles.

❖ **According to the principle of operation of the machine:**

- ➢ Turbomachines: Also called Rotodynamic machines, they are a type of machine in which there exists an exchange of quantity of movement between the fluid and the machine through a rotating part, called rotor or impeller. A fluid circulates continuously through the channels that form the rotor blades. The forces have mainly a tangential direction, and this implies that there is a change in the kinetic moment of the fluid when it passes through the rotor, and, therefore, a torque is transmitted between the rotor and the fluid, and also an exchange of mechanical energy. An example of these machines is a centrifugal pump.
- ➢ Positive displacement machines: Also called volumetric machines, they are machines in which the exchange of energy is mainly in the form of pressure as the fluid passes through a working chamber, in which it enters and leaves in an alternative process. There is a force between the fluid and other moving organs that results in the exchange of energy, but a non-continuous process is made in the exchange of energy. An example of these machines is the rotative machine of gears.
- ➢ Gravimetric machines: These are a kind of machine that uses the gravitational potential energy for transmitting energy to a fluid. They are not very interesting in today's society, but they have had their importance in history. One example could be the Archimedes' screw.

3.2.3 Hydraulic turbines

Hydraulic turbines are the prime movers that convert the energy of the falling water into a rotational mechanical energy and then, consequently, to an electric energy through the use of the generators that are connected to the turbines. The generator is composed of a rotor and a stator.

These turbines are called ‘hydraulic’ because water is the element that is used by them to obtain energy. An elementary hydraulic turbine has, basically, a series of fixed blades (distributor), and other moving blades . The association of fixed members and a movable wheel constitutes a cell. A single-cell hydraulic turbine is made up of three different organs in which the fluid goes through successively. Those are the distributor, the impeller and the diffuser. Moreover, all the structure is supported and centered by a shaft, connected to the generator [10].

On the one hand, the distributor is a fixed part whose mission is to direct the water from the inlet section of the machine towards the entrance to the impeller, distributing it around it, or a part. This means that the distributor can regulate the water that enters the turbine, from closing the passage completely (zero flow), until the maximum flow. It is also an element that transforms pressure energy into kinetic energy. In general, turbines also have another static part called diffuser, whose task is to drain the water, allowing it to recover part of the kinetic energy at the exit of the impeller after the pass of water through the rotating blades.

On the other hand, the impeller is the most important element in a turbine. It is responsible for transmitting the main part of the energy of the water to the machine thanks to its blades. Below in Figure 7 we can see all the previous parts mentioned in a hydraulic turbine.

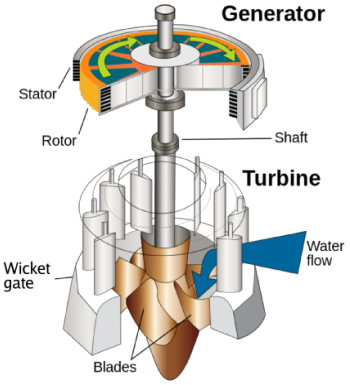

Figure 7: Basic parts of an hydraulic turbine [11]

3.2.3.1 Types of hydraulic turbines

According to the variation of pressure in the impeller, there exists 2 types of turbines:

- **Action turbines:**

  In action turbines, the water leaves the distributor at atmospheric pressure, and reaches the impeller with the same pressure. In these turbines, all the potential energy of the jump is transmitted to the impeller in the form of kinetic energy. In action turbines, the push and the action of the water have the same direction:

- **Reaction turbines:**

  In the reaction turbines the water leaves the distributor with a certain pressure that decreases as the water passes through the impeller blades. Thus, at the outlet, the pressure can be zero or even negative. In these turbines the water circulates under pressure in the distributor and in the impeller and, therefore, the potential energy of the jump is transformed, one part, into kinetic energy, and the other, into pressure. In reaction turbines, the push and the action of the water have different direction:

According to the direction of entrance of the water into the turbines, these can be classified into 3 main groups:

- **Axial turbines:**

  In the axial turbines the water enters parallely to the shaft. Examples of these turbines are **Kaplan turbines**, helix turbines or Bulb turbines. This kind of turbine is used for treating high volumes of water flow (reaching even 1000 m^3/s flow), but, consequently, for giving low water net head. Below in Figure 8 we can see an example of an axial turbine:

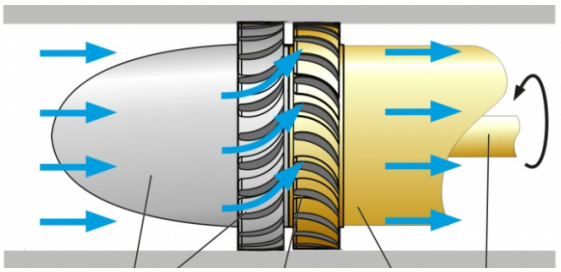

Figure 8: Example of an Axial turbine [12]

- **Radial turbines:**

  In the radial turbines the water enters perpendicularly to the shaft, being centrifugal when the water goes from the inside to the outside, and centripetal when the water goes from the outside to the inside. An example of these last kinds of turbines are the Francis turbines. Francis turbines are used for neutral parameters of work. Nevertheless, they can't reach the water flow through them of an axial turbine and they can't give the net head of a Pelton Turbine. Below in Figure 9 we can see an example of a radial turbine:

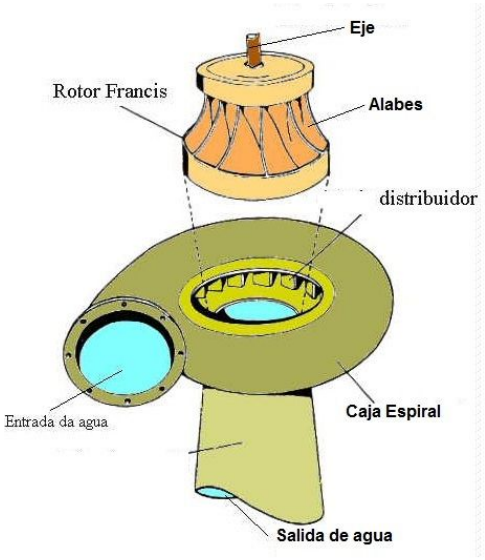

Figure 9: Example of a Radial turbine [13]

❖ **Tangential turbines:**

This kind of turbine is defined that way because water enters laterally or tangentially against the blades. The main example of this kind of turbine is the Pelton turbine.This turbine is used for treating very low water flows, but for reaching high water net head (even 1500 m). Below in Figure 10 we can see an example of a tangential turbine:

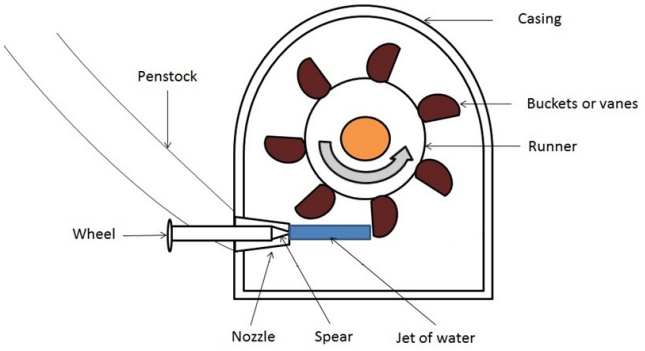

Figure 10: Example of a Tangential turbine [14]

3.2.3.2 Uses of different Hydraulic turbines

In the previous chapters we have seen that there exists a huge range of hydraulic turbines to use in the hydroelectric power plants, and the configuration of them will depend on the quantity of water and the head that can be used by the own plant. In this point we should define two main parameters to select a turbine for a determined installation.

- Water flow (**Q**): The amount of water flowing per unit of time. It is expressed in m^3/s in the International system of units (IS).

- Net head (**Hn**): The net head is defined as the gross head minus all losses due to friction and turbulence. It is expressed in meters [m] in the International system of units (IS). The net head between the entrance (a) and the exit (b) of the turbine can be calculated using the Bernoulli's Formula shown below in Equation 1:

$$Hn = (c_b^2/2g + P_b/\rho g + z_b) - (c_a^2/2g + P_a/\rho g + z_a) + h_f \quad (1)$$

Where h_f are the losses due to frictions and turbulence in the pipes, and the rest of the equation is the gross head.

Once these two parameters are defined, we must also know that the turbines are directly or indirectly connected to the alternator. This means that, as they are connected, they must rotate at a constant speed, so that the frequency of the electric current does not vary. This speed, called synchronism speed, depends on the frequency of the current (f) and the number of pairs of synchronous alternator poles (np).

$$N = 2\pi f/np \ \text{[rpm]} \qquad (2)$$

With this equation, the specific speed (Nq) can be defined for the selection of the turbine in a power plant, depending on the water flow of the own Hydroelectric power plant and the net head that it can provide:

$$Nq = N * (Q^{0,5}/gH_n^{0,75}) \qquad (3)$$

Once we have calculated the specific speed Nq from all the equations mentioned before, we can select a specific turbine for a plant through all the parameters mentioned above. For doing so, below in Figure 11 we can see an ideal distribution of use of turbines for a determined Hn and Nq:

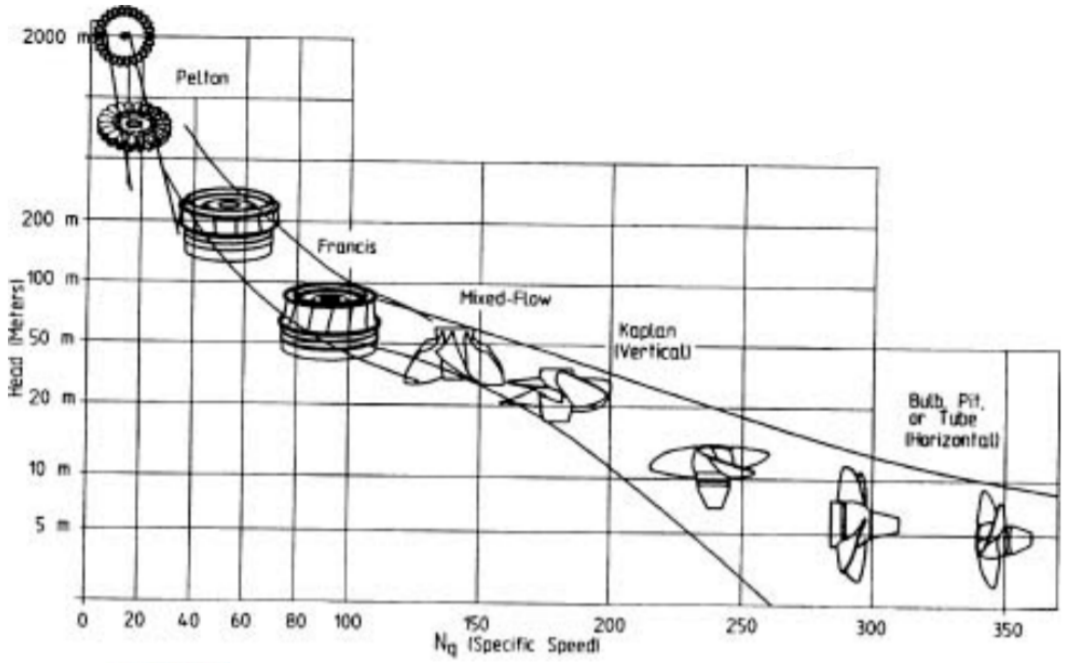

Figure 11: Ideal turbine selection depending on the net head and the specific speed [15]

In the previous figure we can see that for high net heads and low specific speed (therefore, low water flows), Pelton turbines are advisable, while Kaplan turbines can use a high quantity of water flow, but the net head that water can provide is low. Francis turbines are used in a wide range of work, both for normal water flows and normal net heads, and this last fact is the particular reason that makes that this kind of turbines are the most used in the world, followed by the Kaplan turbines.

Once the selection of the turbine has been made, the question is how much energy a turbine can supply to the electricity grid. The usual way of operation of the industrial turbines is to constantly supply the power required by the alternator, while keeping the frequency within a certain reduced margin. This is the reason why it is interesting to study the variations in the efficiency by varying the power or the water flow, keeping constant the net head Hn and the rotation speed N [16].

To answer that, we also have to define the efficiencies of different parts of the turbines. Firstly, the own efficiency of the turbine, that is defined as the mechanical energy that the turbine can provide divided by the hydraulic energy received by the water:

$$\eta_{turb} = P_{mec}/P_{hyd} \qquad (4)$$

Where P_{hyd} is the energy given by the water, and it's defined by the Equation 5 below, and P_{mec} is the power given to the alternator.

$$P_{hyd} = \rho \cdot g \cdot H_n \cdot Q \qquad (5)$$

As we can see, linking the two previous equations, the efficiency of a turbine depends on the water flow that goes through the own turbine. This means that for different flows of water, the efficiency of the turbine will vary.

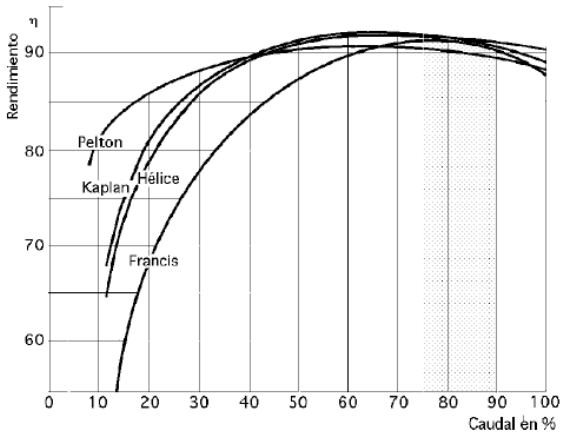

Figure 12: Efficiencies of turbines depending on the % of load [16]

In Kaplan turbines, the maximum efficiency is obtained for loads of water flow between 60% and 70% over the maximum flow possible for the turbine. In Francis turbines we can see an optimal point of efficiency at the 80% of the maximum load possible for the turbine. In this last figure, we can see also that just for very low loads of water, the pelton turbine has a better efficiency than the others.

3.2.4 Kaplan turbines performance

Following the previous concepts, we have to highlight the importance of Kaplan turbines in the industry. As we have seen, these kinds of turbines have a good range of efficiencies and are available for using huge amounts of water flows (they can even reach a water flow of 1000 m^3/s). Particularly, for this study, between all the hydraulic machines mentioned before, we will focus on the Kaplan turbines, as it's the one that we are going to analyze experimentally in the laboratory and with computer software like Ansys or SolidWorks.

Kaplan turbines can be used horizontally and even vertically. This particular reason makes this turbine even more adequate for different styles of work in different hydroelectric power plants. Moreover, the increasingly trend towards the construction for using faster turbines, for specific speeds (n_s) greater than 450 rpm, leads to focus on Kaplan turbines, since in Francis turbines with ns of the order than 400, the water cannot be accurately guided and steered.

The impeller in Kaplan turbines is made up of a few blades, which give it the shape of a ship's propeller. The main difference between helix turbines and the Kaplan turbines is that the rotating blades in the Kaplan turbines are steerable, while in the Helix turbines, the blades are fixed. In both cases, the turbines work with a single direction of rotation. They are, consequently, irreversible turbines. If the blades were steerable and the turbine could work in 2 directions of rotations, we would be talking about a Bulb turbine. As we said, we will focus our explanations and calculations for the Kaplan turbines.

In all hydraulic machines, there exists 3 components of velocity of the water in a point to describe movements, and thanks to the study of the evolution of these 3 terms, there can be defined some other parameters like net head, power, and efficiency of a turbine. The first of them all is the rotation speed (U), that is the velocity in a point of the blade. It depends on the rotation speed of the turbine (n) and the distance between the studied point and the shaft of the turbine. Secondly, the relative velocity (W), that it's described as the velocity of the water seen in a relative reference (commonly, the blade is the relative reference). Finally, the third component of velocity is the absolute velocity of the water (C) that represents the velocity seen in an absolute reference.

In Kaplan turbines, 2 points are interesting for analyzing the performance of the turbine. The first point is the inlet of the blade (described as 1 in Figure 13). The second point of study is the point where water leaves the blade (called point 2 in Figure 13). Knowing all parameters mentioned before, we can analyse the efficiency of the turbine, and, therefore, we can know what is the contribution of the Kaplan turbine to the electrical grid. In Kaplan turbines, for the design conditions, Figure 13 represents the velocity field. The main characteristics of the velocity field is that the relative velocities W_1 and W_2 follow the direction of the blade, meanwhile the absolute velocity of the exit C_2 is axial. The theoretical energy that can provide a Kaplan turbine with all the parameters mentioned is described below in Equation 6:

$$Eth = 1/2 \cdot [(C_1^2 - C_2^2) + (W_1^2 - W_2^2)] \quad (6)$$

Another relation between the E_{th} and thetheoretical net head can be defined at Equation 7 below:

$$Eth = g \cdot H_{th} \quad (7)$$

Therefore, the net head and the velocity field of the blades are related, and, consequently, the efficiency of the turbine too. With all these relationships mentioned above, it's obvious that the variation of the angle of the blades (remember that the Kaplan turbines are characterized by this), will provoke a variation in the efficiency of the system. In Figure 14 we can see the distribution of efficiencies depending on the angle of inclination of the blades. Note that the best efficiencies are achieved when there is an inclination of about 12º-17º, reaching an efficiency of almost 90%. Even with an inclination of 0º, the Kaplan turbine could work, but the efficiency would be around 50%. Compared with other machines in the industry (like car engines or solar panels), the efficiency mentioned is not bad at all. Nevertheless, it's highly recommended to use an inclination of the blades of around 15º if possible.

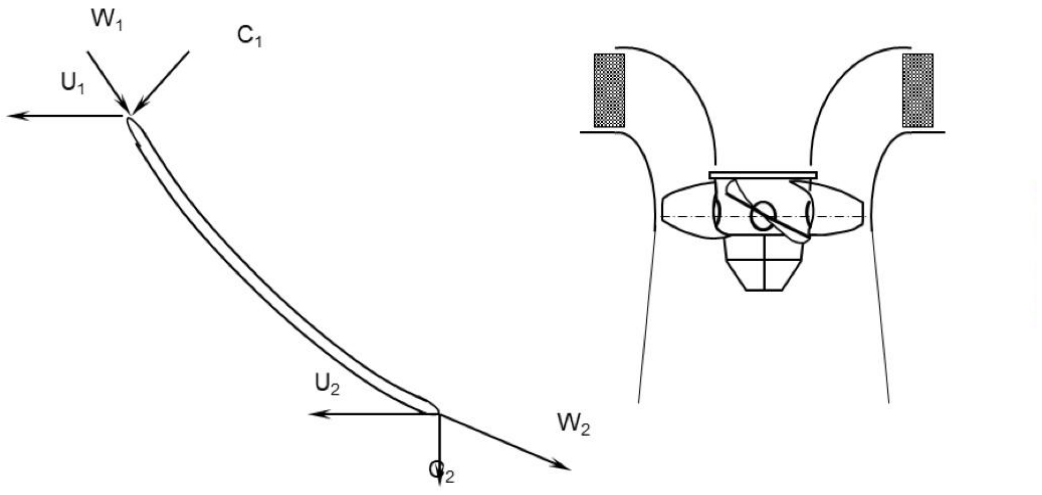

Figure 13: Description of velocity components in a Kaplan turbine [17]

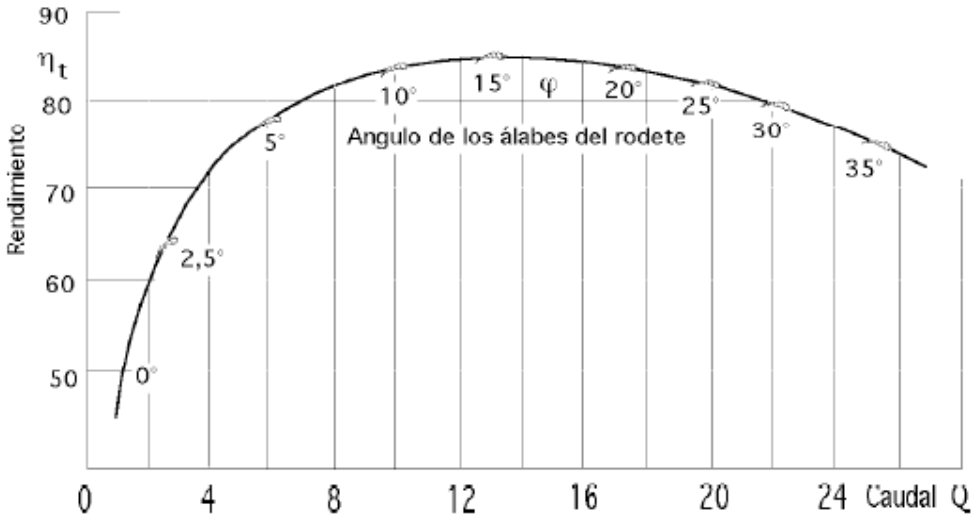

Figure 14: Efficiencies depending on the angle of inclination of the blades [18]

3.3 Most common failures in Kaplan turbines

Continuing with the topic of the Kaplan turbines, we will introduce some theory about the most common failures in hydraulic machines. To know more about the topic of failure in hydraulic machines, we must define what kind of failures are identified currently. There are 4 kind of failures for the hydraulic turbines [19]:

- **Cavitation**: This is a phenomenon that happens in the turbine due to the flow of water through it, and mainly produced because water changes its pressure and velocity while passing through the turbine. It is due to the formation of bubbles of vapour rapidly and its subsequent collapse. In many cases, the force of cavitation is strong enough to destroy metal components. Cavitation occurs when the static pressure of the liquid falls below the vapor pressure, creating vapour bubbles. As the energy must be constant, if the water reduces its pressure the component of the velocity must increase. Therefore, the points in where cavitation often appears are the fast moving blades of hydro-turbines or near the exit of the turbine. The most common causes of cavitation in any turbine are the design profile of the turbine and the constant change in the operating conditions due to water load requirements. The appearance of cavitation provokes vibrations in the unit and noise, and enhances the possibility of failure in the unit.

- **Erosion**: The erosion is a phenomenon that represents the losses of material in a surface due to the contact with another material. In case of hydraulic turbines, the erosion is provoked by the flow of water (with its impurities) at high velocity and due to the impingement of abrasive sediments on the surface of the turbines. Erosion can be provoked too due to the cavitation, as the bubbles can remove material from the turbine surface while they collapse. The most susceptible parts because of erosion are the turbine blades and the guide vanes. Erosion (as cavitation) reduces the efficiency of the turbine, and this affects directly to the electricity generation of the hydroelectric plant.

- **Fatigue**: This kind of failure in machines appears because different components of machines are subjected to repeated alternating or cyclic stress below the normal yield strength and fail progressively by cracking. The appearance of a crack provokes a reduction in the efficiency of the turbine and can be dangerous for all the units of the turbine, because the crack can provoke a collapse in the structure. This kind of failure is the one that we are going to study in this work, and we will simulate the appearance of a crack to analyse possible behaviors (mainly because of the vibration) of the turbine while fatigue phenomenon has started in a simplified Kaplan turbine. The most susceptible parts for appearing a crack in a Kaplan turbine are the turbine blades and, concretely at the point of contact between the flange and turbine runner assembly.

- **Material defects**: The failure due to material defects is very strange, but it actually exists. Material defects could essentially be controlled during the turbine fabrication stages. The fabricated turbine parts must accomplish the standards required by the hydroelectric power plant. Material defects can derive in other failure phenomena like erosion and even fatigue.

3.4 Introduction to vibrations in bodies

As we said in the first chapters, we will use the vibration analysis for trying to reach conclusions about the vibratory response of a simplified Kaplan turbine. We will also see how it behaves, and how it works under the appearance of the effect of fatigue.

3.4.1 Definition and types of vibrations

A vibration [20] is an oscillation of a determined body or structure around a balance position. The balance position is the place that the body will arrive once the force exerted on it is equal to 0. This kind of vibration is called full body vibration, which means that all single parts of the structure move together in the same direction at any time. A vibration in a machine can come from many reasons (i.e cracks, frictions with the environment, frictions of different parts of the machine, external noise…). To be more direct, a vibration comes from an action or force over a body. A vibration is a particular kind of oscillation that is characterized for having high frequencies (f) and low amplitudes (A), this means that the repetitives movements of the bodies are really fast and short. As an example, when someone rings a bell, this one vibrates very fast and the amplitude of the movement is very short.

For measuring vibrations in the time, we can analyse the signals that the own oscillation gives us. A signal is a set of representative values of a phenomenon. There are 2 kinds of signals: stationary and non stationary.

The Stationary signals can be deterministic and aleatory, and they (the stationary signals) are the signals that have the statistical parameters constants in the time. This means that it doesn't matter when or where someone measures a vibration in a machine with stationary signals, because the vibrations remain practically constant. Rotative machines (like Kaplan turbines) produce stationary signals while working.

The deterministic signals are basically those who can be described with a mathematical formula during a period of time. This implies that future values of vibration can be determined by measuring the previous ones. There are two kinds of deterministic signals. Firstly, a periodical signal is the one that has the same shape of wave during the time. The main example of this kind of signal is the sinus signal, which can be seen in the left part of Figure 15. The semi periodical signal is the one that is not periodical at all, but the observer while measuring the signal in the frequency domain can see a kind of periodical behaviour. A semi-periodical signal can be seen also in Figure 15 on the right.

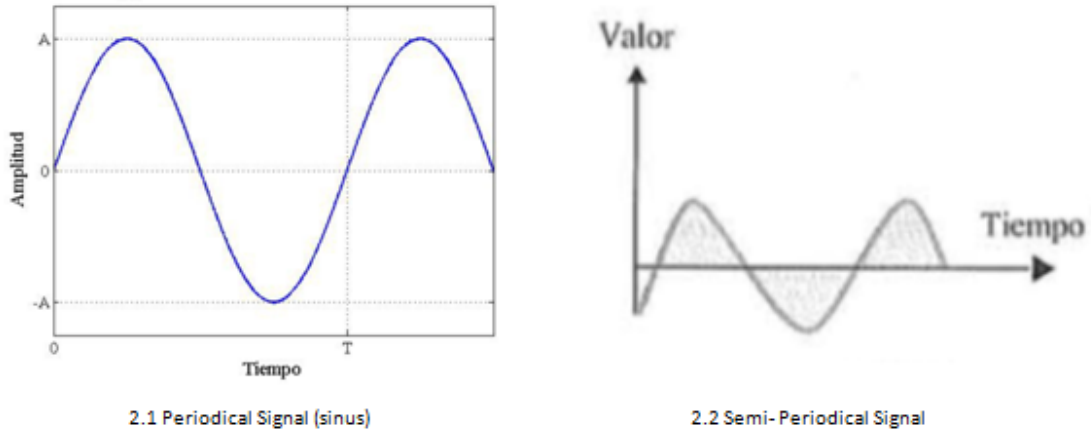

2.1 Periodical Signal (sinus) 2.2 Semi- Periodical Signal

Figure 15. Periodical and Semi-periodical Signals

An aleatory signal is the one which can not be described with a mathematical formula and, consequently, we can't know future behaviors of vibrations in a machine with these kinds of signals.

The non-stationary signals are signals that change their characteristics over time, like the beat of a drum. Regarding these signals, there exists continuous and transient ones. Transient signals are those that begin and end at some point (normally 0), like the hit of a hammer. The continuous signals are those non stationary that are not transient, they don't start and end at a certain point and can endure in time.

3.4.2 Important parameters in a vibration analysis

When measuring vibrations in a structure, three parameters are the main ones to describe its behaviour while oscillating. Oscillations can be described through its waves, and those waves have a displacement (measured frequently in inches), velocity (measured in inches per second) and acceleration (measured in Gs). As we know, the derivative of the displacement is the velocity and the derivative of the velocity is the acceleration. In a reverse path, velocity is the integral of acceleration and the displacement is the integral of the velocity.

For our experiment (and this is what is usually done) we will use accelerometers to measure accelerations, and, automatically, we will obtain the results of displacements and accelerations of different points due to the mathematical relationships explained.

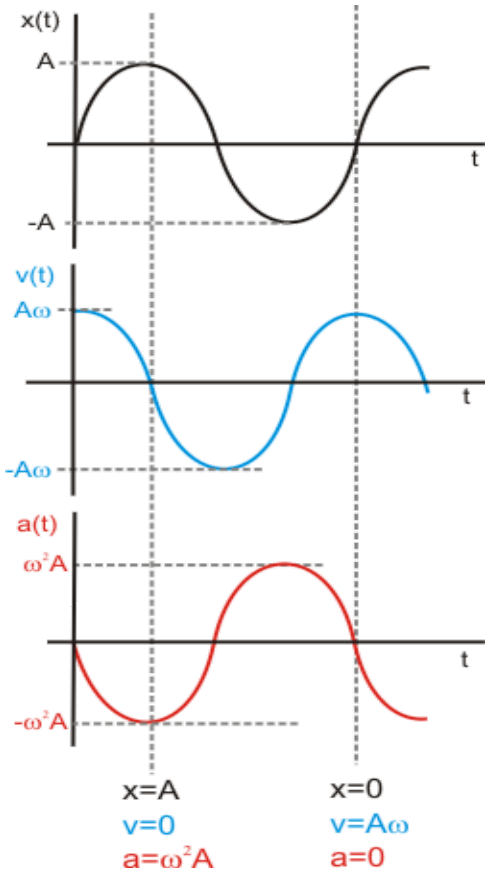

Figure 16: Relationship between Displacement x(t), Velocity v(t) and Acceleration a(t) in a wave [21]

As we see in Figure 16, when analyzing the displacement, the maximum displacement represents a null velocity and a minimum acceleration. It makes sense due to the explanation before of the derivatives and integrals. Therefore, when measuring accelerations we can ensure the effectiveness of the results of displacement and velocities in a point of a body. Accelerometers are put in different places of a structure, and knowing velocities, displacements and accelerations of different parts of a structure we can comprehend the movement of that structure under an effect of vibration, and its evolution during a certain period of time.

3.4.3 Important concepts of vibrations

- **Movement equation:**

A particle's vibration can be determined imagining a system like shown in Figure 17 below:

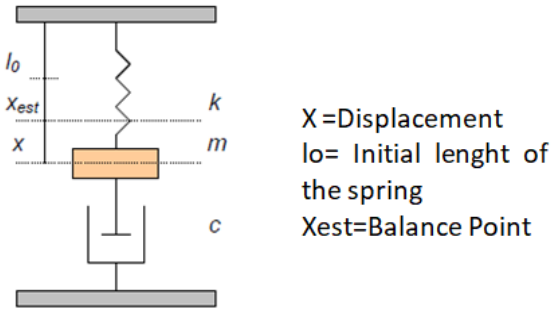

Figure 17: Model of the vibration movement in a point of a body [22]

As we can see in Figure 17, a determined point in a body or structure oscillating is composed of three main parameters regarding its oscillating movement. These parameters are the mass (m), the stiffness coefficient (k) and the damping coefficient (c) [22]. The mass will displace itself (x) from a balance point X_{est} considering the following hypothesis:

- The mass moves vertically without friction.
- The mass of the spring is negligible and the force of the spring is $F=k\cdot x$.
- The mass of the damping device is negligible and it is based on a viscous type friction, with friction force opposite and proportional to speed $F=c\cdot x'$.
- The studied body is in the vacuum environment.
- The parameters m, k and c are bigger than 0.

The damper is the element that represents the energy loss of a system in the form of heat or noise. It has no mass or elasticity. It just represents the loss of energy in the damping coefficient c. On the other hand, stiffness is a mechanical property of the springs that measures the capacity of hardness of these, and, hence, it is related to the property of the material of the structure. It thus represents the capacity of a spring (in terms of material) to increase or decrease with respect to its initial length l_0.

The dynamic equilibrium equation makes it possible to establish the differential equation of the movement shown below as Equation 8:

$$F= m\cdot x'' +c\cdot x'+k\cdot x \quad (8)$$

Where F is the external force applied to the system, $m\cdot x''$ the inertial force, $c\cdot x'$ is the viscous damping force and $k\cdot x$ is the elastic force.

- **Natural Frequency**

The natural frequency is the frequency at which a body vibrates when giving it an external energy. The level of vibrations will depend on the strength of the energy source and the absorption inherent in the system.The natural frequency of a spring-mass system is is given in the following Equation 9:

$$Fn = (1/2\pi)\cdot\sqrt{k/m} \quad (9)$$

As we can see in Equation 9, the smaller is the mass, the bigger is the term of the natural frequency (F_n). On the other hand, the bigger the stiffness coefficient, the bigger is F_n. Therefore, the more rigid a structure is with constant mass, the bigger is its F_n and, therefore, vibrates more in a period of time. If the stiffness reduces its value, the value of natural frequency will be reduced as well.

A large number of spring-mass-damping systems that form a body are called "degrees of freedom", and the vibration energy that is put into the machine will be distributed among the degrees of freedom in quantities that will depend on their natural frequencies and damping, and also of the frequency of the power source. This is why not in the system the way it vibrates is constant.

For example, in a machine powered by an electric engine, a big source of vibration energy is the residual imbalance of the engine rotor. This will result in a measurable vibration in the motor bearings. Nevertheless, if the machine has a degree of freedom with a natural frequency close to the RPM of the rotor, its level of vibrations can be very high, although it can be located at a great distance from the rotor engine.

For this particular project, we will measure the natural frequencies of the structure given in air, as there is no time enough for doing experiments both in water and in air environment. For doing that, we will study the natural frequencies of the structure and we will analyze the way it vibrates at that frequency, what is called Vibration mode.

- **Vibration Mode**

The vibration mode is the way that a system vibrates. The vibration mode will be achieved when the system spring-mass-damping arrives at its natural frequency. There exists an amount of vibration modes equal to the amount of degrees of freedom, and it's equal to the amount of natural frequencies in a structure. The displacement of a point in the structure will depend on its vibration mode and it can be measured in all single points of the structure. This term is also known as mode shape.

3.5 A brief summary about fatigue in machines

In this fifth chapter of the basic concepts we will explain the topic of fatigue. As fatigue has a wide range of study, we will explain the basic concepts of fatigue, being more concrete for the case study and we will try to define and set the relationship between fatigue, crack and failure in a structure.

3.5.1 Definition of fatigue. Fatigue as a multidisciplinar phenomena.

Fatigue is defined by the Society for Testing and Materials (ASTM) as the process of structural change, progresive and localized, that occurs in a material subjected to variable stresses and strains in a point or in various points that produces cracks or complete fracture after a sufficient number of fluctuations.

We should note that this is a really interesting definition, because it covers many parts. Firstly, the definition says "structural change", which refers to the internal change in the structure of the material, "progresive" that means with no return, and "localized" because it affects to concrete parts of material localized. Secondly, the definition mentions the term "variable stresses", which means that this is a phenomenon that does not occur in bodies subjected to static loads, but in bodies or structures that suffer dynamic loads. Thirdly, it is mentioned that it has an effect on the generation of "cracks" that did not exist before, and, finally "complete fracture after a sufficient number of fluctuations", which means that after a high number of fluctuations (cycles of work), the initial crack mentioned before can spread itself until reaching a critical length. Once the longitude of the crack is equal to the critical length, the system will collapse and break down.

Fatigue and fracture are two phenomena of great practical significance. Failures due to fatigue are especially dangerous because, apparently, the structures don't seem to be affected, and visually are not supposed to

collapse in a short period of time. Generally, fatigue is provoked due to a change in the geometry of a body, like holes or changes in sections. Those changes in sections are really significant for the effect of fatigue. Moreover, we should highlight that not only the change in the geometry is relevant for the appearance of fatigue, but also other factors like the material, the loads that are acting over the structure, corrosion, and the manufacturing process. Therefore, we can say that fatigue is a multidisciplinar phenomena.

The phenomena of fatigue and the resistant behavior of cracked bodies, described by the principles of mechanics, are two important and complementary fields. Actually, nowadays they are the cause of the largest number of failures in service in machines, since fatigue failure is produced by the repeated action of loads of values lower than those necessary to produce a static failure of a structure. For this reason, fatigue and fracture are both of interest in various fields of engineering, like in the automotive industry, the civil industry, and, in our particular case of interest, the hydroelectric industry.

Having in mind that fatigue is a multidisciplinary phenomena, the nature of the fatigue is not deterministic, but statistical. Results obtained from studies apparently equals (for example, 2 test tubes with same variable loads applied on them) can vary depending on the experiment that has been carried out. The statistical nature of fatigue determines how to treat the various problems related to it, because it is not possible to ignore this issue both in the theoretical and experimental approaches. In all calculations (including our own study), this fact must be highlighted, because in all the different stages of fatigue that we will introduce soon, the statistical nature of fatigue must be taken into account in order to approach the results expected and obtained to the reality of fatigue in bodies.

3.5.2 Persistent issue and its relation with fatigue

Once we have seen the definition of fatigue, it seems obvious that when some structure, body, or component is created, this has to be designed taking into account the effect of fatigue, being able to be safe and reliable (understanding reliability as the probability that a body they can carry out its function without failure for a given period of time).

A structure is considered safe if its remaining residual resistance is bigger than the external effort applied in every instant of time with a certain security margin. In Figure 18 below, there are two diagrams that show the evolution of some external loads that suffers a structure during its lifespan (on the left) and it's progresive degradation (on the right) associated to the effect of fatigue due to that variable load.

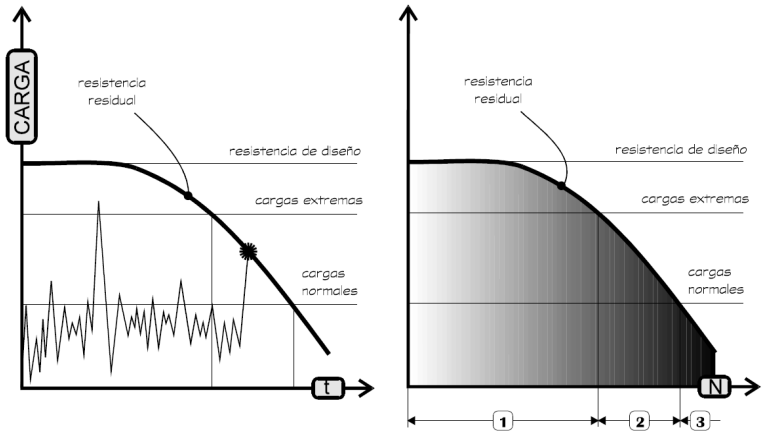

Figure 18: Evolution of degradation of a structure due to variable external loads applied on it [23]

To simplify the explanation, we will set 2 levels of load, the common loads and the extreme loads. In the beginning of the life of the body, the residual resistance is equal to the design resistance and it has to be bigger than the external loads (including the security margin) for not failing. Once the structure starts suffering external variable loads it starts its degradation, and here is where the concept of fatigue appears. When the residual resistance of the structure decreases it is getting closer progressively to the extreme stress values, zone 1 of the graph. During the pass through this first zone, the failure probability has to be practically zero, and when the zone 1 ends, the time reflected has to be the service life time expected.

In zone 2 of the graph, the failure is possible and random. It is an 'random zone', which depends on the load at that time to see a failure in the structure. If there is an extreme external load in this zone, the piece will break down. Finally, the zone 3 is the zone in where the failure is certainly going to happen, as the residual resistance is smaller than the common external loads, but it's not known exactly when is going to happen the failure of the structure, but it will happen in this third zone. If the external load is bigger than the residual resistance, the piece will break for sure. All this explanation of life span of pieces and bodies while suffering variable loads in time is known as the **persistent issue**.

Once we have explained the persistent issue hereinabove, we can consider the previous concepts mentioned of fatigue and fracture from this perspective of relations between loads vs time. This also allows us to study the reliability of the structures and relate it with the concept of **crack**. To relate fatigue and failure with the persistent issue, we must define 3 scenarios while studying the reliability of a structure regarding its capability of work when a crack appears.

- Firstly, the phase of initiation of microcracks. In this first phase, the body starts suffering variable loads but with no appearance of big cracks on it. Microcracks are common in structures. Actually, we can also find them right after the manufacturing process. This is the phase that lasts the longest in time. In this first phase, the microcracks are so small that they have a negligible effect on loss of strength.
- Secondly, a macrocrack appears (we will call it just crack hereinafter). This crack makes the body lose internal resistance and the cracks expand itself in all the body.
- Finally, the third and final phase is the scenario in which the section fails due to the length of the crack and because the residual resistance is smaller than the external stresses. The duration of this period is negligible regarding the previous two mentioned.

As we can see, the existence of these three clearly differentiated phases makes it possible to consider the total fatigue life as the sum of three different periods of life: 1-Life of crack starts. 2- Crack propagation life. 3- Life until the final fracture.

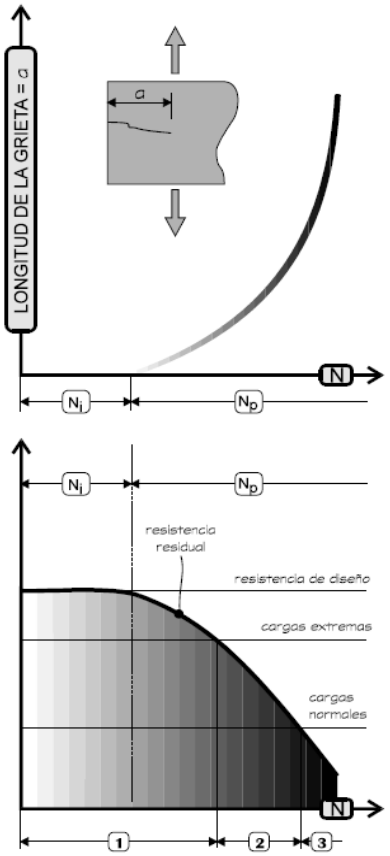

Figure 19: Relationship between the length of the crack and the persistent issue [23]

This 3 phase-scenario makes us relate the appearance of the phenomenon of fatigue with the appearance of cracks and failure with the persistent issue, that, remember, also had 3 scenarios as well. In Figure 19 we can see the relationship between the evolution of the crack with the persistent issue.

Fatigue fractures in ductile metals (such as in a blade of Kaplan turbine) begin in areas with localized plastic deformation due to the effect of the shear stresses, and the direction that the crack should take is the perpendicular to the main direction of stresses in that point. Actually, there are many theories about the phenomenon of fatigue, but, the main considered, and the one we are going to use, is that we could consider the crack as a lack of material in a point due to the internal stresses, and the evolution (propagation of the crack) depends, as we said, on the direction of the shear stresses in those points with lack of material.

3.5.3 Physical foundations

To physically analyse the effect of fatigue in the bodies, we should first define the concept of stress. Stress (σ), in physical sciences and engineering, is defined as force per unit area within materials that arises from externally applied forces, uneven heating, or permanent deformation and that permits an accurate description and prediction of elastic, plastic, and fluid behaviour.

We should mention that for describing the essential components of the stress, a sinusoidal variation of stress is described, but this sinusoidal form of stress can be extrapolated to other kinds of external forces applied over a structure. The easiest type of test to perform, that also describes a sinusoidal external stress, and therefore, the most common to study or describe the fatigue phenomena is the rotary bending test on a cylindrical test tube. During each axis revolution, the same material particle is subjected to tensile stresses and compression of the same magnitude depending on its position relative to the neutral fiber. We should highlight that in fatigue analysis, the studies are directed to the critical points that are supposed to fail due to fatigue. Those points are points that are frequently in changes of geometry or point that suffers directly from the external force on them. In Figure 20 below we can appreciate a temporal variation of a sinusoidal stress applied on a particle of a body.

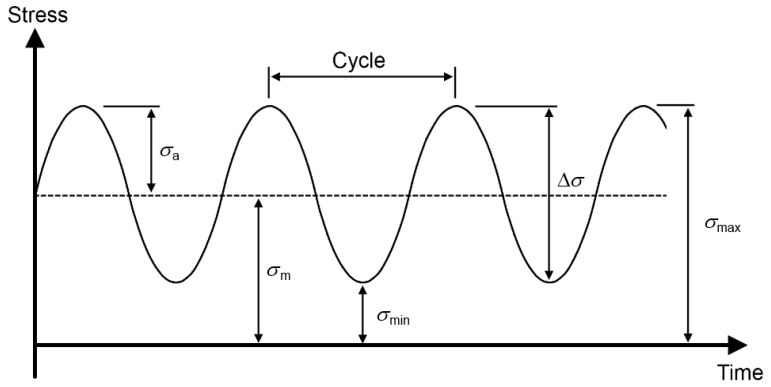

Figure 20: Sinusoidal shape of stress applied in a body [23]

The components that describe this evolution of stresses in the particle are the following:

$\sigma_{max} = Maximum\ stress$
$\sigma_{min} = Minimum\ stress$
$\sigma_a = Alternating\ stress\ (Amplitud) = (\sigma_{max} - \sigma_{min})/2$
$\sigma_m = Average\ stress = (\sigma_{min} + \sigma_{max})/2$
$\Delta\sigma = Range = \sigma_{max} - \sigma_{min} = 2 \cdot \sigma_a$
$N = Number\ of\ cycles\ of\ work$

3.5.4 The S-N curve

The S-N curves are the result of submitting a body to a stress cycle with constant amplitude and fixed average stress, and graphing the number of cycles until the final fracture "N" against the amplitude "σ_a" of the stress applied during the test. The stress is calculated from the loads based on the standard formulas of the material resistance.

Another important term is the fatigue limit S_f. Some materials, under suitable environmental conditions, present an elbow in the S-N curve in the bottom part of the diagram. This elbow represents that below a certain value of the alternating stress, the fracture will not appear because of fatigue, and the amount of cycles that can be made is unlimited. This value is called the "fatigue limit (S_f)" and its existence is characteristic of ferrous materials, such as a Kaplan turbine blade. Finally, another important point in the diagram is the failure limit of steel for static stresses σ_u. Depending on the kind of steel, there will be one or another value.

The S-N curve is often represented in a double logarithmic scale. In Figure 21 below, we can see approximately the S-N curve for steel.

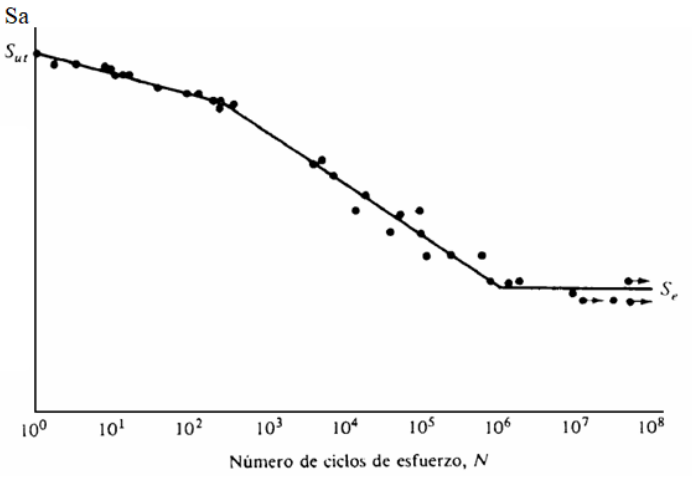

Figure 21: S-N diagram for steel [23]

As we can see in the S-N diagram, there are 2 main zones differentiated in this diagram, the zone of finite duration (approximately, below 10^6 cycles) and the infinite duration zone, with more than 10^6 cycles. Depending on the alternating stress that the critical point of the body is studied, there will be a number of cycles of work or another. The S-N curve is interesting to be studied and applied in the zone of finite life, because it will determine (approximately) the amount of cycles that a body can give in its lifespan.

For our particular case (the study of the phenomena of fatigue in a Kaplan turbine), it's obvious that the S-N curve will not be certainly the previous one represented, as it represents the study of a test tube under a constant external load. However, the S-N curves are usually determined under rotational bending due to their ease of use, and I hope this previous explanation has helped us to understand the concept of fatigue, stresses and amount of cycles. In next chapters we will go deep into fatigue regarding Kaplan turbines.

3.5.5 Crack spread theory

To study and identify the propagation of the crack in a body, we will consider the contribution of theory explained by an experienced university professor to our study. We must say that, as there are many theories of crack spreads, we will consider this one as the professor advised that is more precise for these kinds of bodies (turbines).

Considering an object that suffers external efforts, we will analyse firstly the point that is subjected to higher Von-Mises equivalent strain in all that range of work. It's very likely that this point may be a point that is situated in a place where the geometry of the object changes. Once we have identified that point, we will consider that the crack spreads in that point following 2 rules:

1. The point and its symmetrical are, respectively, the points that are subjected to the highest traction strain (maximum elastic strain) and the highest compression strain (minimum elastic strain). By joining these 2 points with an imaginary line, the crack will spread perpendicularly to that line that links these two points. With this condition we have infinite solutions that are possible, but at least, the initial line of empty (of the crack) is defined. The final direction is defined with the following rule.

2. The point that suffers a higher equivalent Von-Mises strain, if it is in a free surface, will open the crack in a direction following a perpendicular to the surface in that point, because this direction is a perpendicular also to the maximum principal direction of strains (the crack will spread perpendicularly to the main directions of equivalent Von-Mises strains, what makes sense as the strains/stresses will generate an empty space in its maximum point). With this second condition, consequently, the direction of the crack is defined and the theoretical study of a propagation of crack that appears in a free surface can be carried out.

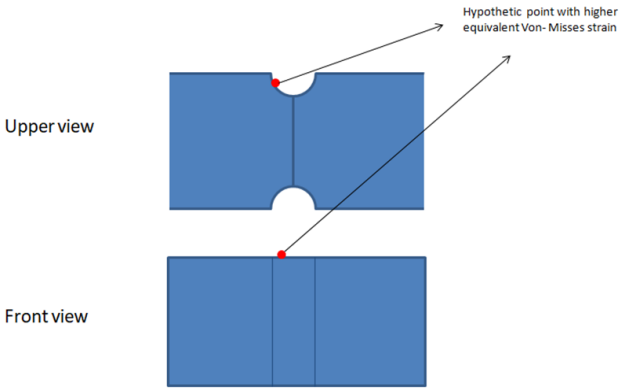

Figure 22 Situation of the point with a higher equivalent Von-Mises Strain

By repeating these 2 rules in an infinitesimal study (opening cracks of tiny length), a study of a propagation of a crack could be done in order to analyse the behaviour of bodies due to the appearance and propagations of cracks on them.

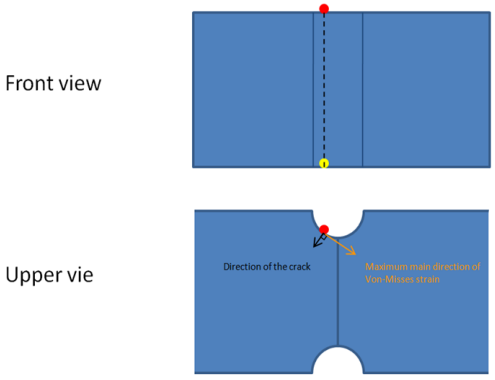

Figure 23: Theoretical direction of the the crack

3.6 Fatigue in Kaplan turbines

In a Kaplan turbine, the blades are the most susceptible part of suffering the effect of fatigue due to the high and variable loads that they suffer. The connection between the blade and the runner is the most susceptible part, as it presents a discontinuity in the geometry and it's frequently the point that suffers more stress and strain. As mentioned earlier in chapter 3.5, the characteristics of fatigue is that this effect usually appears in zones with changes of geometry and that's why in this kind of turbine the large cracks appear in the zone mentioned before [24]. Another possibility (our case study) is that by 'forcing' a discontinuity in the geometry of the blade, the effect of fatigue can be followed in all its phases, and that's what we are going to do, study the effect of the crack in all the phases, from the beginning until the length that will provoke a collapse in the system, the critical length.

The longer the crack, the more vibrates the broken blade and all the structure of the turbine. The more vibrations that happen in the machine, the smaller is the frequency of vibration. Therefore, the main quantitative objective in this project must be to relate numerically the terms 'vibration', 'crack length' and 'natural frequency'.

We will define that the critical length of the crack that appears due to the effect of fatigue is the one that has a size that provokes a critical change in the stiffness in the turbine. As we said in chapter 3.4.3 stiffness is a mechanical property of the bodies that measures the capacity of hardness of them. If the stiffness turns into the half of the original one, the turbine will not work anymore as it used to do, as the mechanical properties would have changed radically. Having set previously the Equation 9, and defining the critical stiffness (k') as the half of the original we have the following two equations:

$$Fn = (1/2\pi)\cdot\sqrt{k/m} \qquad (9)$$

$$k' = k/2 \qquad (10)$$

Combining these two equations we have the following term of the critical natural frequency (Fn') obtained for a critical stiffness and, therefore, due to the effect of a crack with a critical length:

$$Fn' = (1/2\pi)\cdot\sqrt{k/2m} \qquad (11)$$

Knowing the original natural frequency of the turbine, we can establish the critical natural frequency in terms of the original one:

$$Fn' = Fn/\sqrt{2} \qquad (12)$$

Therefore, once we have a $F_n' = 0{,}7071 \cdot F_n$, we will consider that the turbine has a crack that makes the turbine work without efficiency, and at that frequency of work, due to a big crack, provokes an imminent collapse of the system (we would be situated in the zone 3 of the Figure 19).

4. Numerical simulations

In this part of the study we will start with the calculations of the numerical simulations on the simplified turbine we have. For doing so, we will first do a modal analysis, that represents an analysis of the turbine simulated using the air as a fluid of work. We will see the natural frequencies of the simplification of the Kaplan turbine available in the laboratory with simulation software. By studying and identifying the possible initial point of appearance of a crack, we will simulate the spread of this crack, and we will recalculate the frequencies obtained in the Kaplan turbine to see the response of the Kaplan turbine while the cracks spreads. We will use the numerical simulations to have a guide in reality calculations (in the laboratory). Once we have the initial results (natural frequencies of the turbine without crack) we will see four different ranges of work of the turbine. Those are with a length of the crack of 25% of the critical length, 50% of the critical length, 75% of the critical length and finally, the simulation of the turbine with a crack of critical length.

4.1 Presentation of the case study

In this first part of the explanation of the work done it is necessary to introduce the object we are going to simulate. The object is a basic simplification of a Kaplan turbine. The model of turbine is composed of a disk with 6 blades and a shaft. It is very important to note that the geometry of this object has been made for adjusting to the available machine in the laboratory, mainly, in the test rig. The geometry of the turbine created in SolidWorks can be seen below in Figure 24:

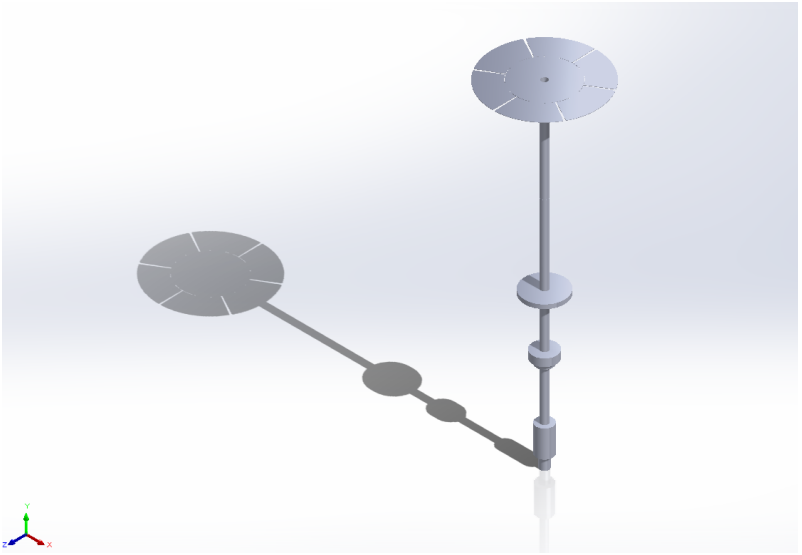

Figure 24: Geometry of the turbine created in SolidWorks

The object is made of stainless steel. The density of the structure is 7750 kg/m³ . The Young's Modulus of the structure is 1,93e+11 Pa, and the Poisson's Ratio equal to 0,31. The boundary conditions are that the shaft will be supported by 2 parts in the test rig. For details of measures of the runner and shaft, attached in the Annex 1 we can see the drawing of the case study, measuring each part of it. Once we have created the Kaplan turbine in SolidWorks, we will import the geometry in Ansys and we will start the simulations of the turbine.

4.2 Modal Analysis

4.2.1 Ansys as a tool of simulation

As we mentioned in chapter 2, one of the objectives of this project was the use and the understanding of numerical solutions softwares like Ansys to extrapolate the simulations into reality. In this case, Ansys will be the software that will analyse the structure by using the finite elements method (FEM).

The FEM is a mathematical method that solves differential equations by linking different parts of a structure with elements and nodes. The amount of nodes and elements will determine the accuracy of the model. The more nodes and elements, the more realistic the simulation will be. However, a huge amount of nodes and elements will make the software take more time to solve the analysis. All the analysis will be carried out with the boundary conditions that will make the analysis even closer to the experiments that will be done after the simulations in the laboratory.

4.2.2 Definition of modal analysis

A modal analysis is the process of determining the inherent dynamic characteristics of a system in forms of natural frequencies, damping factors and mode shapes, and using them to formulate a mathematical model for its dynamic behaviour. The formulated mathematical model is referred to as the modal model of the system and the information for the characteristics are known as its modal data [25].

The most important modal datas are the frequency and the position, because, as we mentioned previously,

knowing these two parameters we can define all the dynamic responses of the structure and, therefore, the different modes of vibration of the turbine. Any vibratory movement can be decomposed in a combination of natural frequencies and associated mode shapes. Modal analysis embraces both theoretical and experimental techniques. The theoretical modal analysis anchors on a physical model of a dynamic system comprising its mass, stiffness and damping properties (mentioned before in chapter 3.4). An example is the wave equation of an uniform vibratory string established from its mass distribution and elasticity properties. The solution of the equation provides the natural frequencies and mode shapes of the string and its forced vibration responses.

4.2.3 Structural modal analysis basics

As we mentioned in chapter 3.4.3, a single element vibrating can be defined by a mass, a damper and a spring. The union of several elements define a structure vibrating. Therefore, every structure can be understood as a superposition of masses, dampers and springs connected between them. The matrix form of the structural equation of a structure subjected to a dynamic load is the following:

$$[\mathrm{M}]\ddot{x}(t) + [C]\dot{x}(t) + [K]x(t) = F(t), \quad where \quad x = \begin{Bmatrix} x_1 \\ x_2 \\ \vdots \\ x_n \end{Bmatrix} \tag{13}$$

As we can see, Equation 13 is the same equation as Equation 8, but in a matrix form. The terms $\ddot{x}(t)$, $\dot{x}(t)$ and $x(t)$ are, respectively, the acceleration, velocity and displacement in the n points or degrees of freedom (DOF) in the time domain. [M], [C], and [K] are, respectively, the matrices of mass, damping and stiffness. They represent the interconnection between the different DOFs of the structure. F(t) is a vector that expresses the force applied on each DOF in the time domain.

The most important parameter of a modal analysis is the natural frequency, because, with it, the vibration, strain, stress and the displacement of a structure can be found and represented with its shape in resonance conditions. From Figure 16 we can see that the displacement x(t) of a degree of freedom follows a sinusoidal shape. Consequently, we can define the displacement of one DOF as the Equation 14 below:

$$x(t) = A \cdot Sin(wt + \theta) \tag{14}$$

Where w is the natural frequency, and θ is the initial phase. For having the acceleration and velocity of a DOF we just need to derive the displacement. In a modal analysis, frequently the damping and the external force are negligible, and, therefore, can be removed from the equation. Finally, combining Equation 13 and the derivations of Equation 14 we obtain the following Equation 15, and it is the way that Ansys has to calculate the natural frequencies and everything that is involved on them:

$$-[w]^2 \cdot x(t) \cdot [M] + [K] \cdot x(t) = 0 \tag{15}$$

For this previous equation there exists only one solution, as the displacement is multiplied by something in the two terms of the equation and it can not be zero, the only solution is that :

$$-[w]^2 \cdot [M] \cdot + [K] = 0 \tag{16}$$

The solutions of this system are the natural frequencies w, and they represent the eigenvalues in this matrix system. We also know that every eigenvalue has an eigenvector associated. The eigenvectors, in this case, are the vibration modes. This last fact makes sense with everything described previously, because, as we said, there just exists one vibration mode for every natural frequency of the structure.

In this last equation, we can see that we have an amount of natural frequencies equal to the amount of degrees of freedom in the structure. In the solutions, Ansys will show us those frequencies that are more relevant for the structure, and we will define previously the amount of natural frequencies that we want to know and study.

4.2.4 Simplification of the case study

In the first part of the numerical simulation, a possible simplification of the case is proposed by the department of Fluid Mechanics. As all the object (shaft+blades) is very big to mesh and simulate, and as the expected result is to see failure due to fatigue in the impeller or its blades, we proceed to study a kind of simulation in order to be more precise with the expected results that we thought we will achieve in the disk with theoretical arguments seen in chapter 3.3.

For doing so, we consider 3 possible scenarios to study. In case that the original model (shaft+disk+blades) gives similar results to the simplifications, we will consider to study just a specific part of all the object:

- **Model A**: The first model represents all the entire structure. It is the original model that we will simulate and analyse in the laboratory, composed, as we said before, of a shaft, a disk and 6 blades. It is the entire simplified model of a Kaplan turbine.

- **Model B**: The second model represents just the disk and its blades without the shaft, with the main characteristic that there is a fixed part that represents the union between the shaft and the disk. This fixed surface is the upper surface of the disk that links with the shaft.

- **Model C**: The third model represents just the disk and its blades without the shaft, with the main characteristic that there is a fixed part that represents the union between the shaft and the disk. This time, the fixed surface is the inner diameter of the disk that joins the shaft.

All these 3 models can be represented in the Figure 25 below:

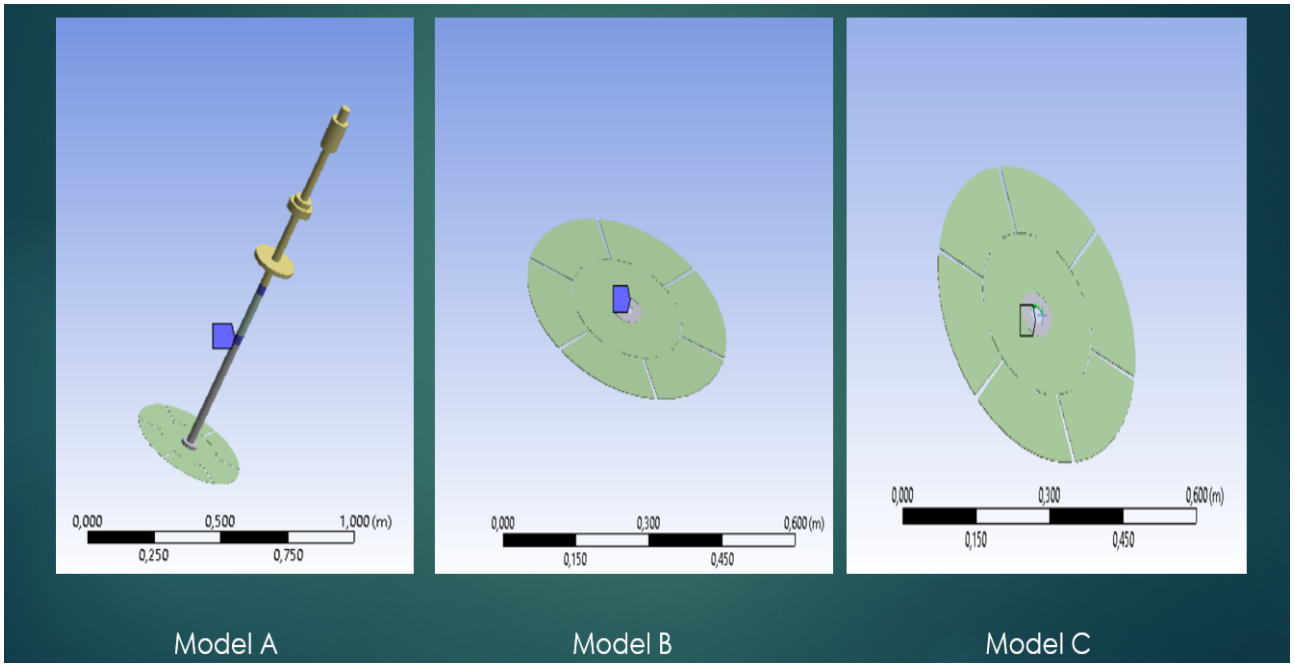

Figure 25: Three different models to analyse to simplify the case

For analyzing these 3 models, we will compare the natural frequencies of the disk and blades, and if there is a small difference between the different frequencies in the disk in every single natural frequency, we will consider a good simplification of the case the model B or C. For doing this analysis, we start a meshing using the minimal mesh that allows all the three models to converge in a result. We will define previously in Ansys the boundary conditions mentioned above. We will also set a number of 10 natural frequencies bigger than 0 to study (the most relevant excluding the DOF of the own structure) and we will start defining a mesh of 5 mm of element size (it is actually the first size number where the 3 models converge in a result). Once the simulation has been completed in all the 3 cases, we proceed to compare the different results obtained.

In Table 1 below we can see the natural frequencies obtained for the simulation with the conditions explained before:

Fn(Hz)	Model A	Model B	Model C
Fn1	21,246	29,966	22,763
Fn2	21,249	29,967	22,787
Fn3	28,873	31,321	27,394
Fn4	28,876	32,209	28,347
Fn5	31,248	32,21	28,349
Fn6	32,105	37,804	37,46
Fn7	32,11	56,304	55,394
Fn8	37,794	61,994	60,605
Fn9	51,805	62,002	60,613
Fn10	51,813	71,212	69,881

Table 1: Natural frequencies obtained in the first simulation

As we can see, we obtained 10 natural frequencies (in Hertz) for every model. In the model A, of those 10 frequencies, four of them (Fn 1, Fn 2,Fn 9, and Fn 10) were natural frequencies of all the structure (disk+shaft), meanwhile, the other six were of the disk. That is why it is highlighted in green. The green frequencies of the three models correspond to the frequencies of the own disk, and those are the frequencies we have to study and compare to see if a simplification can be done in future simulations. In Table 2 below, a comparison between the three models is represented:

Modo de Vibración	Fn Modelo A	Fn Modelo B	Fn modelo C	Diferencia % modelos A-B	Diferencia % modelos A-C
1	28,873	29,966	22,763	3,79%	21,16%
2	28,876	29,967	22,787	3,78%	21,09%
3	31,248	31,321	27,394	0,23%	12,33%
4	32,105	32,209	28,347	0,32%	11,71%
5	32,11	32,21	28,349	0,31%	11,71%
6	37,794	37,804	37,46	0,03%	0,88%
Promedio de diferencias				0,77%	7,17%

Table 2: Comparison of the natural frequencies of the 3 models

Seeing the previous table, we proceed to compare the differences between the different Fn of the disk versus the entire turbine. For doing so, we compare two by two the models B and C with respect to the model A. The average relative differences seen in the frequencies between models A and B are 0,77%, less than 1%, which is an astonishing similarity. Meanwhile, the average difference between models A and C is 7,17%, which is very high for doing a simplification.

Therefore, with this first study, we can **conclude** that for being more precise and to approach ourselves more to the reality of the failures in the disks of a kind of Kaplan turbine, we will proceed hereinafter to simulate in every simulation a simplified model B, which is composed just of the disk with its blades, in where the disk is fixed in it's upper face where there is the connection with the shaft.

4.2.5 Mesh analysis

Once we know that the **model B** previously mentioned is the one we are going to simulate, we proceed firstly to do a mesh analysis in order to be even more precise and effective with the solutions and with the time simulations. For doing the mesh analysis, we will do the same simulations on the disk increasing the amount of elements on it. It's obvious that the more elements in the body, the more time Ansys will take to show the results. We will have to set a balance between time calculation vs precision in the results, and the most balanced mesh will be the selected for continue our study

Firstly, we start measuring the first six natural frequencies in the disk, as they are the most destructives, with an element uniform size of 0,5cm, as we did in the previous analysis. Naturally, the natural frequencies obtained must be the same obtained before. By reducing the element size and exporting the results of the natural frequencies, we can see the Table 3 below:

Element Lenght (m)	Fn1	Fn2	Fn3	Fn4	Fn5	Fn6	Solution_time [s]
0,005	29,966	29,967	31,321	32,209	32,21	37,804	26
0,003	29,944	29,948	31,305	32,19	32,193	37,793	41
0,0025	29,938	29,94	31,299	32,184	32,187	37,789	74
0,002	29,925	29,926	31,288	32,171	32,173	37,776	96
0,001	29,879	29,88	31,252	32,125	32,126	37,733	960

Table 3: Element Size vs Natural frequencies obtained in the disk

As we can see, this table shows what is obvious, the smaller the size of the element, the more time the Ansys has to calculate to give a solution. The last simulation took more than 900 seconds (15 minutes). In this study of different element sizes, there are not huge differences between the simulation results, but in future calculations, a refinement in the zone of the crack will be done, and it will imply more time of simulation just because that refinement of the mesh near the crack produced by the fatigue effect. This is why the solution time shows as an important character, basically the most important one, having seen the low difference between all these results obtained in the mesh analysis. All these previous natural frequencies obtained from the table 3 can be represented in Figure 26 below:

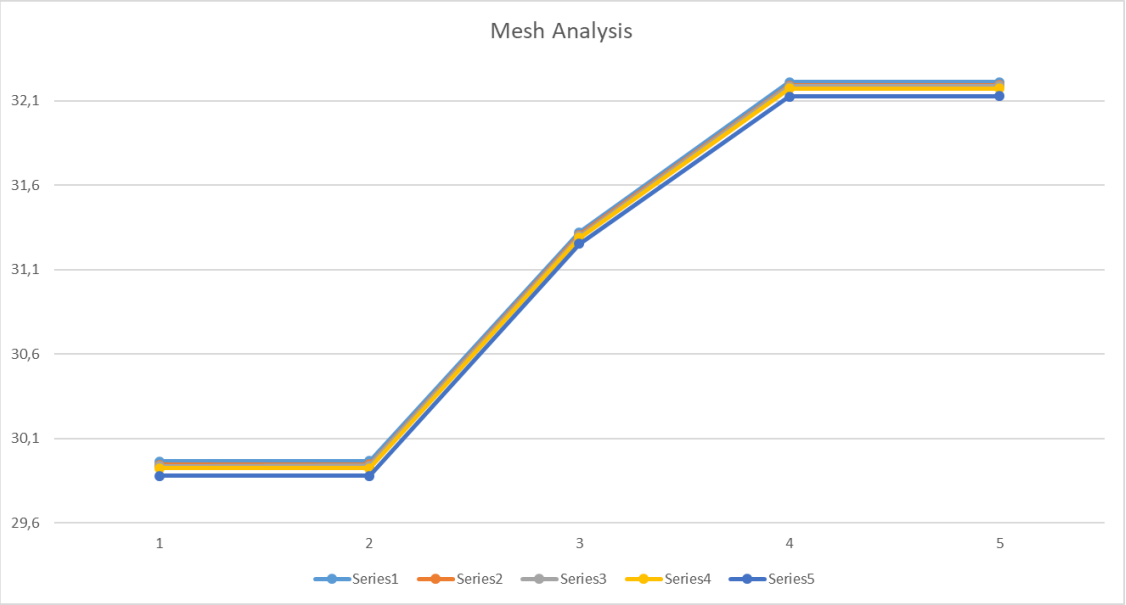

Figure 26: Curves of the natural frequencies depending on the series of simulation (element size)

As we can see in Figure 26, there are five curves that represent the five series of the natural frequencies obtained for each different element size mesh. It's seen that the last one (the Series5, that represents the natural frequencies obtained for an element size of 1mm) is a little bit far from the rest of the series. The rest of the curves are practically overlapped. This means that for the first 4 simulations of different element sizes the results are practically the same. Now we have to proceed to see the differences between 2 consecutives element sizing to see the increment of different parameters (basically, F_n and the simulation time) between two consecutives simulations. Once we have a small difference of results between different meshes with a small increase in the time calculation, we will decide the ideal element size for our mesh on the disk for future simulations. In Table 4 below, we can see this calculations made:

	Fn1	Fn2	Fn3	Fn4	Fn5	Fn6	Average of differencies
Δ Dif mesh 1-2	0,07%	0,06%	0,05%	0,06%	0,05%	0,03%	0,05%
Δ Dif mesh 2-3	0,02%	0,03%	0,02%	0,02%	0,02%	0,01%	0,02%
Δ Dif mesh 3-4	0,04%	0,05%	0,04%	0,04%	0,04%	0,03%	0,04%
Δ Dif mesh 4-5	0,15%	0,15%	0,12%	0,14%	0,15%	0,11%	0,14%

Table 4: Difference between different consecutives meshes

In Table 4 we can see what we mentioned before. The average difference between the first and second kind of mesh is 0,05%. The average difference between the meshes 2 and 3 is more than half, as it is 0,02%. Therefore, we can conclude from this study that from the element size of 5mm to a smaller one we must obtain a result that is very close to reality. As the results are very similar, we must now check the parameter of time of simulation. The simulation time with the element size of 5mm takes just 26 seconds, and the following (the mesh with element sizes of 3mm) takes just 15 seconds more, and this is the reason why the element size selected is 3mm for obtaining the natural frequencies of the structure without cracks on it in a reasonable time of simulation (less than a minute).

Reducing even more the mesh to 2,5 mm would not contribute too much to our study, as the simulation time increases more than 30 seconds to see practically the same results. Finally, in Figure 27 below we can see the disk and its blades meshed with an **element size of 3mm**, the one we will use to obtain and determine the definitive natural frequencies of the disk.

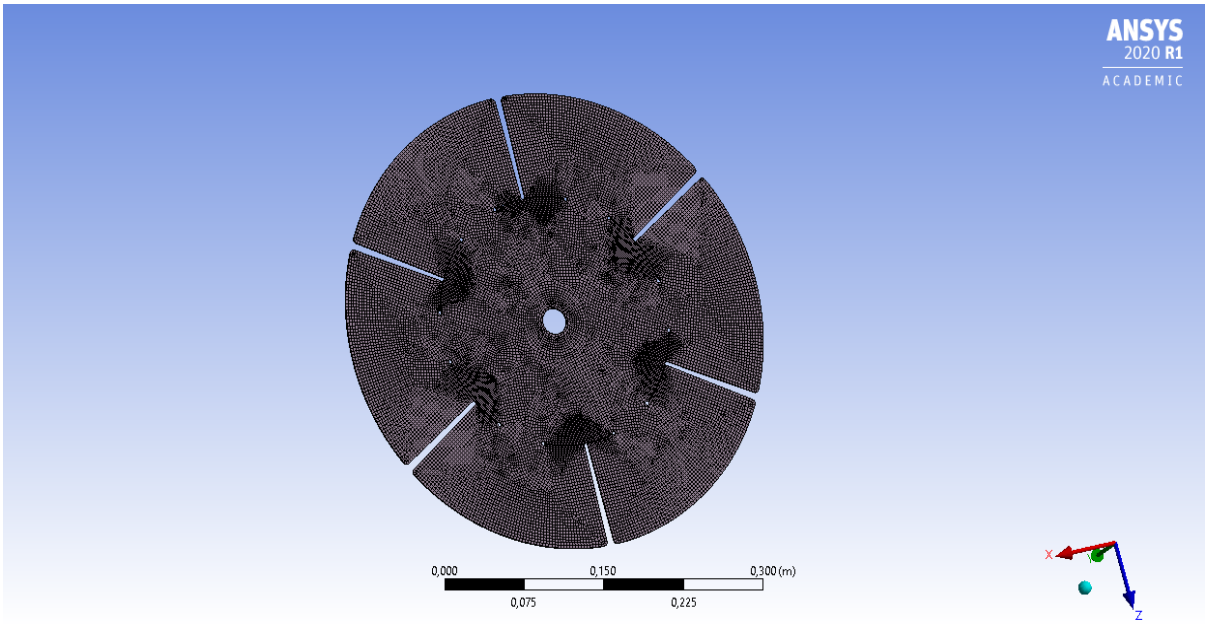

Figure 27: Disk with the mesh of 3 mm selected

However, although we have set an average element size of 3mm in the disk in this chapter, in future simulations it will be very likely to make a refinement of the mesh in other zones of the disk like the holes or cracks, as they are more important to analyze and see a more precise result on them, in order to understand the behaviour of the disk under the effect of fatigue and to see the direction of the expansion of the crack.

4.2.6 Initial conditions for the study of the propagation of the crack

Once we have the initial conditions for simulating the disk (to obtain the natural frequencies and its corresponding vibration modes), we have now to proceed to investigate two main things. Firstly, where will be the place where the crack may appear, and secondly, the initial direction of this spread. Starting with the first simulation with the mesh conditions explained before, we focus our attention on the points of every vibration mode that suffers a bigger strain.

Of all the possible vibration modes of the disk, we will study the first 3 deeply, as the low frequency values are

the most dangerous for the integrity of the structure. Effectively, when simulating, we can see that the biggest strains (and therefore, stresses) are suffered in the first 3 vibration modes. Those are called 1ND (nodal diameter) and 0NC (nodal cercle). For the 1ND vibration mode, it's called like that because the displacement forms an unique line of low displacements values (the nodal line) passing through the axis of the diameter (1ND). Regarding the 0NC mode shape, we can see a shape of displacements centrated in the axis and displacing with respect to its center. As there is always a symmetric form for the 'X'ND, being X integer numbers, the first 2 vibration modes are symmetrics, and they are the 1ND and its perpendicular. The third mode shape found was the 0NC. Below in Figure 28 we can see the movement of the disk with respect to its initial position in the first six vibration modes, and in its maximum displacement point. There are two 1ND modes that are symmetrical, one 0NC, two 2ND, that are also symmetrical, and one 3ND.

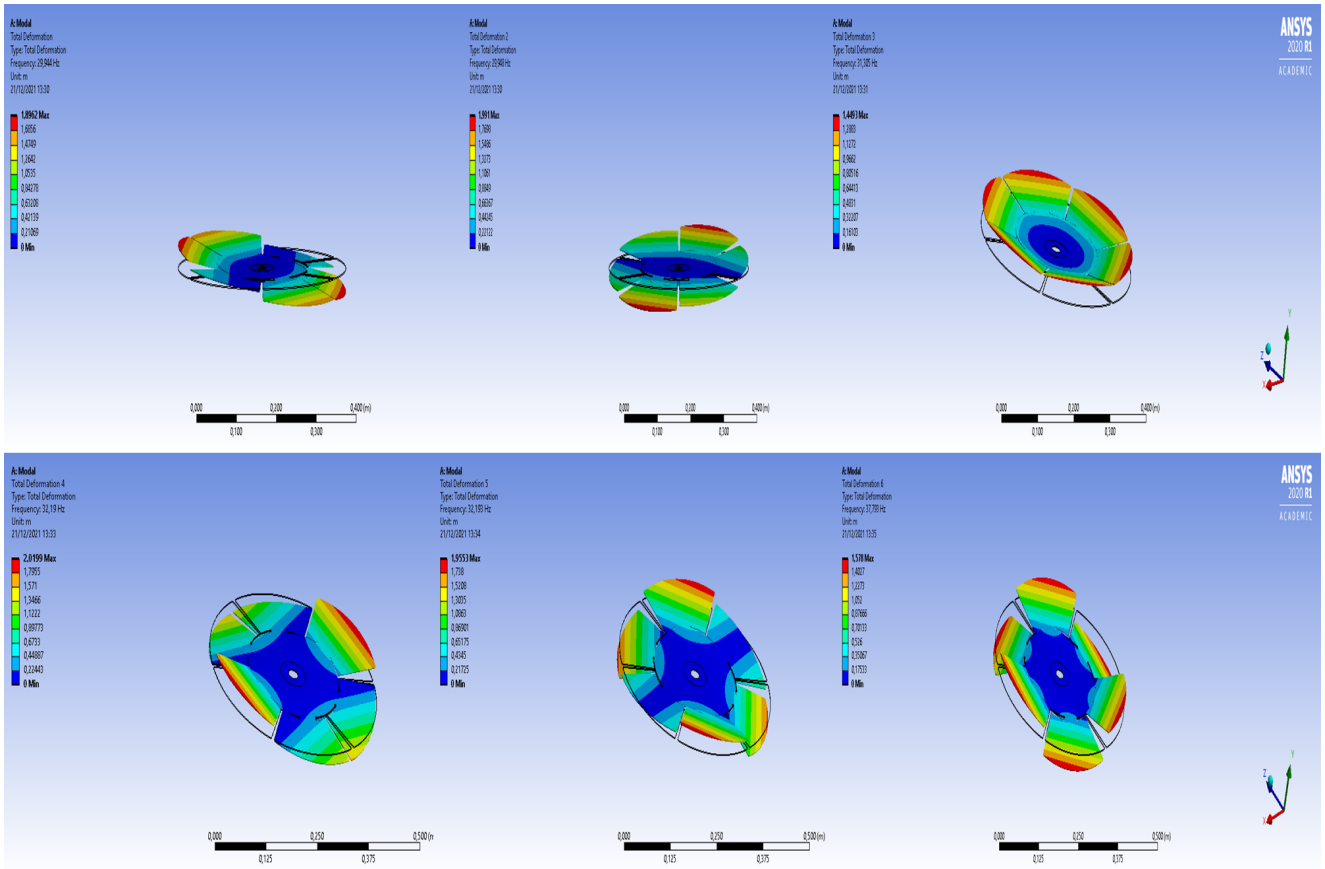

Figure 28: Deformation of the disk depending on the vibration mode

The deformation modes that Ansys offers as a result are a good method to understand how the structure will move or displace. However, numerically, it does not contribute at all as the results do not represent any value. Figure 28 given is just a frame of many videos that ansys shows in order to understand how the structure displace itself depending on the natural frequency that excites the body, having in dark blue the nodal lines, that are lines with displacement practically 0.

For having an idea about the point of the appearance of the crack, we have to study the point of the disk that suffers a bigger equivalent Von-Mises strain, and, from there, we will have to analyze the vectors of the principal direction of strains in that point, as we explained in the chapter 3.5.5.

First, as the first simulation is the most important one as it will determine the origin of the crack, an additional mesh refinement is done in the zone of the holes, as they are supposed to be the places where the crack will appear (because, as we see in the theory of fatigue effect, these are the points that changes the constant geometry in the disk). The new mesh refined can be seen in Figure 29 below:

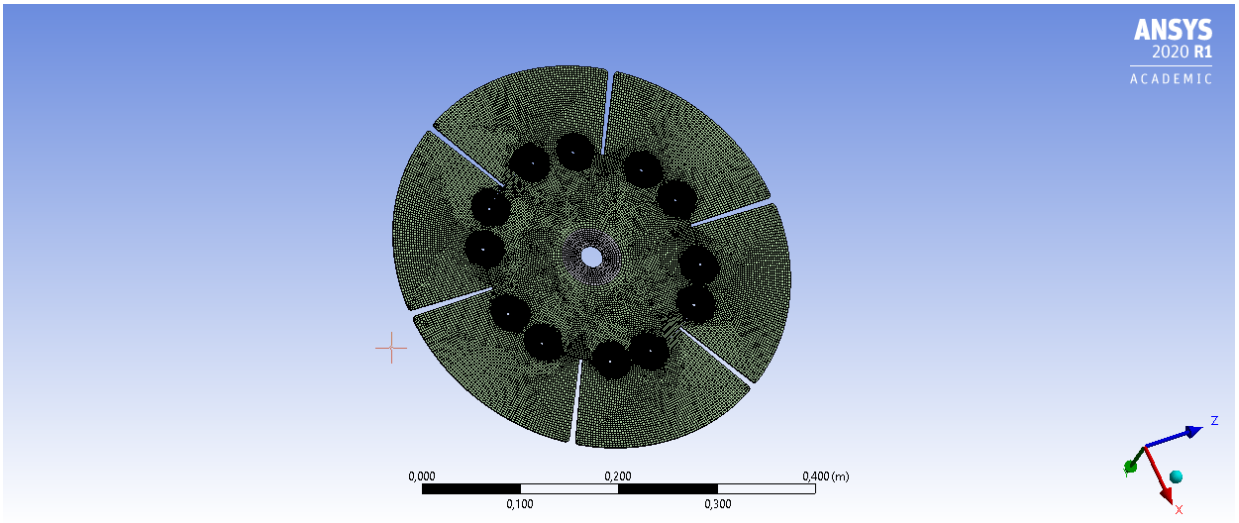

Figure 29: Additional mesh refinement in the holes

By executing a deformation and a strain analysis in Ansys, and waiting 30 minutes for this simulation we get the following results:

Result	Natural Frequency [Hz]	Mode Shape
Fn_1	29,897	1ND
Fn_2	29,897	1ND
Fn_3	31,265	0NC
Fn_4	32,139	2ND
Fn_5	32,139	2ND
Fn_6	37,73	3ND

Table 5: Results of the simulation after the refinement of the zone of the holes

As we can see, the natural frequencies obtained are not much different than those obtained in the previous results of Table 2 with a poorer mesh. This simulation was done mainly because of the need to identify the initial point where the crack may appear. In the strain results, we can see effectively the maximum equivalent strain is in the zone of one hole of the disk for the first natural frequency, concretely (by situating the axis properly to see it) it is in the blade that is situated more far for the nodal line, and in it's smaller cut of geometry, as we can see in the Figure 30:

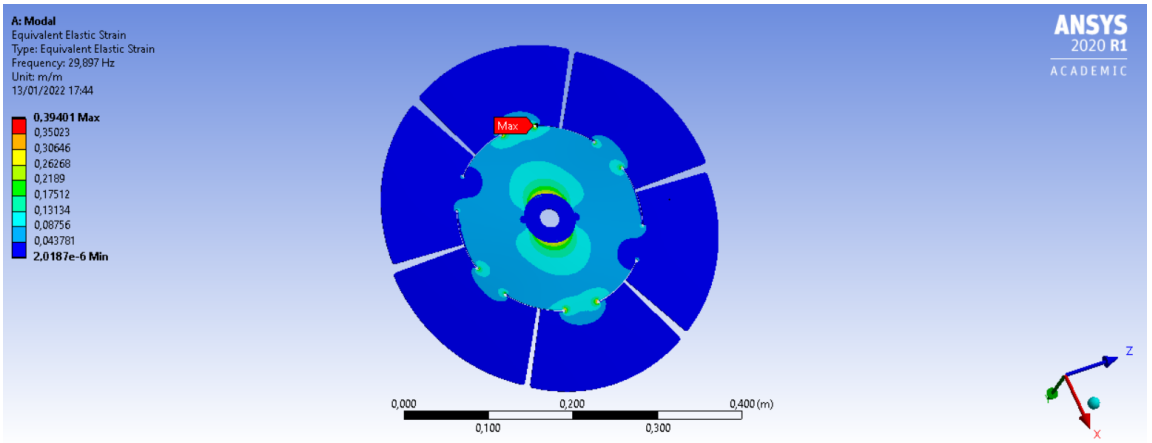

Figure 30: Maximum equivalent elastic strain (Von-Mises strain) in the disk

Figure 30 shows the results of the first strain analysis for the first natural frequency. As we can see below in Figure 31, the maximum equivalent strain is located in one of the holes of the blades. Concretely, if we consider the blades moving in the direction of clockwise, and being the first blade in the 12.00, the hole that apparently will suffer the crack is the first hole of the 1st blade (the short-cutted one). The maximum strain that the disk will suffer if it moves at this frequency is 0,394 m/m and it will be suffered in the beginning of the movement. The maximum displacement will be in the edge of the fourth blade while the turbine vibrates at 29,897 Hz.

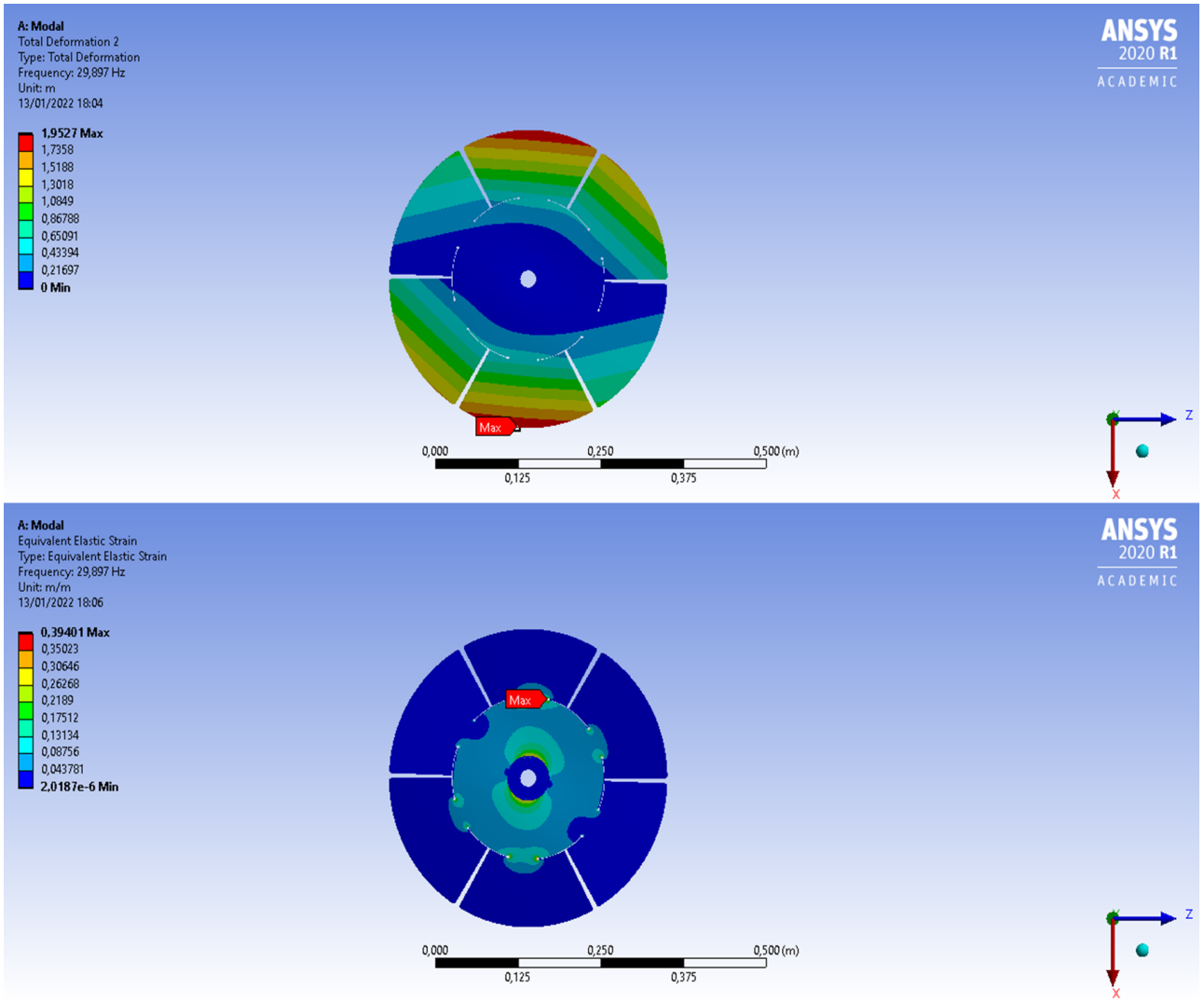

Figure 31: Comparison between deformation analysis and strain analysis

This last comparison of Figure 31, actually, will be very important, because from this situation of the nodal line and the hole of maximum equivalent strain, we will obtain the exact blade of the reality (the blade we will simulate and where we will force a crack in the laboratory) that will collapse due to the effect of fatigue. We will continue this explanation in chapter 5, the enlargement of the project.

For now on, therefore, we will analyse the first natural frequency in every simulation for the crack spread, as we will consider that the fracture of the disk may appear due to the vibration provoked by the first natural frequency in the turbine.

By zooming in the zone of the maximum equivalent strain, the zone shows the distribution of strains studied. As we can see in Figure 32 below, the maximum equivalent elastic strain (Von-Mises) is in the edge of the geometry in a change of section, coinciding with the theory explained about fatigue effect in chapter 3.5.5.

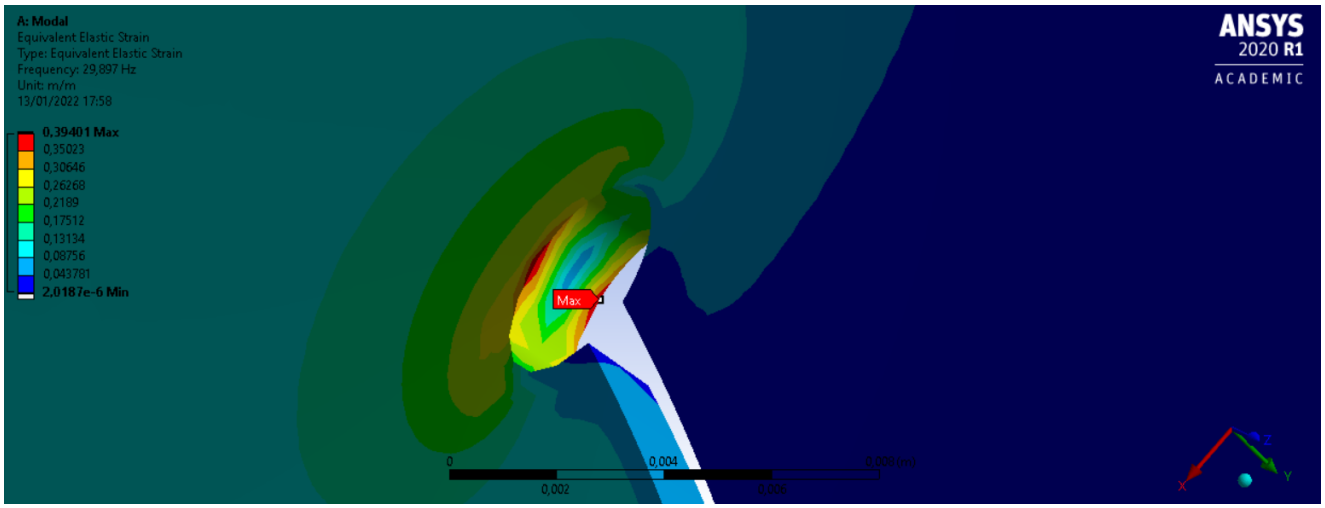

Figure 32: Zoom in the zone of the hole that will suffer the crack

If we analyse this point, the theoretical maximum principal strain should be here, and watching this position, it should coincide with the point with maximum strain working in traction. Therefore, symmetrically in the other face, near this point, there should be the point that is working in maximum compression. Effectively, watching Figure 33 below, the theory explained coincides with the results given by Ansys. The maximum principal elastic strain point works in traction mode with a maximum strain of 0,39 m/m. The minimum principal elastic strain point works compressing the point al -0,39 m/m:

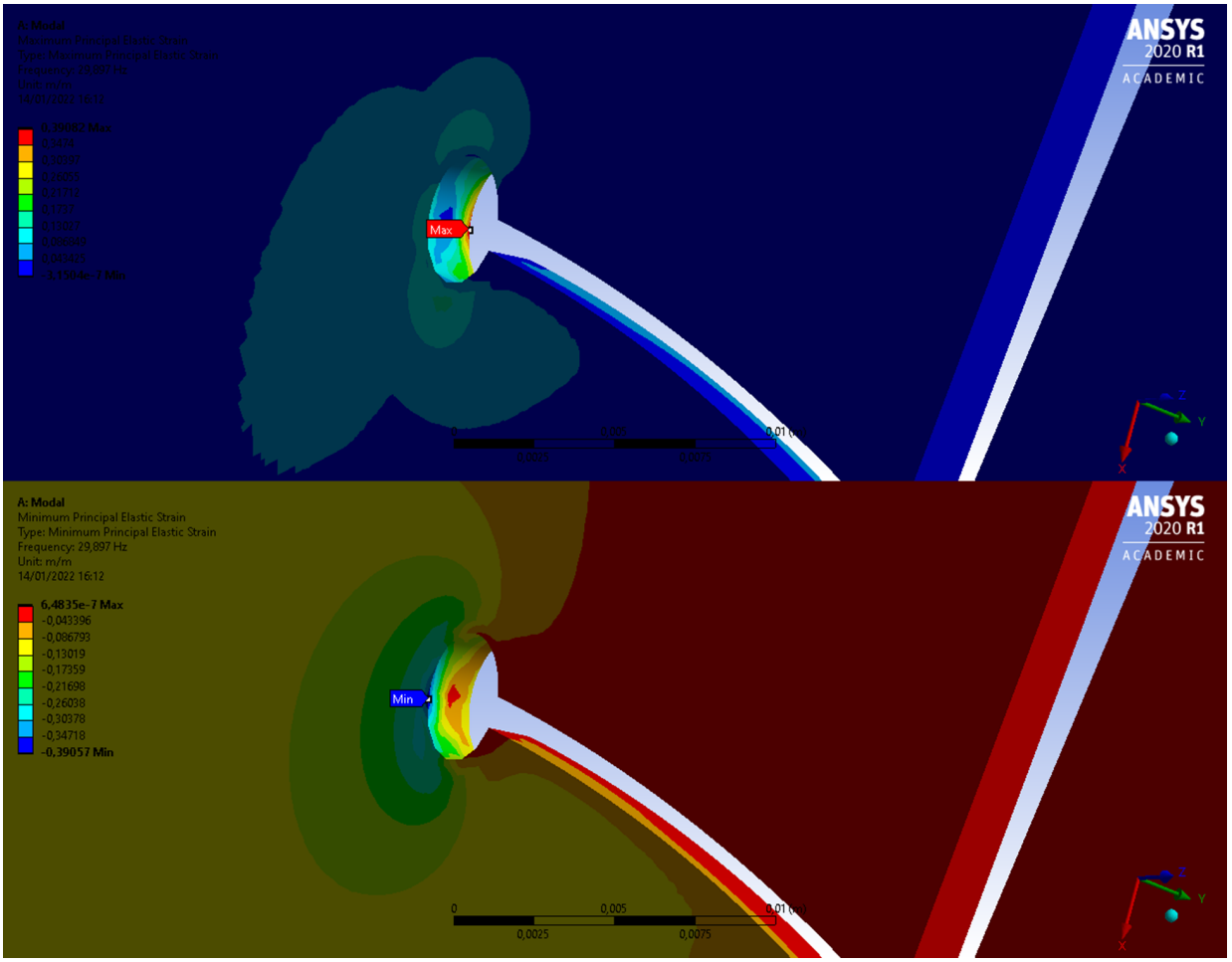

Figure 33: Points with maximum and minimum principal elastic strain

Therefore, once we have obtained these two points, the crack should be perpendicular to the line that links these points. As we mentioned in chapter 3.5.5, the direction of the crack will be set by the second rule explained. The length of the first crack (the second simulation we will do) will be set in 0,5 mm, as it is important to know exactly the distribution of strains in the beginning of the appearance of the crack and its direction. Other future microcracks, depending on the results obtained, will have a length of a maximum of 4mm, but we will try to approximate it to reality and not create too many cracks bigger than 2,5 mm, at least in the firsts simulations.

For creating a new microcrack it's necessary to identify the point where the crack will spread from this simulation. We can identify it in Ansys by selecting the exact coordinate of the point (node), and then, we will identify that point in the drawing of the Solidworks, and by creating a new sketch and extrapolating the 2 rules mentioned in chapter 3.5.5 to the software SolidWorks we will create the new micro cracks one after another.

Nevertheless, before starting doing microcracks, it's important to know until what point we will consider that the crack will be long enough in order to make the blade collapse. As we explained in Equations 9, 10, 11 and 12, the critical frequency of the turbine is Fn'=0,7071·Fn. Therefore, in our case, Fn'=0,7071·29,944 = 21,17Hz.

Consequently, the behaviour of the turbine when a crack appears will not be analyzed by the length of the crack, but by the vibration (natural frequency) change of the turbine. Consequently, we expect to see a relation between the vibration of the turbine and the length of the crack that appears due to fatigue. Actually, if the crack can be simulated properly and the directions of the crack are accurate in every microcrack created, we should see a graph representing the vibrations of the turbine versus the length of the crack similar to the one explained in Figure 18, watching a reduction of the residual resistance of the turbine while the crack spreads.

Moreover, as this project is expected to be an extense project, it is interesting for us to analyse the behaviour of the turbine in different points with the appearance of the crack. To be more concrete, we will study the performance of the turbine when having cracks with length of 25% of the critical length, 50% of the critical length, 75% of the critical length and the turbine performance (if it is possible and has not collapsed before) when having a crack with critical length. We will study the displacements of the blades, strains of different important points, and the vibrations modes of the simplified turbine, and we will see how the frequency decreases while the crack spreads. Finally, we will try to relate these variations of the frequency in the turbine with the effect of fatigue on it.

For identifying the points mentioned before, we will consider a linear regression analysis in order to identify the critical points to study. Knowing the first natural frequency in the beginning and the frequency of critical length, we only need to create a regression line and identify the frequencies. In Equation 17 below, we can see the linear regression to analyze the frequency variation.

$$F_n = a \cdot L_{crack} + b \qquad (17)$$

Where L_{Crack} is measured in %, and F_n in Hz. Knowing also that in the initial situation, there is no crack (L_{Crack}=0%) for a Fn=29.944, and that the crack has its maximum length (L_{Crack} =100%) when the natural frequency is the critical mentioned before, Fn=21.17 Hz, we can set and create a regression line to identify the intermediate points. Below in Figure 34 we can see the theoretical evolution of the first natural frequency of the turbine while the crack spreads. We must highlight that the variation of frequencies are not expected to be linear with the variation of length of the crack, (for instance, we don't expect to see that for every increment of a determined length of the crack the decrement of frequencies is constant and linear). Theoretically, as we said, the evolution of frequencies should be similar to Figure 18.

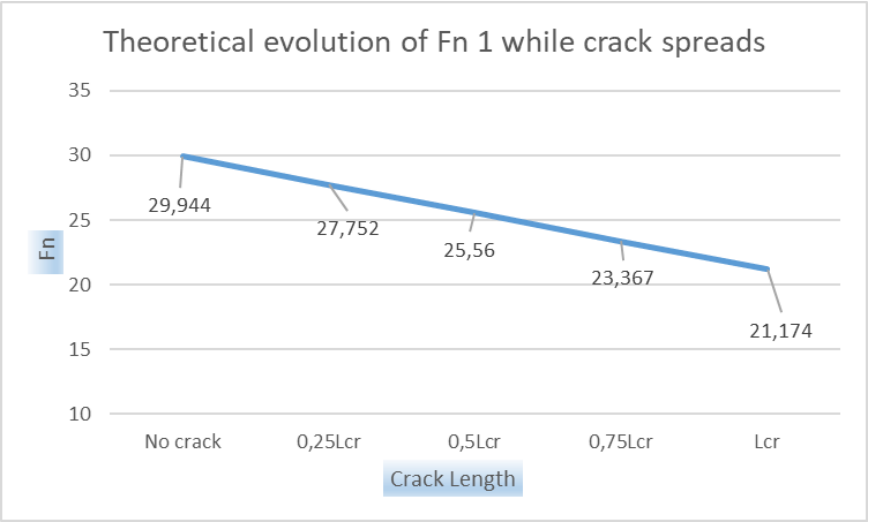

Figure 34: Evolution of Fn1 while crack spreads

4.2.7 Numerical study of the propagation of the crack

4.2.7.1 First Simulations and crack appearance

Once we have identified the four points where we will focus our attention and study in detail, we proceed now to create in our model a sufficient amount of microcracks to study the behaviour of the turbine while the crack spreads. Once we have studied the initial condition (turbine without crack), explained in the previous chapter, we proceed now to open in SolidWorks the first microcrack. Every single crack we will create will have a thickness equal to the thickness of the disk (1,5 mm) and the length will depend on the simulation we will be doing, but it will not be longer than 4 mm in any case.

For this first microcrack created, the main characteristic is that the length of the crack will be 0,5 mm, as it is important to know well the behaviour of the crack in the first instants when a microcrack appears. Figure 35 shows the sketch created in SolidWorks, that will be the model we will use to import to Ansys and to do the following simulation and identify the new microcrack that will appear:

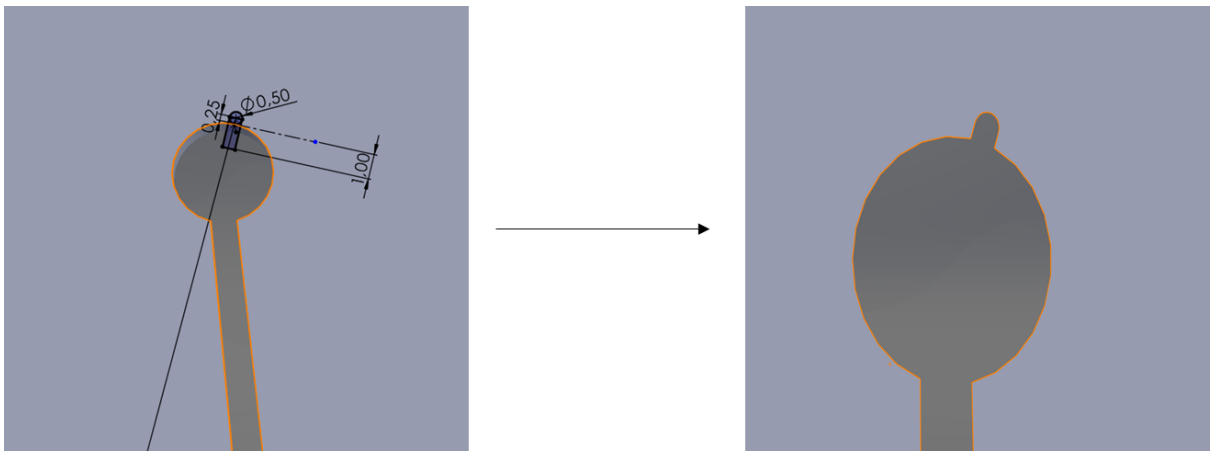

Figure 35: Sketch of the first crack that appeared in the model

By importing the sketch to Ansys, and doing a second simulation in the turbine (with the first crack on it), we proceed to analyse the results of displacement, strains and vibrations. Firstly, we create a mesh similar to the previous one, with an element length of 3 mm. Moreover, an additional refinement will be done in the zone of the crack, as it is important to focus our attention on the point and to identify clearly what is happening in every

point of the edge of the crack. We select a triple refinement, the maximum permitted. We can see the refinement of the mesh in the zone of the crack in Figure 36 on this next page.

Once we have set all the parameters in Ansys (material assignment, proper meshing, boundary conditions, solution settings…), as we did in the previous simulation, we proceed to simulate the turbine and do a new displacement and strain analysis. To comment briefly on the results, the analysis of displacement did not variate at all with respect to the previous simulation. Nevertheless, the appearance of a new microcrack changed the strain distribution, as in the first simulation the maximum equivalent elastic strain was in the hole, and now it is located in the microcrack.

As we explained before, for creating a new microcrack, it's important to identify the new point with a higher equivalent elastic strain. Effectively, after doing a new modal analysis, we can check that the new point with a higher Von-Mises strain is a point in the crack created. We can see this distribution of strains in the zone of the microcrack and the mesh in the Figure 36 below:

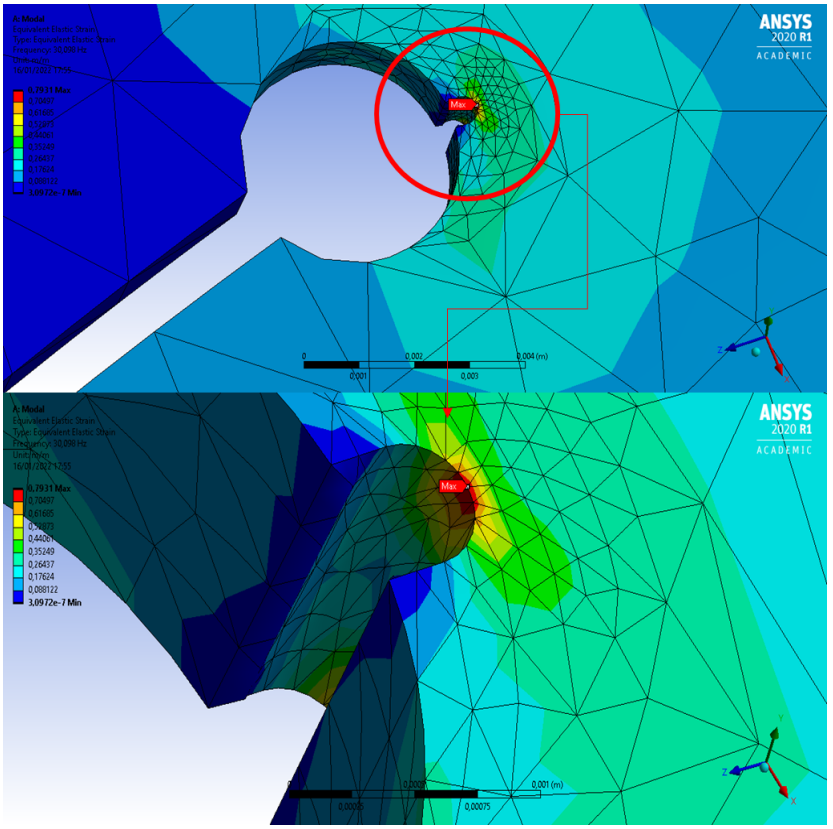

Figure 36: Strain analysis with the first micro-crack in the turbine

Once we have obtained the node with higher Von-Mises strain, we can proceed again to apply the 2 rules mentioned in chapter 3.5.5 and open the second crack in our model. By doing this simulation after simulation, we should be able to obtain a crack approximate to a real one that could appear. We will now focus the explanations and figures of the simulations on the four critical points mentioned before, and in the path followed in order to arrive at the critical point obtained.

4.2.7.2 Crack length equal to 25% of the critical length

The objective after the first two simulations was to try to reach, as we said, a real crack that follows fatigue effect principles and try to measure its contribution to the turbine vibration. The first critical point, therefore, was a point where the stiffness of the turbine worsened enough to reduce the natural frequency of the turbine by 25% with respect to the critical natural frequency. Therefore, and as we showed in Figure 34, for having a crack of length equal to the 25% of the critical length, the frequency should have reduced its value up to 27,75 Hz.

The first 3 cracks created had a length of, respectively, ⅓ of the thickness, ⅔ of the thickness and the thirdone a length equal to the thickness of the disk (1,5 mm). After these 3 simulations, the natural frequency of the first mode shape did not vary at all (actually, it increased a very low value, but we will consider it as the same result, just because the mesh is not the same for every simulation, as the total surface of the turbine changes simulation after simulation). Below in Figure 37 we can see the results for the simulation with 3 cracks, with a crack with a total length of 3 mm:

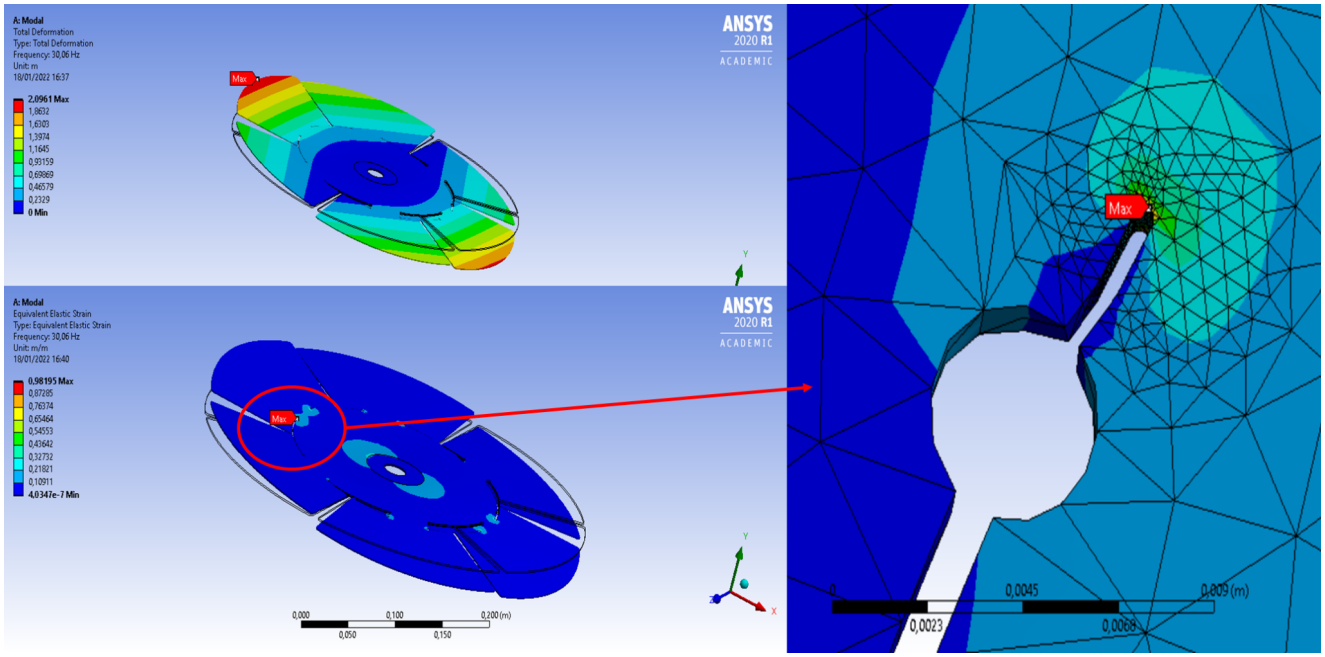

Figure 37: Solution of strain and displacements of the disk after a 3 mm crack

The first three natural frequencies obtained for this simulation were 30,06 Hz (1ND), 30,116 Hz (1ND) and 31,424 Hz (0NC). As we can see, the difference of frequencies with respect to the previous simulation are negligible, as that small change can be even caused because of the mesh distribution. Nevertheless, we can see something now that did not happen before. While the crack spreads, for the first natural frequency (considering that frequency as the one that creates the crack while the turbine vibrates), the damaged blade with the micro crack is the one that has the biggest deformation (one point in the edge of the blade). This means that the blade in which the crack appears will be the blade that will displace more with respect to the central point and, therefore, will finally break due to the effect of fatigue. This last observation is obvious, but this behaviour has been seen after 3 microcracks, and was not seen in the firsts simulations.

After these firsts three different simulations, the following ones were similar until the achievement of the crack with a length enough to make the turbine vibrate at 27,75 Hz. Some of them have one determined length, and some others had another length, but this length was never bigger than 2,5mm. After 20 simulations (therefore, 19 microcracks created in the turbine), the results obtained were the ones we will comment on now.

As we see in Table 6 below, 20 simulations were needed in order to see a change in the frequency of approximately 2 Hz, it's quite a lot. The variation of frequencies microcrack after microcrack, therefore was being reduced 0,1 Hz after 0,1Hz (approximately). The total length of the crack after these 20 simulations was of 3,3 cm (33 mm). This means that the average length of the crack created was of 1,65 mm. We must highlight for the understanding of the reader that the natural frequency achieved in this 20th simulation was 27,93 Hz and the following one (21st simulation) was 27,50 Hz, and this is the reason why we stopped here, as it is right the previous point before achieving a crack of length equal to the 25% of the critical length.

Crack Number	Lcrack [mm]	Fn1 [Hz]
0	0	29,98
1	0,5	30,09
2	1,5	30,08
3	3	30,06
4	4,5	29,94
5	6	29,92
6	7,5	29,86
7	9	29,81
8	11	29,73
9	12	29,69
10	13,5	29,61
11	15	29,54
12	17	29,42
13	19	29,3
14	21,5	29,13
15	25	28,85
16	26,5	28,71
17	30	28,28
18	31	28,2
19	33	27,93

Table 6: Evolution of the first natural frequency with the spread of the crack. 0-25%Lcrit

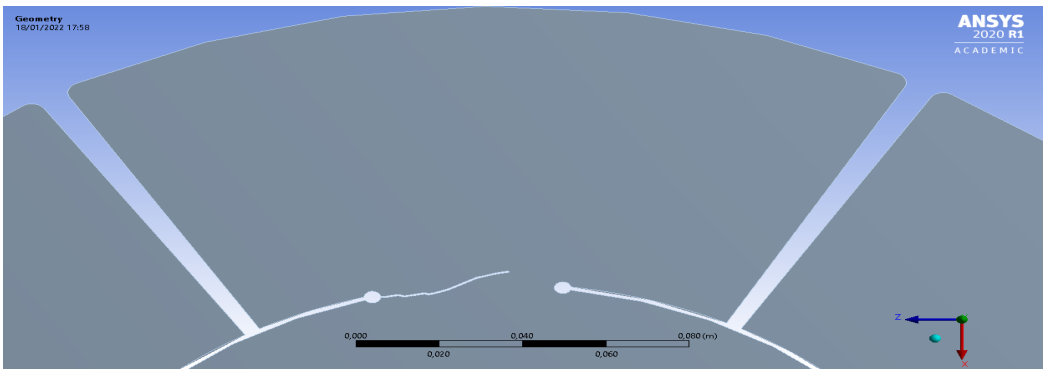

Figure 38: Sketch of the turbine with a crack of length = 25%Critical Length

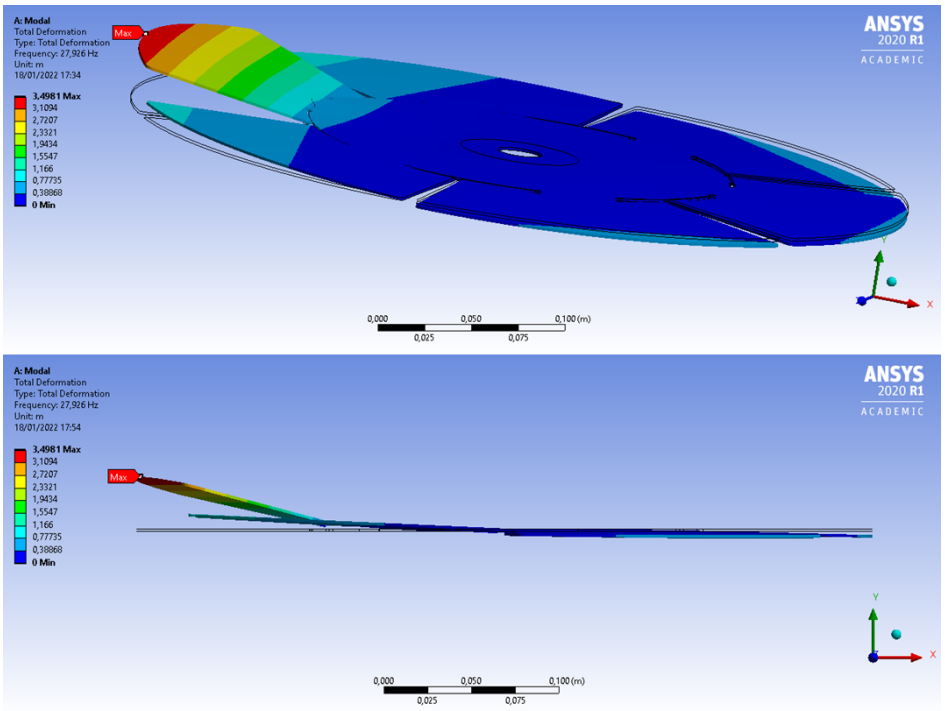

Figure 39: Displacement of the blade with a crack of length = 25%Critical Length

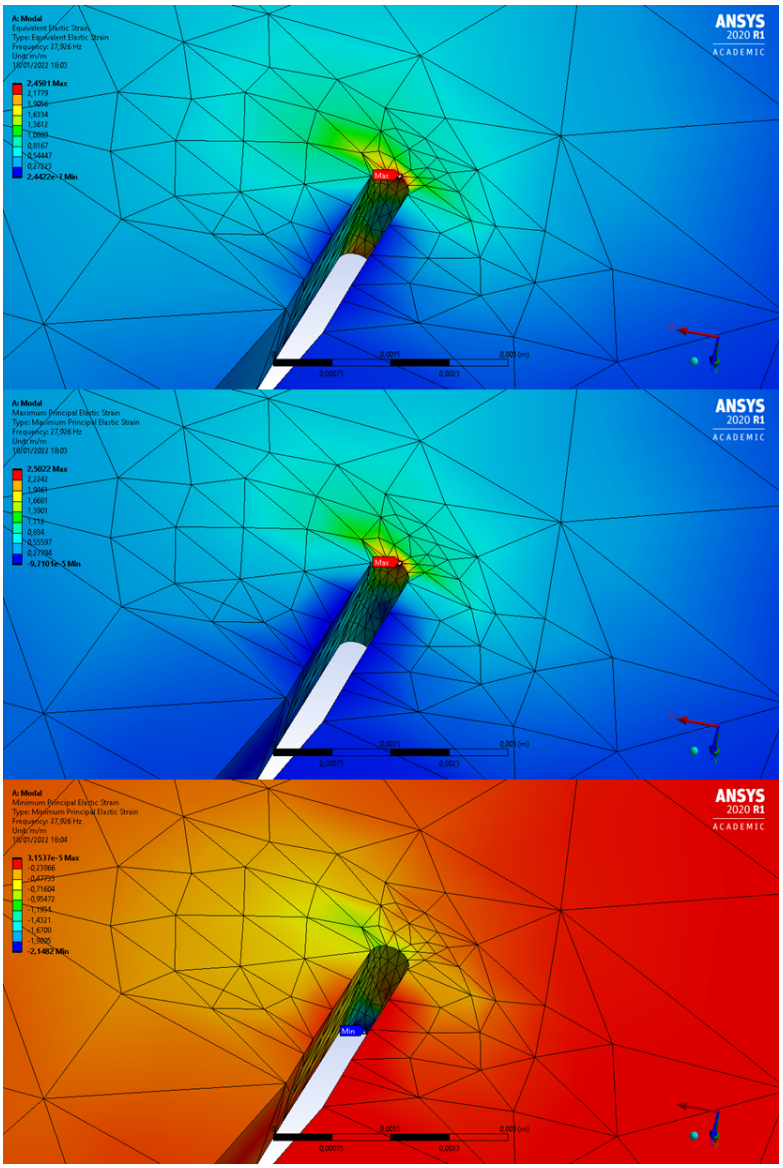

Figure 40: Strain analysis with a crack of length = 25%Critical Length

Regarding the deformation analysis, as we can see in Figure 39, the displacement of the turbine with respect to the blade where the crack appears is negligible. The maximum displacement point continues being one point of the edge of the damaged blade, and the initial nodal line has practically become in all the disk, as the blade is moving almost free with respect to the disk.

Regarding the strain analysis, as we can see in Figure 40, it does not change at all with respect to the first cracks mentioned before. The maximum value of equivalent strain (Von-Mises Strain) is one point of the edge of the crack. The maximum principal elastic strain, and the minimum principal elastic strain still follows the first rule mentioned in chapter 3.5.5, as one point of the edge of the crack is working in traction and the symmetric one on the other face of the disk is working at compression. For now on, the analysis strain will be not explained and shown anymore, as it is repetitive in all the experiments and only contributes to determine the direction of the crack, but not to see the displacement of the broken blade or the variation of frequencies in the turbine.

With reference to the vibration analysis, the appearance of the crack provoked by the first vibration mode should have provoked a variation in the first natural frequency, as we said previously. Nevertheless, the behaviour of the other 2 main vibration modes, as we can see in Table 7, is quite different:

Vibration mode	Natural frequency with the first crack analysed [Hz]	Initial Natural frequency (no crack) [Hz]	Difference with respect the initial conditions (no crack)
1 (1ND)	27,93	29,897	-6,58%
2 (1ND)	30,07	29,897	0,57%
3 (0NC)	30,95	31,265	-1%

Table 7: Variation of frequencies of the first 3 vibration modes with a crack of length=25%Critical Length

As we can see in this previous table, the variation of frequency due to the appearance of a crack mainly affects the first vibration mode, as the variation of the second and third variation modes are as maximum, 1%. Effectively, if we see the deformation of the turbine in the 2nd and 3rd vibration modes, they have not almost changed, as it follows the previous pattern of movements (it could be better appreciated in Ansys with the video analysis that the software provides), as we can see in Figure 41 below.

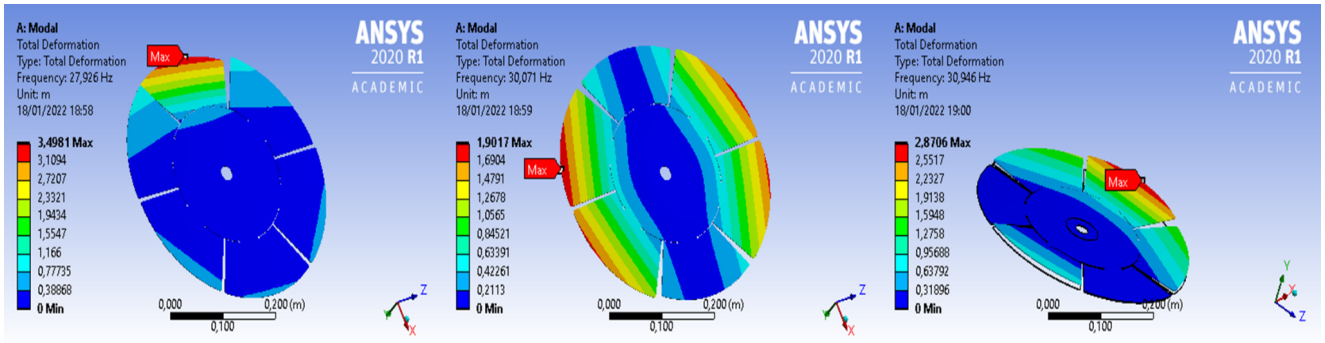

Figure 41: Vibration modes analysis with a crack of length = 25%Critical Length

To sum up, for a crack of length equal to the 25% of the critical length, we have reached the following conclusions:

- From the initial point of appearance of the microcrack, until reaching this point, it is necessary to have a long crack (and therefore, many simulations in Ansys) to see a variation in the behaviour of the turbine. In our case, a 33 mm crack.

- This change of behaviour affects only and mainly if the turbine vibrates in the first vibration mode, as it is the only one that sees a big decrease in its natural frequency due to the appearance of the crack.

- For the mode shape we are following (1ND), the maximum displacement point in the turbine is in the blade that suffers the crack, and the initial nodal line has turned in a kind of nodal surface (approximately 70% of the disk), as, regarding the center of the disk, the cracked blade moves a lot.

4.2.7.3 Crack length equal to 50% of the critical length

Once we analysed the results and the behaviour of the turbine with a crack length equal to the 25% of the critical length, we proceed now to try to achieve a crack length equal to 50% of the critical length in our model of Kaplan turbine. For doing so, the procedure has been followed the same way as we were doing.

Our first step was to take the 20th simulation (with a crack length of 33 mm) and follow the rules mentioned in chapter 3.5.5 to increase the length of the crack. The objective in this part of the project was to see a decreasement in the first natural frequency while the crack spreads, and obtain a value equal to F_{n1}= 25,56 Hz.

Crack Number	Lcrack [mm]	Fn1 [Hz]
20	35	27,5
21	37,5	27,06
22	40	26,59
23	42,5	26,11
24	44	25,75
25	45	25,5

Table 8: Evolution of the first natural frequency with the spread of the crack. 25%Lcrit-50%Lcrit

As we can see in Table 8 above, in contrast with the previous analysis, there were needed just 5 simulations to achieve the next analysis point. The variation of frequencies microcrack after microcrack generated was being reduced 0,5 Hz after 0,5Hz (approximately). The total length of the crack after these 5 simulations (25 in total) was of 4,5 cm (45 mm). This means that the average length of the crack created until this point was of 1,8mm. In this interval of study, the maximum length of a crack created until this point was 2,5mm. The Table 8 also shows that the behaviour of variation of frequency in this interval of crack length follows a different pattern from the previous interval (0-25%Lcrit). The decrease of the first natural frequency of the turbine is bigger in this interval, having the same microcrack lengths than before. At first view, the natural frequency of the turbine has decreased 2 Hz just with 1cm of crack, when in the previous analysis (chapter 4.2.7.2), the turbine needed a crack of an approximate length of 3 cm to decrease the same value (2Hz). We will analyse deeply every interval result at the end of this study and we will try to identify the different ranges of work that the turbine has if a crack appears on it.

To start analyzing the results, we must focus our attention on the sketch obtained in SolidWork with the crack until this point, which can be seen in Figure 42 on this page. As we can see in the sketch, the crack does not change drastically its direction, as it continues approaching to the other hole, but never ends touching it. Seems that simulation after simulation it tends to approach the edge of the damaged turbine.

Regarding the deformation analysis, as we can see in Figure 43, the displacement of the turbine with respect to the blade where the crack appears is still negligible. The maximum displacement point continues being one point of the edge of the damaged blade. Nevertheless, as the crack spreads we can see the point of maximum displacement tending to move to the same side of the blade where there exists the crack. It also makes sense, as this part of the blade is freer than the other side, and not only can move vertically, but also moves with a certain inclination. The initial nodal line has increased even more the surface with low displacement, as the damaged blade is moving almost free with respect to the disk for the first mode shape, even more than in the previous simulation.

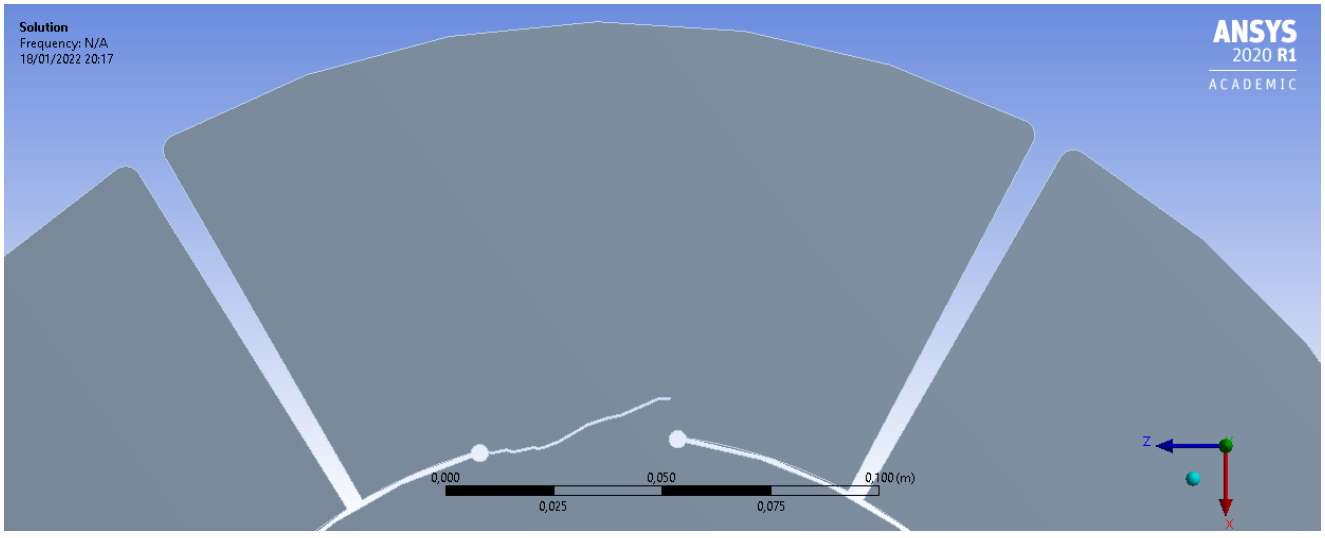

Figure 42: Sketch of the turbine with a crack of length = 50%Critical Length

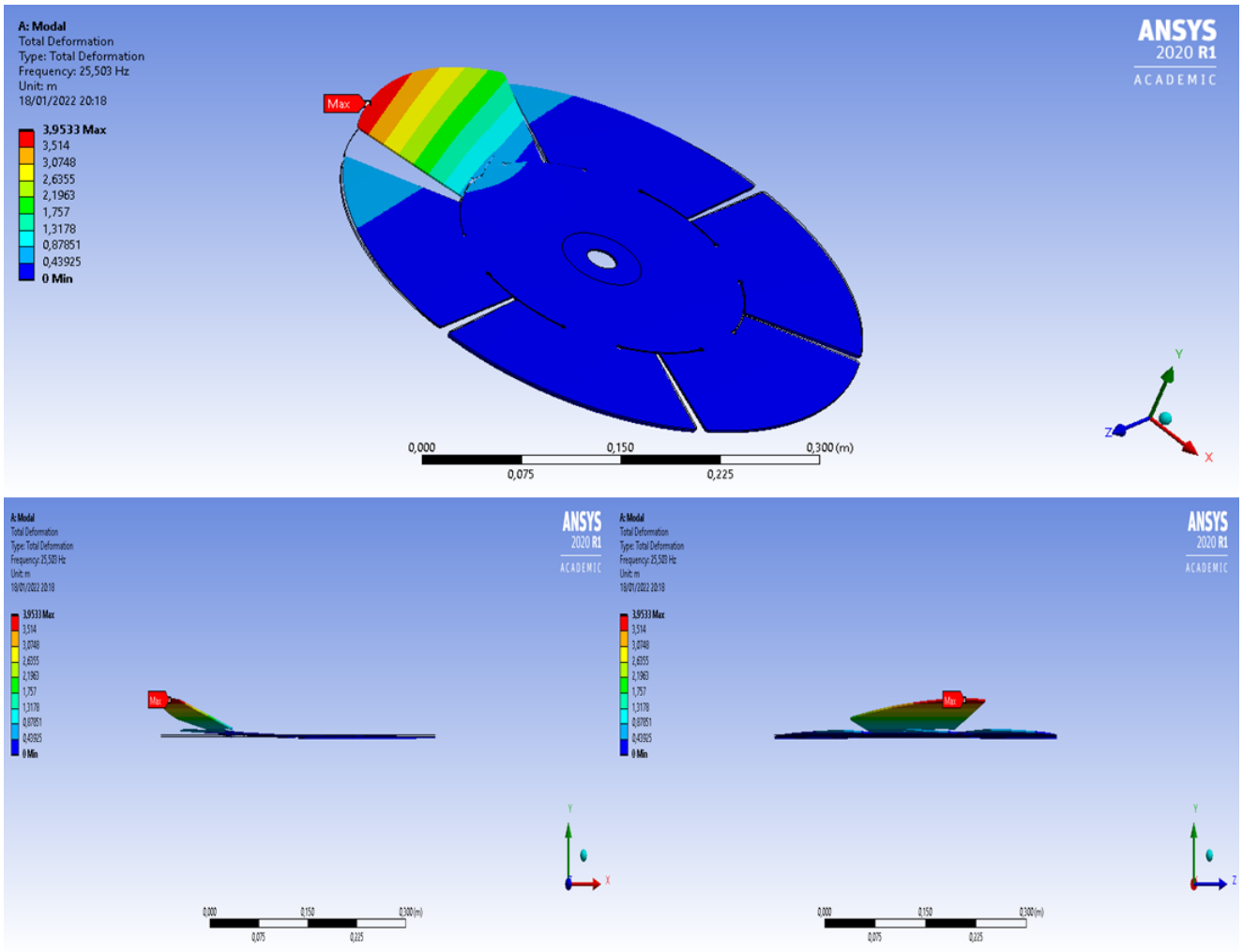

Figure 43: Displacement of the blade with a crack of length = 50%Critical Length

Finally, it is interesting too to analyse the vibration of the turbine in its first three vibration modes as we did before. As we can see in the following Table 9, the variation of frequency due to the spread of a crack still mainly affects the first vibration mode, as the variation of the second and third variation modes are negligible with respect to the variation of the first vibration mode.

Vibration mode	Natural frequency with the crack analysed [Hz]	Initial Natural frequency (no crack) [Hz]	Difference with respect the initial conditions (no crack)
1 (1ND)	25,5	29,897	-14,7%
2 (1ND)	29,86	29,897	-0,12%
3 (0NC)	30,75	31,265	-1,64%

Table 9: Variation of frequencies of the first 3 vibration modes with a crack of length=50%Critical Length

If we see the deformation of the turbine in the 2nd and 3rd vibration modes, they have not almost changed the way they vibrate, as it follows the previous pattern of movements, as we can see in Figure 44 below.

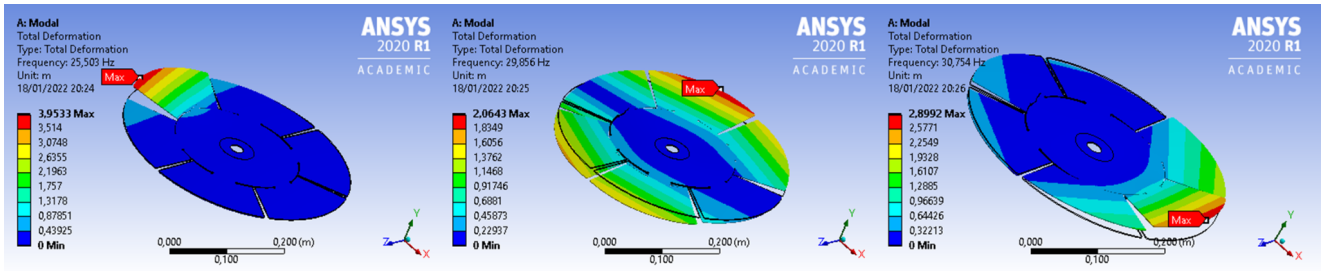

Figure 44: Vibration modes analysis with a crack of length = 50% Critical Length

Finally, after doing an amount of 25 simulations and reaching the crack of length equal to 45 mm, the conclusions we reach for this part are the following:

- This change of behaviour still affects the turbine vibrating only in the first vibration mode, as it is the only one that sees a big reduction in its natural frequency due to the appearance of the crack.

- In this interval of study, it seems clear that the behaviour of reduction of frequency because of the crack has changed, because now only a few cracks (5) were needed to reduce 2 Hz approximately the first natural frequency.

- For the first vibration mode, the maximum displacement point in the turbine is in the blade that suffers the crack, and the initial nodal line has turned in an almost nodal surface (approximately 80% of the disk), as, regarding the disk, the damaged blade moves a lot, and with this crack, the blade is moving even in other directions (not only vertically).

4.2.7.4 Crack length equal to 75% of the critical length

Once we analysed the results and the behaviour of the turbine with a crack length equal to the 50% of the critical length, we proceed now to try to achieve a crack length equal to 75% of the critical length. For doing so, the procedure followed has been the same until now.

Our first step was to start from the 25th simulation (with a crack length of 45mm) and, from that point, follow the rules mentioned in chapter 3.5.5 to increase the length of the crack simulation after simulation. The objective was in this part of the project to see the first natural frequency achieve a value of 23,37 Hz. Once we did the simulations, and after doing only 3 more cracks, the results obtained of the simulated disk with the cracks and the natural frequencies were the following:

Crack Number	Lcrack [mm]	Fn_1 [Hz]
26	47,5	24,73
27	50	24,11
28	53	23,35

Table 10: Evolution of the first natural frequency with the spread of the crack. 50%Lcrit- 75%Lcrit

As we can see in Table 10 above, continuing with the behaviour seen in the second interval of study (25%Lcrit-50%Lcrit), there were needed just 3 simulations to achieve the next point of analysis. The variation of frequencies microcrack after microcrack generated was reduced 0,7Hz after 0,7Hz (approximately). The total length of the crack after these 3 simulations (28 accumulated in total) was 53 mm. This means that the average length of the crack created until this point was 1,9 mm. In this interval of study, the maximum length of a crack created until this point was 3mm. Table 10 also shows that the behavior of variation of frequency in this interval follows a different pattern from the first interval studied (0-25%Lcrit), but similar to the previous one (25%Lcrit-50%Lcrit). At first view, the natural frequency of the turbine has decreased 2,2 Hz just with 5,5 mm of crack, a smaller crack length with respect to the previous analysis.

To start analyzing and understanding the results, we could start watching the sketch obtained in SolidWorks with the crack until this point, which can be seen in Figure 45 below. As we can see in the sketch, it seems that simulation after simulation the crack tends, as it did before, to spread to the other side of the blade, but in this case, and this is different from the previous interval study, the crack seems to avoid approaching the other hole, as it is opening slowly in these simulations to the edge of the blade.

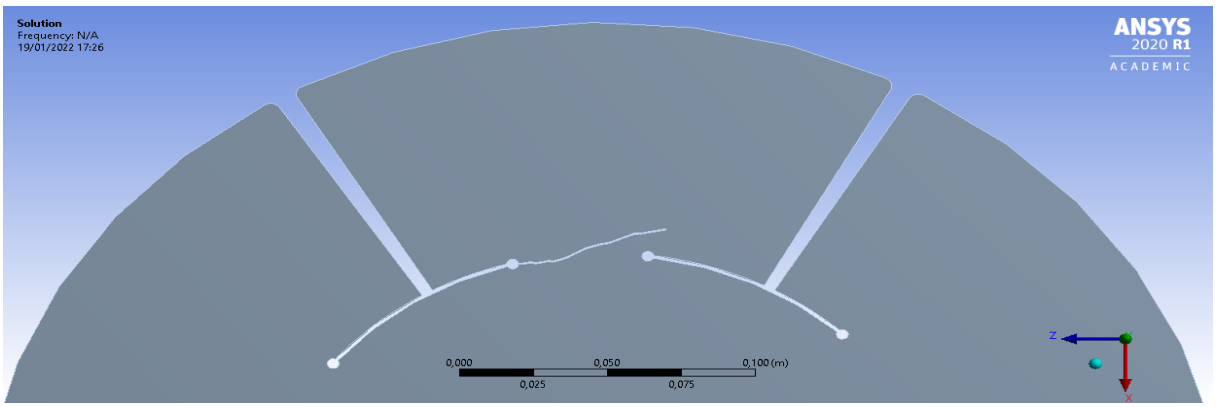

Figure 45: Sketch of the turbine with a crack of length = 75%Critical Length

Regarding the deformation analysis, as we can see in Figure 46, the displacement of the turbine with respect to the blade where the crack appears is negligible. The only element that seems now to vibrate with a bigger amplitude is the damaged blade. The maximum displacement point continues being one point of the edge of the damaged blade. Moreover, in this case, the point of maximum displacement is practically the corner of the blade, but not exactly the corner. As the crack spreads, we can see the point of maximum displacement tending to move to the same side of the blade where there exists the crack. It also makes sense, as this part of the blade is practically free now. The initial nodal line has increased even more the surface with low displacement, as the blade is moving almost free with respect to the disk, even more than in the previous simulation. Now, as we can see in Figure 46, the displacement of the blade with the crack is the one with more amplitude for the first vibration mode studied.

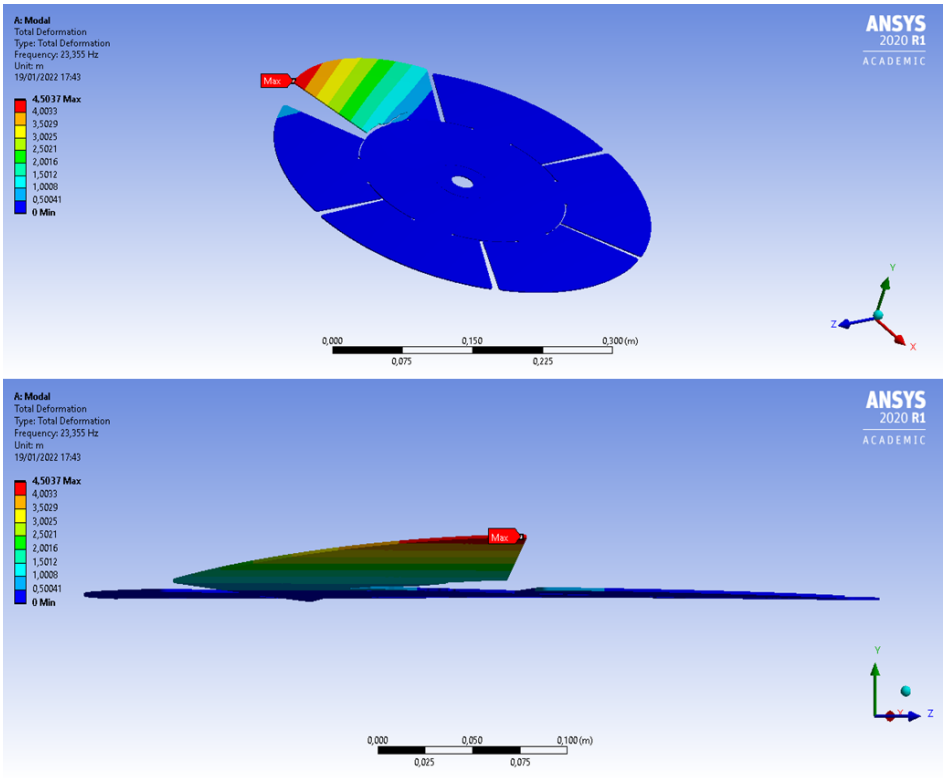

Figure 46: Displacement of the blade with a crack of length = 75%Critical Length

As we did in the previous intervals, it is interesting too to analyse the vibration of the turbine in its first three vibration modes. As we can see in the Table 11 below, the variation of frequency due to the spread of a crack still mainly affects the first vibration mode, as the variation of the second and third variation modes are still negligible with respect to the variation of the first vibration mode.

Vibration mode	Natural frequency with the crack [Hz]	Initial Natural frequency (no crack) [Hz]	Difference with respect the initial conditions (no crack)
1 (1ND)	23,35	29,897	-21,90%
2 (1ND)	29,53	29,897	-1,22%
3 (0NC)	30,63	31,265	-2%

Table 11: Variation of frequencies of the first 3 vibration modes with a crack of length=75%Critical Length

If we see the deformation of the turbine in the second vibration mode it has not almost changed the way it vibrates, as it follows the previous pattern of movements. Nevertheless, with this length of crack, the behaviour of the third vibration mode has started changing. The movement of the blades in this 3rd vibration mode is not the same, but the frequency still is quite similar to the obtained in the first simulation, with just a difference of 2%. As we did in the other points of study, we can see in Figure 47 below the different vibration modes for the turbine with this crack.

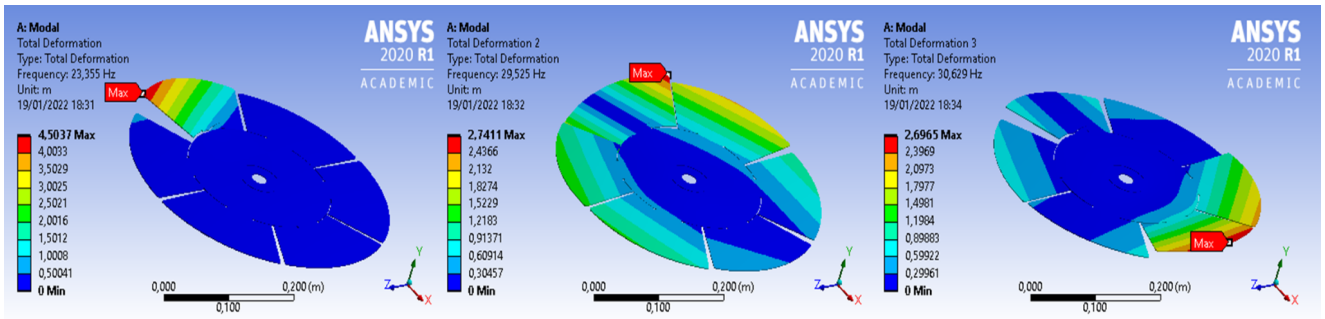

Figure 47: Vibration modes analysis with a crack of length = 75% Critical Length

Finally, the conclusions we can reach after all these simulations are the following:

- This change of vibratory behaviour still affects the turbine vibrating mainly in the first vibration mode, as it is the only one that sees a bigger reduction in its natural frequency due to the appearance of the crack. However, the original 0NC vibration mode (third natural frequency of the disk) is starting to feel the effect of the crack in its frequency and in its way to vibrate.

- In this interval of study, the reduction of the first natural frequency continues with a behaviour similar to the previous one, (even with a more aggressive reduction of the frequency due to the spread of the crack) as the variation of frequencies microcrack after microcrack generated was being reduced approximately 0,7 Hz after 0,7 Hz

- The maximum displacement point in the turbine is in the blade that suffers the crack for the first natural frequency, and the initial nodal line has turned in all the disk but the own damaged blade, which means that the blade is vibrating practically alone with respect to all the structure. We can guess that the failure due to fatigue in a real experiment should be almost imminent, if it has not happened already.

4.2.7.5 Crack length equal to the critical length

After analysing the behaviour of the turbine with a crack with a length of 75% of the critical length, we will now comment on the results we have with a crack that is supposed to break the blade definitely, a crack with a critical length. Note that, theoretically this interval is not defined at all, as the turbine could have broken due to fatigue earlier, but we will show the results for this critical point.

The first step was to start from the 28th simulation (with a crack length of 53mm) and follow the rules mentioned in chapter 3.5.5 to increase the length of the crack. The objective was in this part of the project to see a Fn_1 equal to 21,17 Hz. The results obtained after the simulations are shown inTable 12 below:

Crack Number	Lcrack [mm]	Fn_1 [Hz]
28	53	23,35
29	54	23,16
30	56	22,9
31	60	22,3
32	64	21,83
33	65,5	21,75
34	69	21,46
35	72,5	21,19

Table 12: Evolution of the first natural frequency with the spread of the crack. 75%Lcrit-Lcrit

As we can see in Table 12 above, in contrast with the 2 previous analyses, an amount of 8 simulations were needed to achieve the final point of study of this project. The variation of frequencies microcrack after microcrack generated in this interval was smaller than in the others, as it decreased just 0,2 Hz after 0,2 Hz (approximately). The total length of the theoretical broken disk of the turbine is 72,5 mm. This means that the average length of the crack created until this point was of 1,8 mm. In this interval of study, the maximum length of a crack created until this point was 4 mm, as we did not see a big change in the strain analysis and the strain distributions. The reduction of the first natural frequency of the turbine is similar to the first interval of study (0-25%Lcrit). At first view, the natural frequency of the turbine has decreased 2 Hz with almost 20 mm of crack, which is a lot, as in the previous analysis just 3 micro cracks of approximately 5 mm were needed to see a big reduction in the natural frequency of the turbine.

To start analyzing these last results, we will first see the result of the sketch obtained in SolidWork with the crack until this point, which can be seen in Figure 48. As we can see in the sketch, the crack has changed drastically its direction, as it now goes directly to the edge of the blade, directing it to a place near the corner of the blade mentioned. During this interval of study, no change in the direction of the crack was observed practically, and it went almost constant to the point mentioned in the eight simulations.

Regarding the deformation analysis, as we can see in Figure 49, for the first vibration mode, the displacement of the turbine with respect to the blade where the crack appears is still negligible. The maximum displacement point continues being one point of the edge of the damaged blade. This time, the corner of the blade has finally become the point with bigger displacements after all the simulations. The initial nodal line has increased and now it is practically all the disk, excepting a part of the damaged blade.

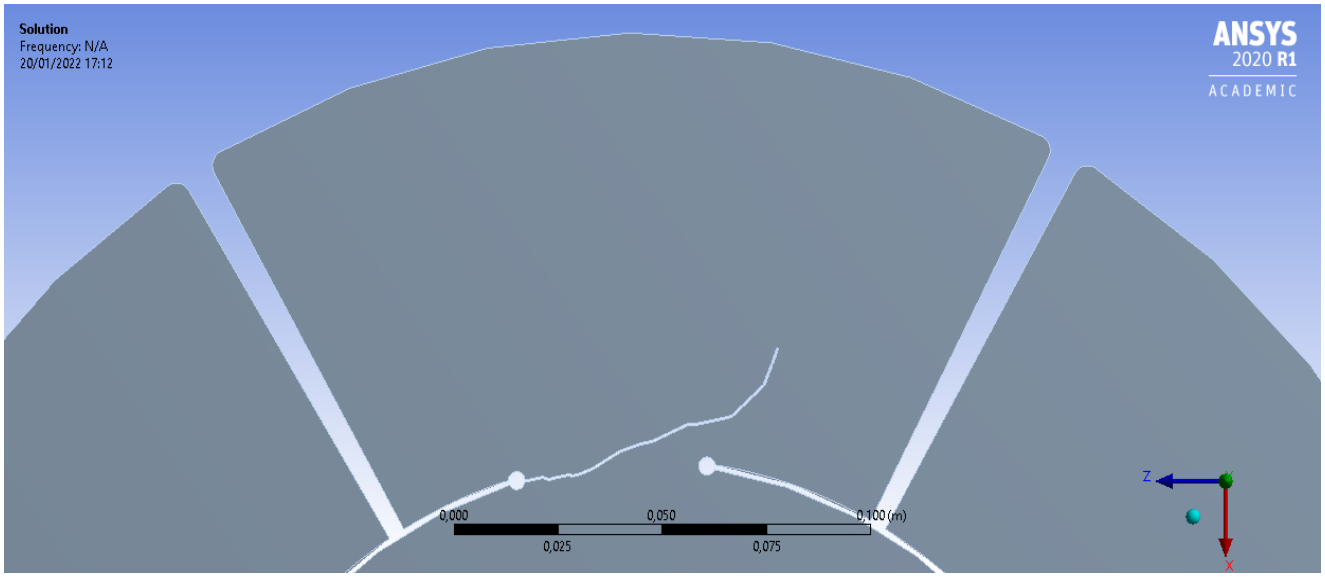

Figure 48: Sketch of the turbine with a crack of critical Length

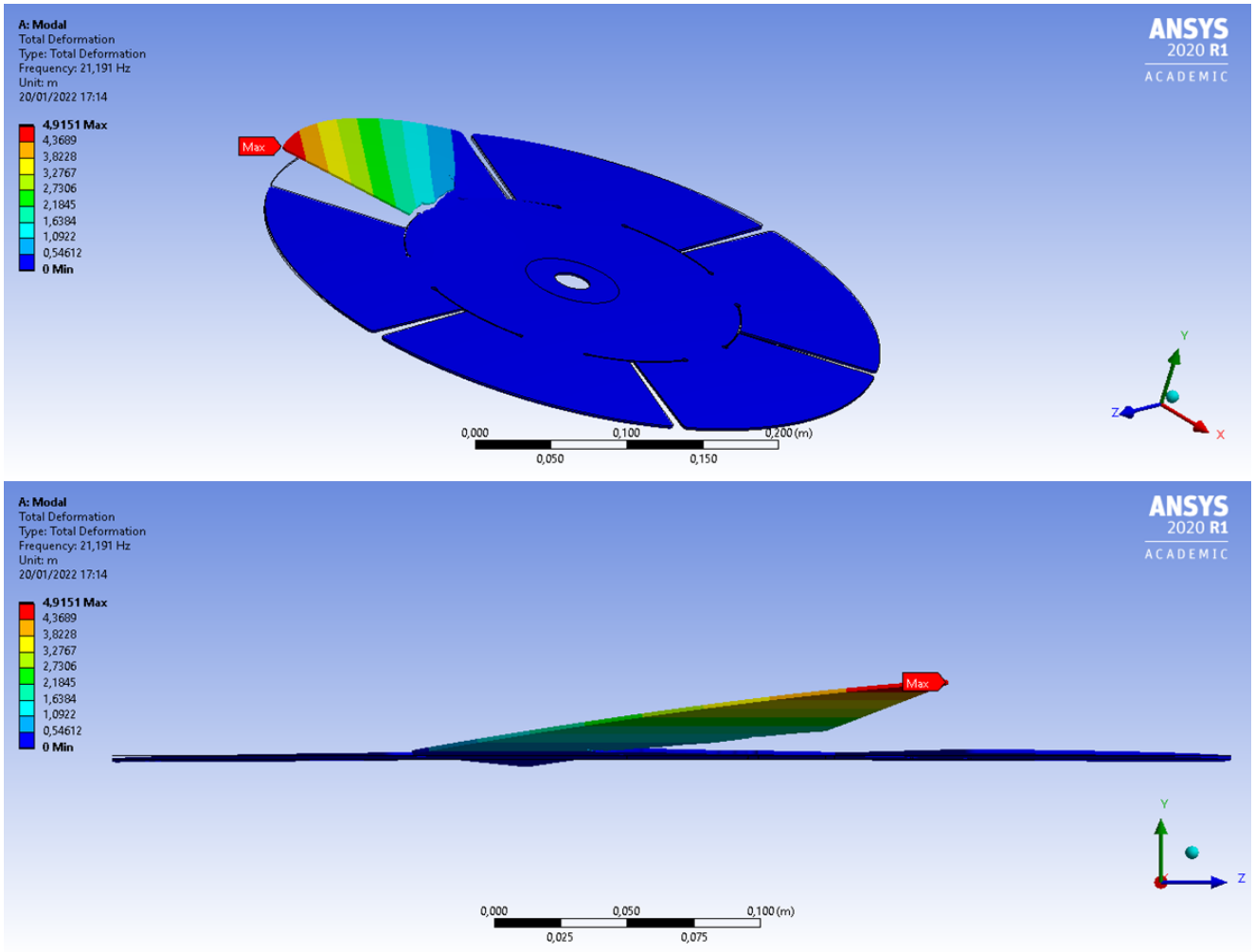

Figure 49: Displacement of the blade with a crack of critical Length

Finally, as we did before in the previous simulations, it is interesting too to analyse the vibration of the disk in its first three vibration modes. As we can see in the following Table 13, the variation of frequency due to the spread of a crack still mainly affects the first vibration mode, as the variation of the second and third variation modes are as negligible with respect to the variation of the first vibration mode.

Vibration mode	Natural frequency with the crack analysed [Hz]	Initial Natural frequency (no crack) [Hz]	Difference with respect the initial conditions (no crack)
1 (1ND)	21,19	29,897	-29,12%
2 (1ND)	29,05	29,897	-2,83%
3 (0NC)	30,52	31,265	-2,38%

Table 13: Variation of frequencies of the first 3 vibration modes with a crack of critical length

Nevertheless, in this last simulation we can appreciate something we did not see in the previous simulations. The second natural frequency has changed a lot in this occasion, as with the previous simulations, the maximum variation observed was a decrease of 1,22% with respect to the original frequency. This time in this interval, the result has almost doubled, which means that this final crack actually could affect the second mode shape as well. The variation of the frequency of the third mode shape remains in the same line as before. We see for this third natural frequency a small decrease in its value, but not far from the other simulations. All these explanations and mode shapes can be seen below in Figure 50 in the displacement analysis.

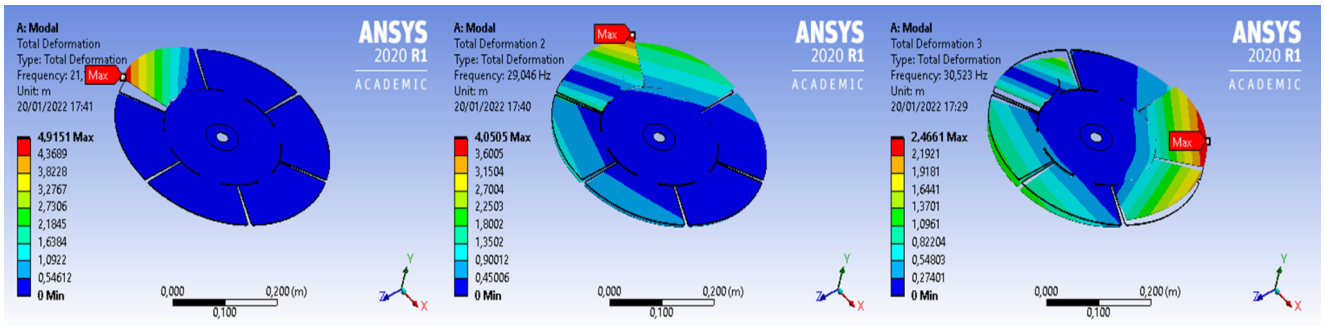

Figure 50: Vibration modes analysis with a crack of critical length

Finally, the conclusions we reach in this interval of study are the following:

- This change of behaviour still affects the turbine vibrating mainly in the first vibration mode, as it is the only one that sees a big reduction in its natural frequency due to the appearance of the crack (29,12%). However, the other 2 mode shapes, on this occasion, have seen with this final crack a variation, but not as big as the first mode shape.

- In this interval of study, it seems clear that the behaviour of reduction of frequency because of the length of crack has changed, because now an amount of 8 cracks of total length of 19,5 mm were needed to reduce the first natural frequency 2 Hz, meanwhile in the two previous simulations, just 3 or 4 cracks of very few millimeters were needed to reduce the value of the first natural frequency of the disk. The way to operate in this interval of study was similar in some way to the first interval, as there were needed many cracks to see variation in the frequency of approximately 2 Hz..

- For the first mode shape, the maximum displacement point in the turbine is in the blade that suffers the crack, concretely in the corner of this blade. The initial nodal line has turned in an almost nodal surface (approximately 95% of the disk), as, regarding the disk, the damaged blade moves a lot only in its 'free' part where the blade is damaged. The collapse of this blade is imminent, as the point with bigger displacement is the only point in the turbine with an amplitude even 4 times bigger than the other points of the other blades of the turbine.

4.2.8 Conclusions of the numerical modal analysis

Now, once we have explained the four different critical points separately, it would be interesting to have a global idea about the phenomena of fatigue in our model of turbine due the spread of the crack in the four phases as a whole. As we said, our global study tends to be a project that could be extrapolated to all turbines, and to all the different phases that the turbines could suffer due to the appearance of a crack because of fatigue.

Firstly, in the Annex 2, we can see the drawing of the disk with the crack of critical length in a better way than in the figures shown before in each interval. It is interesting to see the shape of the crack, as it is unique because of the turbine style, and it can be representable and measurable, as we have done it by simulating the appearance and spread of the crack microcrack after microcrack. The sum of all the microcracks appearing in each simulation is the crack of critical length. Due to the results obtained during the spread of the crack, we can confirm that absolutely the simplified Kaplan turbine has changed the way it vibrates and, therefore, its range of work and its efficiency, as the disk did not behave equally in the different intervals of study.

Secondly, it is also interesting to put in common the different intervals of the turbine to see how all of them together are represented. It is also interesting to see if there is a linear behavior in the first natural frequency (supposed to be the destructive one we are following), that we said we were not seeing apparently. Effectively, in Figure 51 below we can see maybe the most important result we have obtained in this study so far:

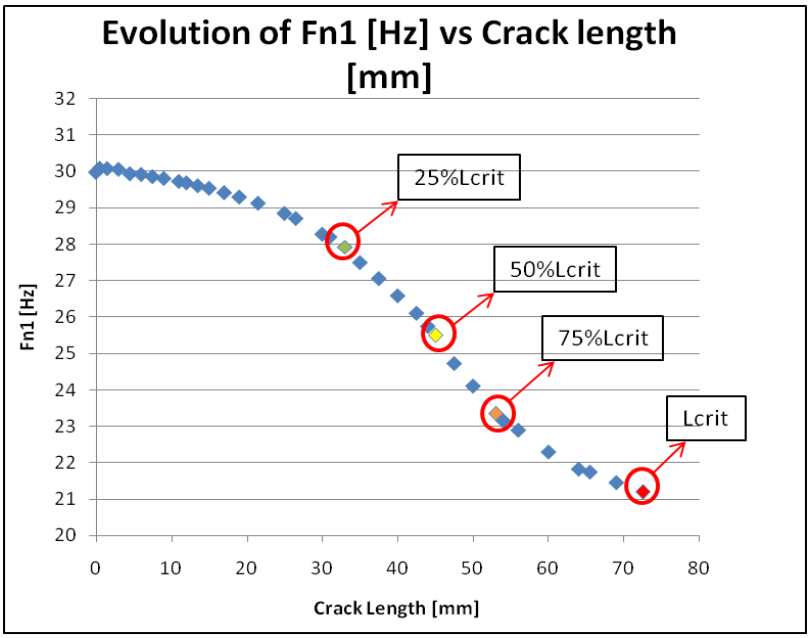

Figure 51: Evolution of the first natural frequency vs the length of the crack

For having an idea, this graph has been created by combining the four tables of the four different intervals studies that represents the crack length and the first natural frequency we are following (tables 6, 8, 10 and 12 of the project in one). As we can see in Figure 51, the evolution of the first natural frequency of the turbine with respect to the length of the crack that appears due to the effect of fatigue is not linear during the lifespan of the turbine. Moreover, there are 3 differentiated zones:

- Zone 1: Interval approximately of a crack of length 0 mm to 17mm: In this zone, the first natural frequency did not almost change, as we did an amount of 12 simulations and the first natural frequency was in this last simulation 29,42 Hz, just an 1,73% smaller than the original one without any crack in the simplified turbine. The evolution of the reduction of the frequency due to the fatigue because of the appearance of microcracks in this zone is linear, and practically horizontal, as the first natural frequency remains practically steady.

- Zone 2: Interval approximately of a crack of length 17 mm to 53mm: In this zone, the first natural frequency changed differently. In the first simulations of this interval, it changed more or less steady, but when the crack approached itself to a length of 25% of the critical length, the reduction of frequency in the turbine was practically exponential. In this second zone, definitely, there is not a linear behaviour of the reduction of frequency.

- Zone 3: Interval approximately of a crack of length 53 mm to 72,5mm: In this last zone, which coincides with the last interval studied (75%Lcrit-Lcrit), the behaviour of reduction of frequency in the turbine changed, as it was necessary to create longer cracks in order to see a big reduction in the frequency of the structure. Moreover, as we see in Figure 51, this last interval is more or less linear and very different from the previous mentioned.

Once I analyzed these three zones, and having introduced concepts of fatigue earlier in chapter 3.5 it came to my mind that frequently in machines that are submitted to external and variable loads, there exists a pattern in the evolution of the internal resistance vs the amount of work that they suffer. We are talking about Figure 18 of chapter 3.5.2.

When I saw that figure again, I did realize that not only three zones were differentiated in the common case mentioned, but also that our graph created that related the reduction of frequency of our model of turbine with the crack length (Figure 51) was very similar to this. We can see this two graphs in one below in Figure 52:

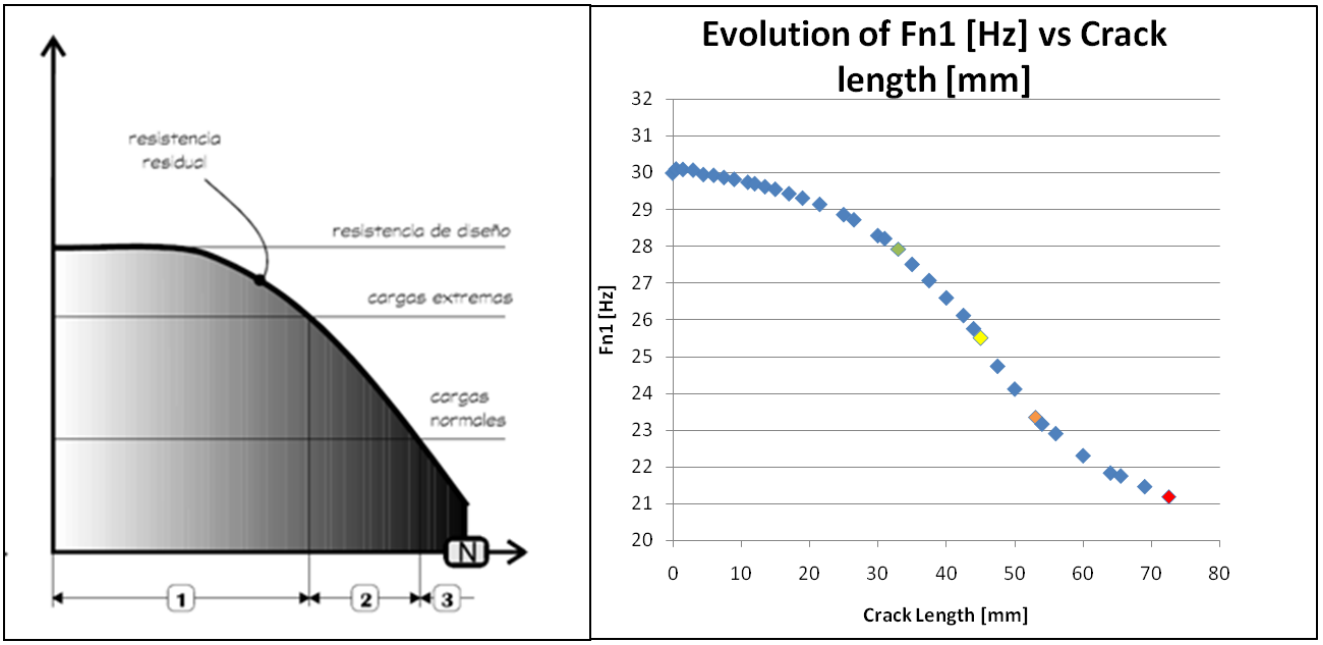

Figure 52: Comparison between theory of fatigue and results of decreasement of frequency in our turbine

Watching these two graphs compared, and having differentiated 3 zones also in our study, we can say that absolutely there exists a relationship between reduction of frequency in our model of turbine, the spread of the crack, and lifespan of the own turbine. We can also say that the tools used (high refinement methods in Ansys combined with precise sketches in SolidWorks), and theory used for following and simulating a crack that appears in machines (chapter 3.5) are good enough to follow a characteristic behaviour of a crack spread in our model of hydraulic turbine that suffers the effect of fatigue.

To sum up, we can resume the conclusions and observations of this numerical study we have made:

- The expansion of the crack caused by the effect of fatigue in relation with the reduction of the frequency in our model of turbine definitively is not linear, and there are 3 intervals of work when the turbine suffers a crack and when this crack spreads through the disk in our model of Kaplan turbine.

- The fact that there exists a similarity between the graphs of residual resistance of machines under external loads and the reduction of frequencies due to the appearance and spread of a crack makes us to confirm that there are numerical relationships between the variation of the vibration of a turbine, the crack length ,and the lifespan of the own turbine.

- The fact of the appearance of this crack does not affect practically to other regimes of work of different frequencies, because, as we have seen in the interval simulations, until the critical point, the other 2 mode shapes practically did not change. This fact could be very important as the turbines do not work currently in constant regimes of work.

- It is possible to simulate in Ansys the appearance of a crack and its spread in a hydraulic turbine, as Ansys nowadays offers tools of high refinement of models that allow it to follow even microscopic elements as a crack. Of course, depending on the types of turbines, the direction of the cracks will be different, as they depend on the shape of the turbine, the material, and even irregularities in the manufacturing process. Regarding this last comment, it is important to note that, as we said, fatigue is a multidisciplinar phenomena. Anyway, a real failure due to fatigue in a simplified hydraulic machine has been seen by doing a microscopic analysis in Ansys.

- Finally, combining all these conclusions mentioned above with the objective proposed at the beginning of the project, it would be possible to improve the predictive maintenance of the hydraulic turbines by doing simulations and studies like I have done. Our simplified model studied could be an initial point to amplify the brand of predictive maintenance to other hydraulic machines that could be analyzed in softwares (like Ansys) before starting working in the hydroelectric power plants to avoid failures because of the effect of fatigue.

5. Experimental analysis

For the enlargement of the project, the professors of the department of fluid mechanics proposed to study and compare the simulations I have done in Ansys with the real model they had already bought for analyzing experimentally. The intention was to try to identify the behaviour of the turbine in real life and try to see if it was at least similar to the one simulated in Ansys in the previous part of this large project. If the experimental results were close enough to the ones simulated before, this project could be even more a good first step into the predictive maintenance of Kaplan turbines.

5.1 Introduction to the experiment

Regarding the experimental part, it is important to say that this part of the project was made in the laboratory of fluid mechanics in the School of Industrial Engineers in Barcelona (ETSEIB), which is part of the polytechnical university of Catalonia (UPC). The mentioned laboratory has a room where a test rig is frequently used for different studies. In our case, this modal analysis of a model of a Kaplan turbine was carried out using this test rig with normal temperature and pressure conditions (NTP), at 20ºC and a pressure of 1atm. Therefore, the influence of external temperature and pressure should not affect the results obtained, as not extreme conditions (such as high increment of temperatures) were experimented during the simulation in the test rig.

For analyzing the results, some instrumentation was needed in order to simulate the vibratory behaviour of the turbine. The instrumentation used was the following mentioned:

- One hammer: The use of the hammer is basically for exciting the turbine at different points, and, therefore, provoking a vibration of the disk and the shaft. Due to the use of this hammer, we will try to analyse if due to a punctual external force/excitement it is possible to obtain clearly all the natural frequencies and mode shapes of the turbine.

- Two uniaxial accelerometers: The uniaxial accelerometers will be the sensors that will measure the acceleration of different points of the turbine. Having explained before in chapter 3.4.2 the relationship between acceleration and displacement, it seems obvious that for trying to obtain different displacement of points, it is enough to use accelerometers, and not other sensors that there were in the laboratory like gauges are needed, as they won't contribute at all to the project. Actually, it is important to note that the sensors (and the wires connected to them) have a mass that may alter our results a little bit. Fortunately, the mass of these sensors is small in comparison with the mass of the disk of the turbine. The main characteristic of these kinds of sensors is that they measure the acceleration in just one direction, and this will be vertical (Z) in our study.

- Two triaxial accelerometers: The triaxial accelerometers have the same purpose than the previous mentioned, but in this case, these sensors can measure the acceleration of one point of the turbine in the three directions of the space. For our study, the horizontal acceleration of the points (X,Y directions) are not interesting at all, but as there were not more sensors, we used them also for analyzing the vertical displacement of different points. The mass of these kinds of sensors is bigger than the uniaxials, as they are bigger. Fortunately, as we said before, the mass of these sensors is small in comparison with the mass of the disk of the turbine, so they should not change at all the results obtained of frequencies and mode shapes.

- NI-9231 module: This is an 8-channel module that can measure signals from integrated electronic piezoelectric (IEPE) and non-IEPE sensors, such as accelerometers and tachometers. This module can perform the high dynamic range measurements required for modern measurement accelerometers. It is the module that connects the accelerometers with the chassis that will provide the information acquired to the laptop. The 8 channels will be, respectively, 1 for the hammer, 2 for the two uniaxial sensors, and 5 for the triaxial sensors (there will be one coordinate X in a triaxial sensor that we will not measure as there are not more channels in the module).

- Chassis compact cDAQ-9185: It is an Ethernet CompactDAQ chassis designed for distributed sensor measurement systems. The chassis controls timing, synchronization, and the data transfer between the modules and an external server (laptop in our case). With this chassis, it is possible to perform various analog I/O, digital I/O, and counter/timer measurements.

- Labview software: To store and read the results of the simulations we will carry out, it is important to use some tool that provides us to read the results we obtain from the turbine and that shows us graphical results such as natural frequencies or vibration modes. For doing so, the department of fluid mechanics uses a software called Labview, which basically does what I have mentioned. By creating a determined program, it creates charts and graphs about the results of the simulations that are carried out with all the measurement tools introduced before. This software, obviously, needs a computer in order to work. There is one laptop in the laboratory exclusively for the analytical results of the laboratory.

All these components that will give us the possibility to study and analyse the results of the real turbine are shown below in Figure 53:

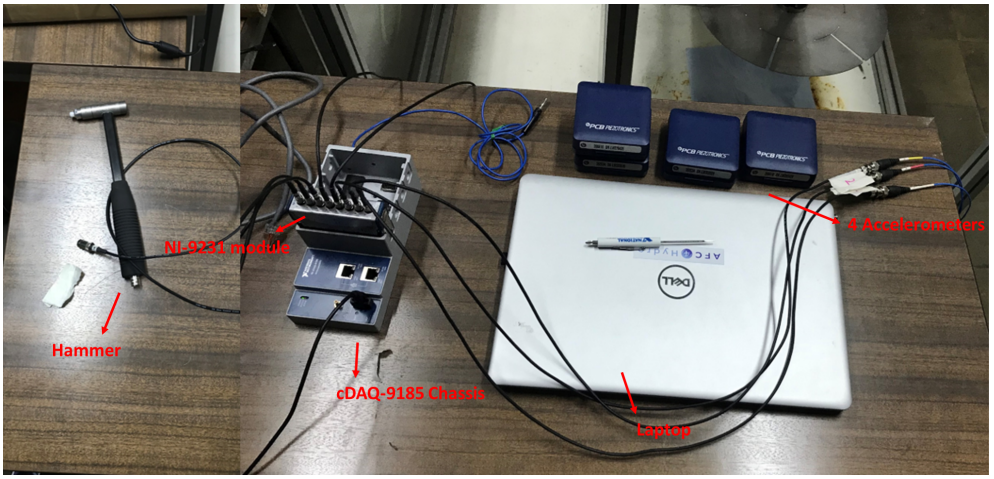

Figure 53: Tools used to measure the vibration behaviour of the turbine

Finally, the key element for this study is the simplified turbine, which has the same geometry and parameters as mentioned in chapter 4.1. The setup of the turbine in the test rig can be seen in Figure 54:

Figure 54: Turbine in the test rig

5.2 Modal analysis

5.2.1 Experimental modal analysis basics

For having the results in the frequency domain through the accelerometers, it is necessary to apply the Fourier Transform (FT) to Equation 13. The Frequency Response Function (FRF) is obtained and shown below in Equation 18:

$$\{X(j\omega)\} = [H(j\omega)]\hat{A}\cdot\{F(j\omega)\} \qquad (18)$$

Where $\{X(j\omega)\}$ and $\{F(j\omega)\}$ are the corresponding vectors x(t) and F(t) in the frequency domain. Therefore, $[H(j\omega)]$ is the Frequency Response Function (FRF). From now on, this $[H(j\omega)]$ will be analyzed in the laboratory thanks to the Labview software, and will provide us the results of the modal parameters. The vectors $\{X(j\omega)\}$ and $\{F(j\omega)\}$ are measured simultaneously with accelerometers for the response and due to the impact hammer. The modal parameters can be extracted through the FRF, which can be also expressed as Equation 19 below:

$$[H(j\omega)] = \sum_{r=1}^{N} \frac{j2\omega_r Q_r \{\vartheta\}_r \{\vartheta\}_r^t}{(\theta_r^2 + \omega_r^2 - \omega^2) - 2\theta_r j\omega} \qquad (19)$$

Where ω_r is the natural frequency, θ_r is the damping factor, $\{\vartheta\}_r$ are the mode shapes that define the deformation shape and Q_r is a constant factor for every mode r. N is the total number of modes, and r is the vibration mode studied. With these two equations it is enough for having and extracting the modal parameters. As we said, the software will calculate these parameters mentioned above and will provide us the results of the modal analysis graphically and numerically [26].

5.2.2 Analysis of the initial conditions

Once we have introduced the basic concepts about the experimental modal analysis we will do in the laboratory, and once introduced all the instrumentation that we will use too, we carry on this project studying the initial conditions of the turbine in terms of initial frequencies and mode shapes. This part is related with chapter 4.2.6, as this is the first step in order to analyse all the following states of the turbine when a crack appears on it. Moreover, in this chapter there will be an extra calculation, as initially it is not known what blade is the one that suffers the crack. By knowing and identifying the nodal line, it is possible to know the initial point of the appearance of the crack.

The first thing I did was to install the disk in the test rig. Once installed, it was necessary to classify the 6 blades and orientate them in an unique position for all this enlargement study. This position of the blades will be the same in all the experiments, even in the measurements of the cracked disk, as it is very important to respect the position of the blades. For doing so, I marked with a pen all the blades, and, to measure the vibration response of the turbine, my director Xavier recommended that I draw 12 points, distributed symmetrically all around the turbine. These points are the points where the hammer will impact, and due to this impact in all these points we will measure with the sensors the natural frequencies of the turbine and its vibration modes. All the setup and the points of study can be seen below in Figure 55:

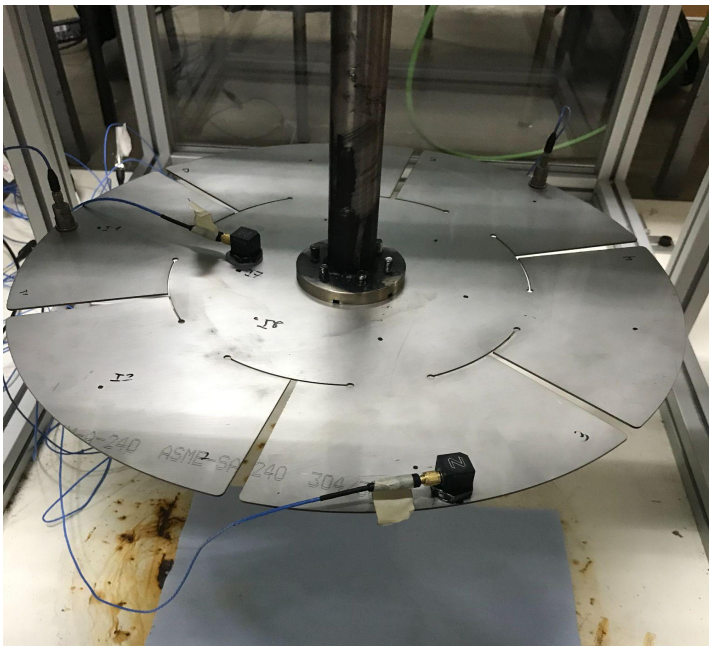

Figure 55: Distribution of the points of study and accelerometers in the turbine

Figure 55 above shows the distribution of the blades and points marked in the reverse of the clockwise, being the first blade the closest to the instrumentation (and chair and table) shown in Figures 53 and 54. It is very important to always have this distribution of the blades as from this position, we will identify the nodal lines of the different vibration modes. For the points of impact, there are in the first experiment two rows of points with respect to the center of the disk. First, there is one point of impact drawn in the middle of each blade at approximately 3.5 cm from the edge (I1,I2….I6). Secondly, we drew another line (another circle line) of points at approximately 3 cm from the shaft of the turbine (I7,I8…I12). The direction of these points is the same as the direction of the first 6 points. That way, we have a pair of points aligned from the edge of each blade to the center of the disk, I1-I7, I2-I8… (see Figure 55 for better understanding). We cover with these points different principal parts and directions of the disk of the turbine.

Regarding the positions of the accelerometers, it is important to distribute them in some way so that they do not coincide in a determined vibration mode in the modal line all of them, because this way the sensors would not measure anything and maybe some natural frequency could be missed as there would not be response of displacement. For doing so, the positions of the sensor are the following:

- Triaxial accelerometer T35Z: In the edge of the blade number 3
- Triaxial accelerometer T28Z: Centered, and aligned with the blade number 1
- Uniaxial accelerometer U29: In the edge of the blade number 5
- Uniaxial accelerometer U30: In the edge of the blade number 1

In Figure 55 the distribution of the sensors explained before can be seen for better understanding. The placement of these sensors (mainly the ones of the edge of the blades), as we can see, form a kind of triangle. This way, we can ensure that at least, for a 1ND vibration mode, at least one sensor will be able to detect some displacement. Once we have all the things prepared, blades identified and sensors distributed properly, everything is ready to start measuring, and we proceed to start the modal analysis in the turbine.

The first part of the experiment has three steps. First, it is necessary to obtain the natural frequencies of the turbine, identify the correspondent mode shape, and compare them to the ones obtained in our simulations in Ansys. As we said, this first part of the study corresponds to the chapter 4.2.6 of this project in real life (in the laboratory). Secondly, and this part is different from the others done, it is necessary to identify the blade where the crack will appear. This will be done by drawing an imaginary nodal line with the amplitudes obtained from different points of the blades. Basically, the measured amplitude in the FRF represents the displacement

tendency of the points per unitary force applied on the hitted point. This amplitude is, for better understanding, a kind of acceleration of all the points measured for a determined natural frequency. Studying the entire range of frequencies, we will analytically see the displacement tendency of each point that is impacted. The use of 4 sensors will be very helpful in order to compare results with different sensors, keeping in mind that if the structure preserves a linear behavior, the results of the frequencies of all the sensors should be equal. Let's move on now to the first part of this study, that is to identify the natural frequencies of the turbine.

Firstly, to identify the natural frequencies and the displacements of different points of the turbine, an amount of 5 hits were made in every point mentioned before (I1,I2,I3…I12). In total, thus, 60 good hits were needed in order to have an idea about the vibratory behaviour of the turbine. We made 5 hits per point because it was not enough with one unique measure per point, as there were mistakes while measuring. The Labview software, in this and all experiments we will do from now on will calculate, prepare and show the average of these 5 impacts per point. It is important to note that we spent two days measuring the 12 points, as the hammer impacts are not always good enough because of the sensibility of all the measurement instruments of the laboratory and, approximately, per good point obtained for analyzing, around 5 were not valid for the software.

Once I had the correct data measured, I proceeded to analyse the results of the modal analysis by watching the natural frequency of the structure and the vibration mode for every natural frequency. There were two ways to analyse the vibration modes, but I will explain just one as it is the one we used in all the experiments. Basically, the experiment consisted in obtaining the amplitude of the points where the hit was done. The sensor will provide us the information about these amplitudes (positive or negative) and knowing these values, we could draw the nodal line applying a kind of Bolzano's theorem, that says if in a continuous function (in our case, displacement) there exist one value positive and one negative, that function must be 0 in some value of the range. Let's' see now in Figure 56 the results obtained of frequencies obtained thanks to the sensor T_28_Z, the sensor that clearly showed all the natural frequencies of the turbine:

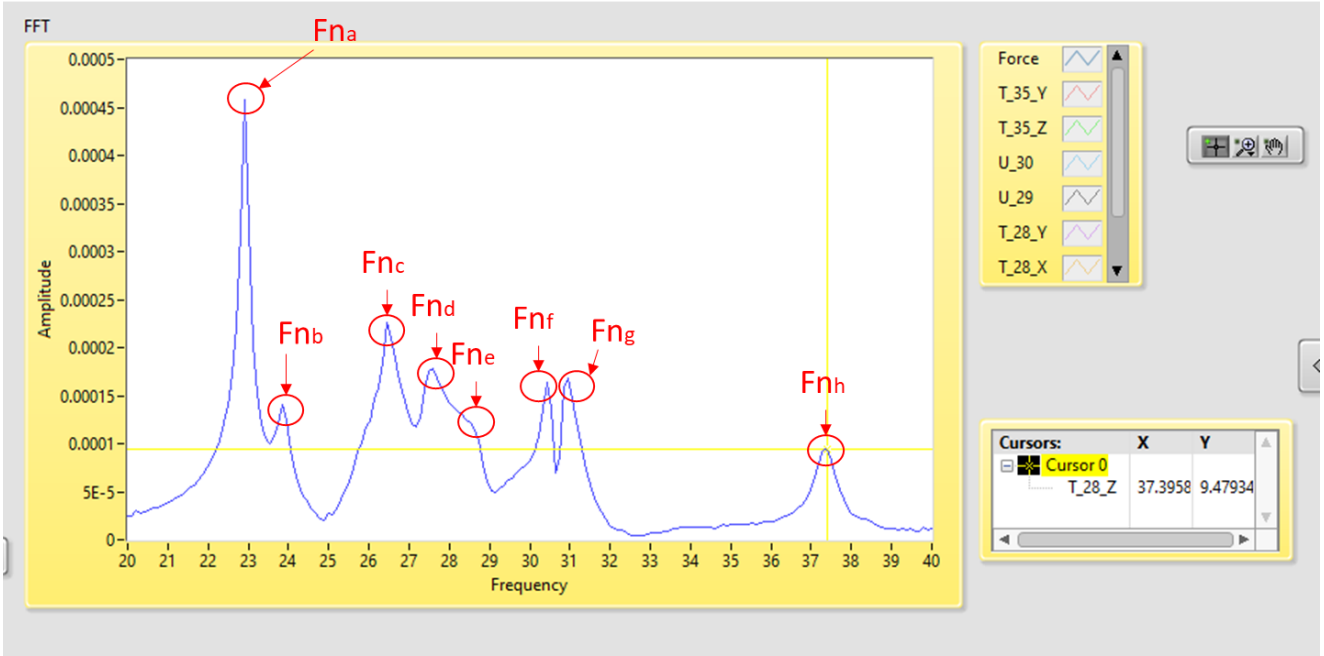

Figure 56: Results obtained of frequency for the initial conditions

As we can see in the image, the results obtained are 8 peaks of amplitude of the response to frequency. There were many more from 60 Hz and up, but we centrated our study in the first vibration modes, as they are supposed to be the easiest to excite and, thus, the most dangerous. Beneath 20 Hz did not appear more natural frequencies for the structure. The following Table 14 shows us the values obtained, with the first impressions and thoughts:

Natural frequency obtained	Value [Hz]	Comments/First thoughts
Fn_a	22,92	It is likely to be a Fn of the turbine (disk+shaft)
Fn_b	23,85	It is likely to be a Fn of the turbine (disk+shaft)
Fn_c	26,45	-
Fn_d	27,5	-
Fn_e	28,75	-
Fn_f	30,52	It is very likely to be a 2ND mode
Fn_g	31,25	It is very likely to be a 2ND mode
Fn_h	37,40	It is very likely to be a 3ND mode

Table 14: Natural frequencies for the initial conditions

Once I had the results of frequencies, the next step was to link the natural frequencies obtained in the laboratory (Fn_a,Fn_b...) with the ones we obtained in the simulation in Ansys (Fn_1,Fn_2...). At first view, it seemed clear that there were 3 of them identified. Firstly, the Fn_h corresponded to Fn_6 of Table 5, as the result was practically the same and the next Fn in the model corresponds to the same natural frequency obtained in the experiment (not represented in the Figure 56), that is 56,30 Hz. Then, another initial thought was that the 2 lowest natural frequencies obtained (Fn_a,Fn_b) corresponded to the natural frequencies of the structure (disk+shaft), as they had to appear in the experiment and both of them had the lowest values of frequency. However, it was necessary to analyze its behavior to affirm if those frequencies corresponded to all the structure or were from the own disk.

Apparently, if the natural frequencies were ordenated as Ansys showed, the Fnc should correspond to the Fn1, Fn_d should correspond to the Fn2, and Fne to the Fn3. However, it is not possible neither to affirm so, as we have to identify first the experimental nodal lines, and identify first the 0NC mode (as it will be the easiest to draw). For drawing this and other experimental mode shapes we will explain the procedure step by step next.

First, thanks to the Labview software it is possible to identify the position of one point while vibrating at a certain frequency (in our case, the points studied are I1,I2…I12). For understanding this, see Figure 57 below:

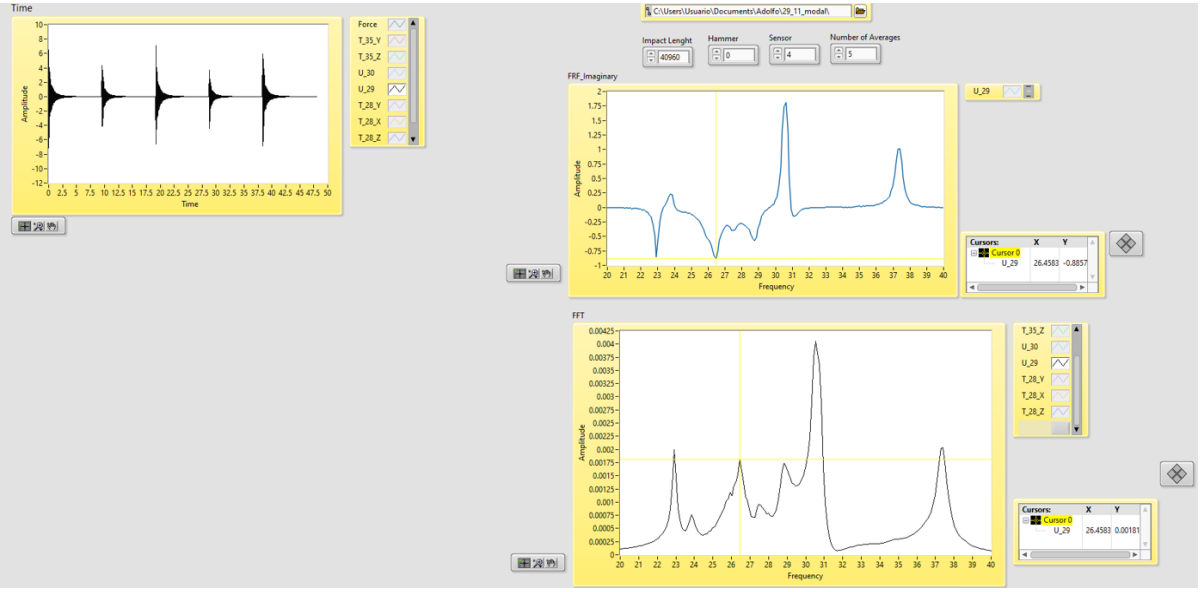

Figure 57: Results of the Labview for one point impact (I11) for the initial conditions

As we can see in Figure 57, there are three main graphs. Firstly, at the bottom of the image, there is the graph of amplitude of response of frequencies of the turbine that the accelerometers read for an impact in the point I11 (in this case). The peaks of amplitude will represent the natural frequencies. The natural frequencies are the same as shown in Figure 56. Over this graph, there is the frequency response function (FRF) of this point and finally, on the left, there are the 5 different hits that we have made for having an average of results.

The procedure to identify the modal parameters is easy. For every average of impact (12 points in total with a 5 impact average) we can identify the response by exiting the turbine in each impact. The FRF will provide us the amplitude of displacements measured for the natural frequency seen in that point. However, depending where a point with low displacement is situated with respect to the others (for example, a point in a nodal line), the results are not as easy to identify. That's why we use four sensors. Although one unique sensor would have been enough for obtaining the results, the use of four of them will clearly show us even 'hidden' responses of peaks of frequencies.

By joining and drawing the amplitude of the different simulations done for every natural frequency, it will be enough to identify the vibration modes of each frequency we have obtained. In this first study, as the points we have drowned in the blades vibrate more than the ones that are near the shaft, it will be enough to measure the amplitude of these 6 points and identify where a '0' displacement point is. The '0' value of amplitude will represent a nodal line.

Firstly, we will try to identify the displacement of the points of the turbine at Fn_a=22,92 Hz. By representing the amplitude of the 6 points of the center/edge of the blade, using the uniaxial sensor U30, situated on the first blade the results obtained were the following shown in Figure 58 below, where we can see the values of amplitude for the 6 points for that natural frequency:

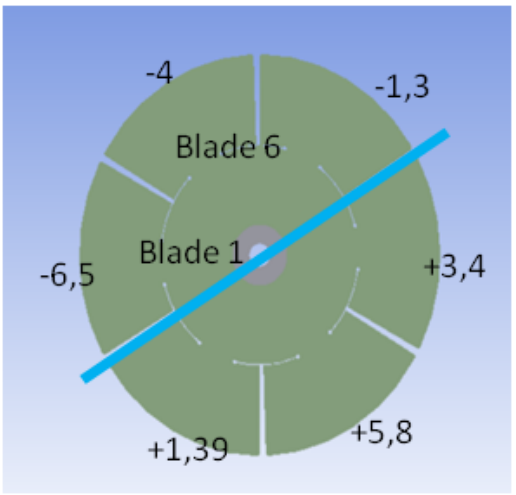

Figure 58: Mode shape of Fn_a

As we can see in Figure 58, the displacement of the disk is separated in two parts, one with positive tendency and the other with negative tendency. This means that the mode shape obtained corresponds to a 1ND mode shape, as the experimental nodal line (represented in blue) divides the different movement of different points of the disk. We can see the nodal line drawn (approximately) between the blades 1-2 and 4-5. Although it was clearly a 1ND mode shape, my manager Xavier Escaler told me that also the natural frequency of the structure (Shaf+Disk) could be represented as this, so it is too soon to say that this is the 1ND mode shape we used for creating and analyzing the evolution of the crack. We will see if some other 1ND mode shape appears and we will try to identify the point of appearance of the crack due to this mode shape.

Secondly, to identify the displacement of the points at Fn_b=23,85 Hz, we will do the same as before, by using the same uniaxial sensor U30. Figure 59 below shows the tendency of displacement of the points of the edge of the blades, and the nodal line found for this frequency:

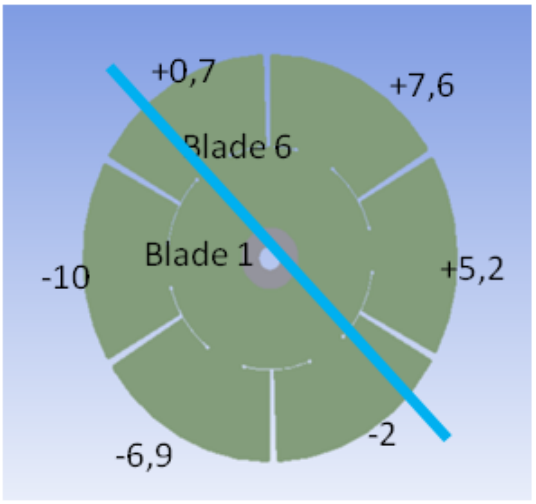

Figure 59: Mode shape of Fn_b

By analyzing this figure, it is obvious that we have found a perpendicular mode shape to the previous found for Fn_a. Nevertheless, as we said before, it is too soon to say that this is the perpendicular to the 1ND we are following (even though it totally coincides with the Ansys). We will have to identify first if this is a vibration mode because of the movement of the axis.

Thirdly, we will try to identify and draw the mode shape for the Fn_c=26,45 Hz. By representing the amplitude of the 6 points of the edges of the blade, using the uniaxial sensor U29, situated on the fifth blade, the results obtained were the following shown in Figure 60 below, where we can see the situation of the sensor and the values of amplitude for the 6 points for that natural frequency:

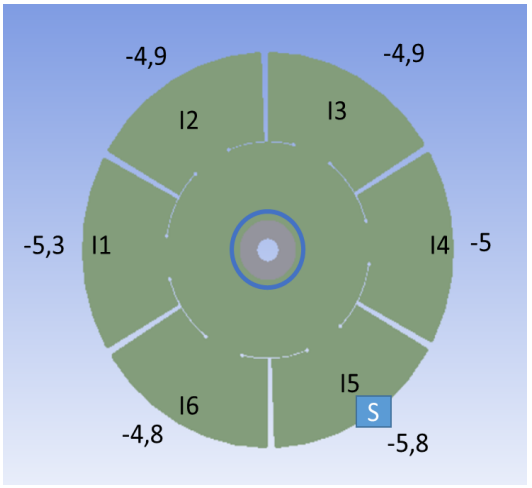

Figure 60: Mode shape of Fn_c

As we can see in the figure, the displacement of all the points is practically equal for all of them. Therefore, and with no doubts, the Fn_c corresponds to the Fn_3 obtained in Ansys, where the mode shape was the 0NC. It corresponds, graphically, to the frame on the top of the right of Figure 28.

For analyzing the following natural frequency, Fn_d=27,5 Hz, we proceeded to do the same as explained before. This time, for using different tools we had in the laboratory, the sensor used was the Triaxial T35Z, which was situated practically on the edge of the third blade. As we can see in Figure 61 in the next page, there are three blades in a row with positive displacement and 3 of them in a row with negative displacement. Therefore between the 2 pairs of points that turn from positive to negative passes the nodal line. We can see the nodal line drawn (approximately) between the blades 1-2 and 4-5 (as happened for the Fn_a=22,92 Hz) in Figure 61 below:

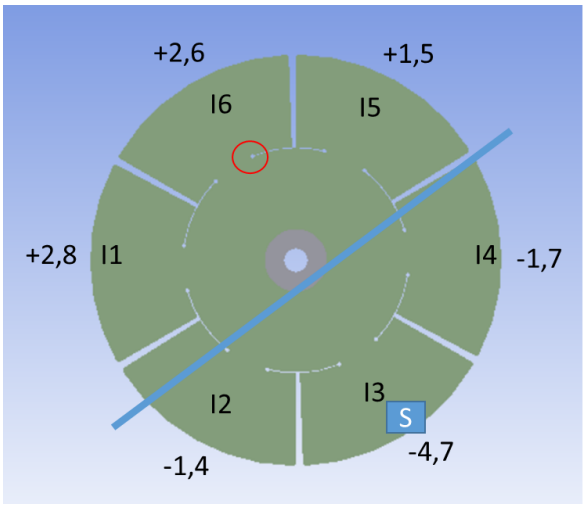

Figure 61: Mode shape of Fnd

Consequently, I can confirm that this mode shape corresponds also to a 1ND. We can see that the points of the blades will displace with respect to one nodal line (the blue drawn). However, due to the existence of another 1ND mode shape, it is not possible to say that this frequency and mode shape are the one I used for doing the crack spread. However, with this result found, I have just identified the point where the crack will appear in our disk. Comparing this Figure 61 and the Figure 58 with the Figure 31, I reached the conclusion that the red-circled point of the blade 6 in this Figure 61 is the point where the crack begins, as comparing it with Ansys, the circled hole of the Figure 61 is the one where the crack begins in the numerical simulations.

Finally, to be sure that the other mode shape is another 1ND (the perpendicular to the previous one), I did the same as explained before. This time, I used the triaxial sensor T28Z in order to draw the theoretical nodal line of this mode shape. Effectively, the results expected can be shown in Figure 62 below, as it is the last 1ND mode shape we needed to find and the nodal line is almost perpendicular to the previous one:

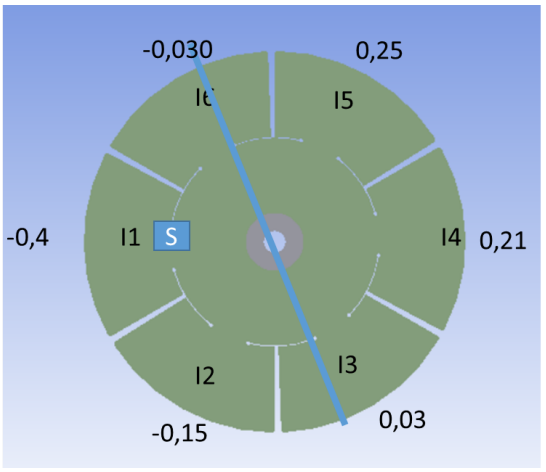

Figure 62: Mode shape of Fne

Finally, to confirm the experimental results of the other mode shapes, similar drawings were made and matched totally the mode shape expected to get (the Ansys results). Once I obtained all this information, I proceeded to compare and see the difference of the results obtained with the expected in Ansys. For knowing how far from reality I was, I compared the results obtained with the ones of model A and B studied in Ansys (chapter 4.2.4 of this project).

To see the results compared, the Table 15 below shows the natural frequencies obtained experimentally versus the ones obtained in the Ansys with the not simplified model and the simplified model (respectively, A and B) and the respective differences between the experimental and numerical simulations.

Number	Experimental Mode shape	Experimental Fn[Hz]	Fn Model A [Hz]	Difference Experimental vs Model A	Fn Model B [Hz]	Difference Experimental vs Model B
1	(1ND)	22,92	-	-	-	-
2	(1ND)	23,85	-	-	-	-
3	(0NC)	26,45	31,24	18,10%	31,26	18,18%
4	(1ND)	27,5	-	-	-	-
5	(1ND)	28,75	-	-	-	-
6	(2ND)	30,52	32,11	5,21%	32,13	5.27%
7	(2ND)	31,25	32,11	2,75%	32,13	2.81%
8	(3ND)	37,40	37,79	1%	37,73	0,8%

Table 15: Comparison between the Fn obtained experimentally with the numericals of models A and B

By beginning seen the difference of frequencies between models, as we can see in the Table 15, for the four 1ND mode shapes (as there are two of the disk and other two of the structure (disk+shaft)), it is not possible to compare them yet with Ansys until more experiments determine the real 1ND mode shape of the disk that will provoke the failure due to fatigue.

We can also see that the most precise results were obtained with model A, as it was expected, because that model is the one closest to reality. Regarding the third result obtained, it seems obvious that there is a huge difference in the 0NC mode shape, but, curiously, the two numerical models A and B have practically the same value of frequency (31,24 Hz). This difference is not actually weird, and it can be explained by the boundary conditions of the experiments. The boundary conditions of the shaft in the laboratory is that it is fixed in two surfaces by bearings, in the same points as in the Ansys simulations. Nevertheless, it is obvious that there is no possibility to have an all surface fixed in reality, as there are only a few points of the shaft that are fixed (enough for holding the turbine). In contrast with this, Ansys takes an all surface as that software has the possibility to simulate it as if it was ideal. In addition, not only this boundary condition is important. In the Ansys simulations it is not shown the test rig that holds the turbine, and this could lead the experiment to have some other differences between models. Anyway, this 0NC mode shape is not important at all for our study, as it will not contribute to the spread of the crack due to a 1ND mode shape.

Focusing again in the 1ND mode shape, the differences between the models will be represented, as we said, once we identify clearly which ones of them found in the experimental analysis of displacements correspond to the real 1ND mode shapes in Ansys, and which ones of them are mode shapes of the structure. The first natural frequency with a 1ND mode shape, as we said, is the most important one for the project, as it has been the one chosen for simulating the appearance of a crack. From this point of differences in the natural frequencies between both experimental and numerical models, and having identified the point of origin of the crack, we will proceed to open the crack, and with the cracks opened in intervals of 25% of the critical length of the crack (as we did in the numerical simulation) we will see how the difference of the natural frequencies changes, and if there is a possibility to relate both models (experimental and numerical), and see if the results of frequencies, vibration modes, and fatigue can be followed not only in Ansys but in a real model too.

Finally, for the other mode shapes, as we can see, the differences are very low in all the results, having also values of error of 1% in the mode shapes with higher natural frequency, like in the 2ND or 3ND.

5.2.3 Experimental analysis with a Crack length equal to 25% of the critical length

Once I obtained the results of the initial conditions and saw that the situation that was studied (failure due to the first vibration mode) was similar to the simulations obtained in Ansys, I proceeded to dismantle the disk from the shaft and took it to the manufacturing workshop. There, with a laser machine and the drawing in Solidworks, the qualified worker proceeded to open the crack that corresponded to the 25% of length of the critical crack length in the blade identified in the previous chapter. The cracked disk can bee seen below in Figure 63:

Figure 63: Disk with the first crack

When I received the disk shown before, I proceeded to install it again in the test rig and put the accelerometers in the same place as the first experiment. Once I have all installed again, I proceeded to start taking measures again by hitting exactly the same points of the first experiment (2 points per blade, one in the middle of the blade closer to the edge and one in the middle and closer to the shaft). An image of myself measuring in the turbine can be seen below in Figure 64:

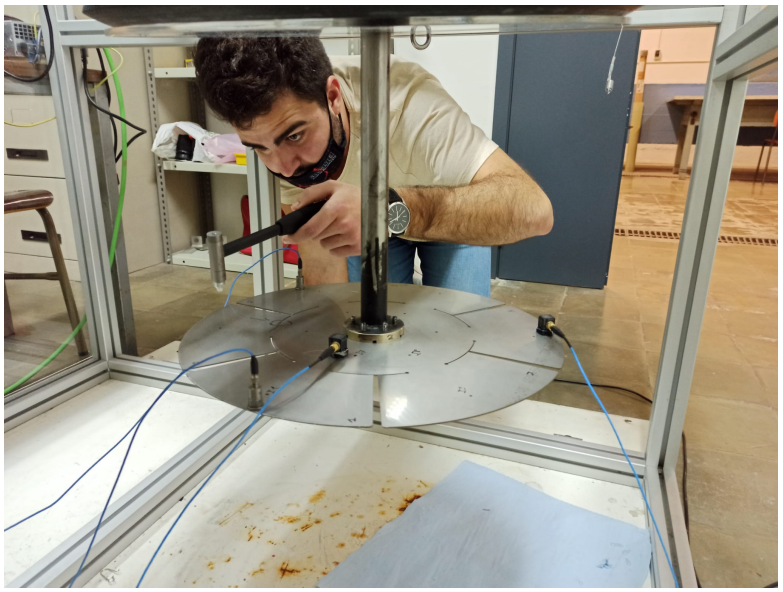

Figure 64: The author of the project hitting the disk

After measuring the disk by impacting in every point an average of 5 good hits, I proceeded to use the Labview and to analyze the results. At first view, the results of mode shapes were not as clear as in the first experiment, as the points closer to the edge of the blade didn't provide much information to distinguish mode shapes of the turbine this time. The frequencies obtained, however, were appearingly good with the points measured. The mode shapes of the natural frequencies with the initial points studied, however, did not contribute at all to clearly identify the vibration mode, and therefore, to identify the frequency followed for the crack. This is why we decided to increase the amount of measures per blade. Moreover, my director recommended me to hit the shaft in two different points to see if the natural frequencies were the same obtained in different parts (disk and shaft). The amount of points measured, in this simulation (and next simulations with longer cracks) per blade doubled the one of the initial conditions, and the approximate distribution of them can be seen in Figure 65 below, where we can appreciate the third blade and 2 additional points to hit in the corners of the blade.

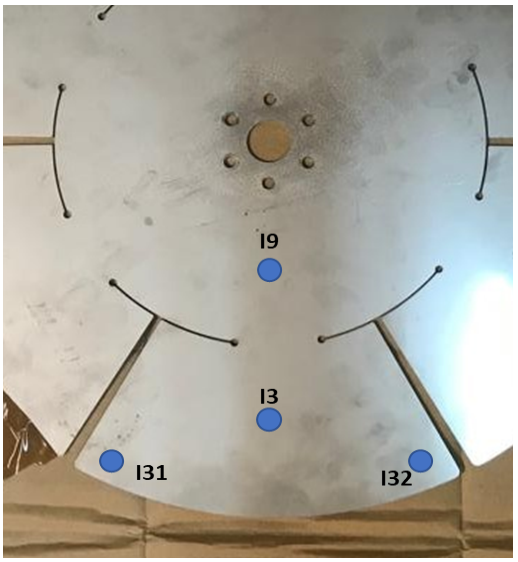

Figure 65: Distribution of the points to study per blade

Once we increased the amount of points to study, the results were clearer this time, and now we will then discuss them. For instance, in Figure 66 below we can see the frequencies obtained for the turbine measured with the uniaxial sensor U_29 :

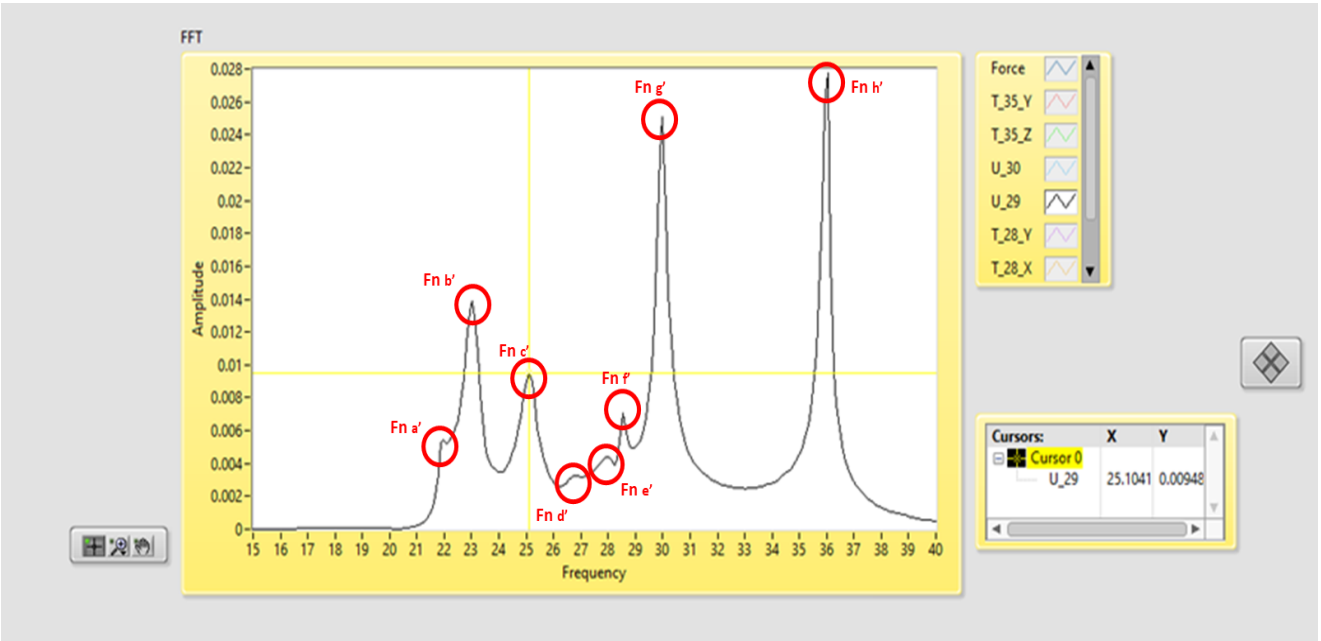

Figure 66: Natural frequencies seen in Labview with a crack of length equal to 25%Critical Length

Figure 66 shows the natural frequencies of the turbine obtained by hitting in the point I1_1 (left corner of the blade 1) and measured by the sensor U_29. There are clearly 8 peaks of frequencies in the range of 0Hz-40Hz. In Table 16 below we can see the results and some initial thoughts about the results obtained:

Natural frequency obtained	Value [Hz]	Comments
Fna'	21,88	-
Fnb'	22,91	-
Fnc'	25,10	-
Fnd'	26,66	-
Fne'	27,91	-
Fnf'	28,6	-
Fng'	30,1	It is likely to be a 2ND mode shape
Fnh'	36	It is likely to be a 3ND mode shape

Table 16: Experimental results of the natural frequencies with a crack of length equal to 25%Critical Length

Once we obtained the natural frequencies of the turbine, we compared the results with both models A and B studied in the numerical analysis by drawing the mode shapes of the disk like I did in the previous chapter (example of Figure 61). On the one hand, I realized that with the first crack of 3,3cm the natural frequencies of model A and model B were slightly different. Nevertheless, the first three natural frequencies of both models were similar (2 of the turbine and the 1ND vibration mode we were using for the crack). On the other hand, the mode shapes were different depending on the model studied (variated how the blades displaced), and that's why to identify the mode shapes and the respective natural frequency in the experiment, we added the shaft to the cracked disk and identified in Ansys the real mode shapes with the cracked disk and the shaft incorporated. The mode shapes for the model A obtained in the range from 0 to 40 Hz in Ansys were the following of Figure 67:

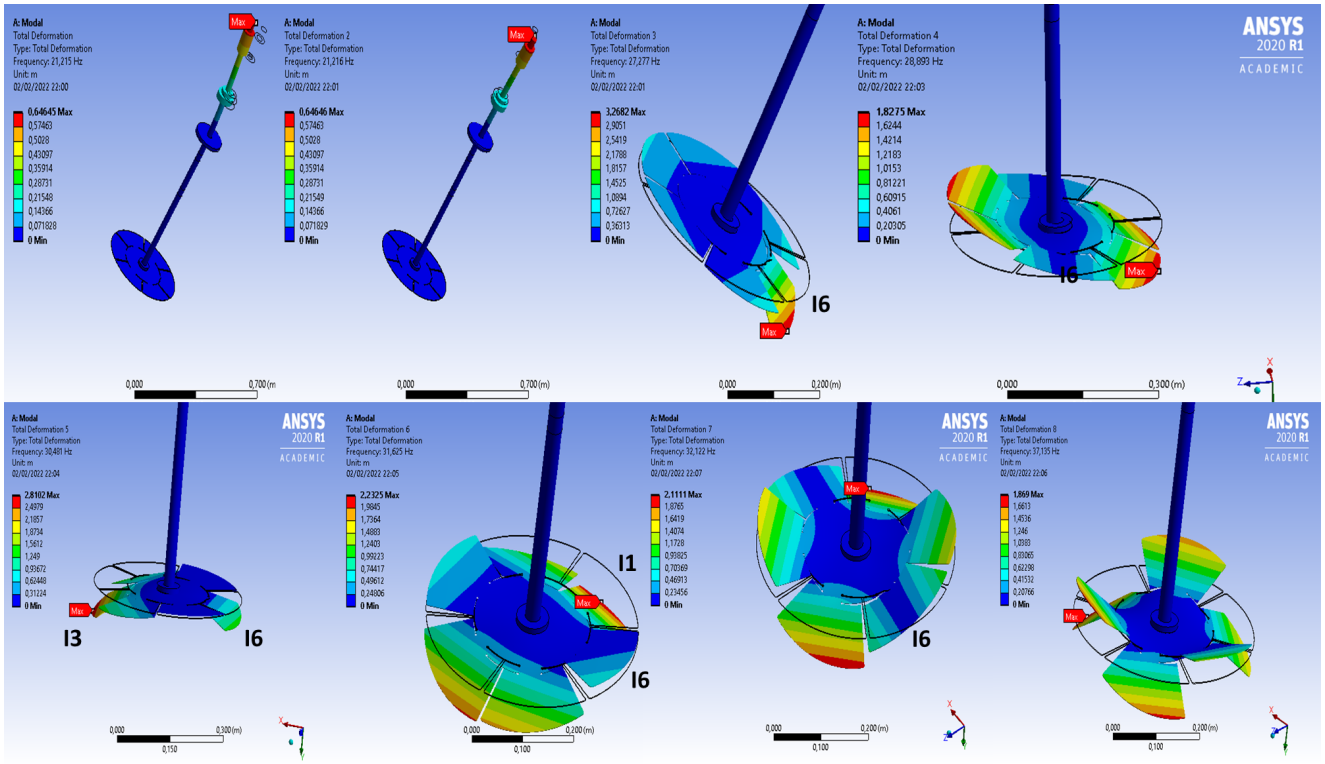

Figure 67: Numerical mode shapes obtained with a crack of length equal to 25%Critical Length

As we can see, there are an amount of 8 natural frequencies in this range, and that coincides with the experimental results obtained in the turbine in the test rig. From this point, the following step was to identify (if possible) the initial 1ND mode shape (the one we are following for doing the crack) between all the frequencies obtained and see if it behaves like the simulation in Ansys. The procedure was the same as explained in the previous chapter. By analyzing the amplitude of displacement for a determined frequency, the mode shape could be drawn studying all the points impacted with the hammer. An example of this can be seen in Figure 68 below, that represents the amplitude of different points at different natural frequencies with the frequency response function. For example, in this figure we can see that for the natural frequency 25,10 Hz the amplitude of displacement of point I5_1 had a value of -4,87.

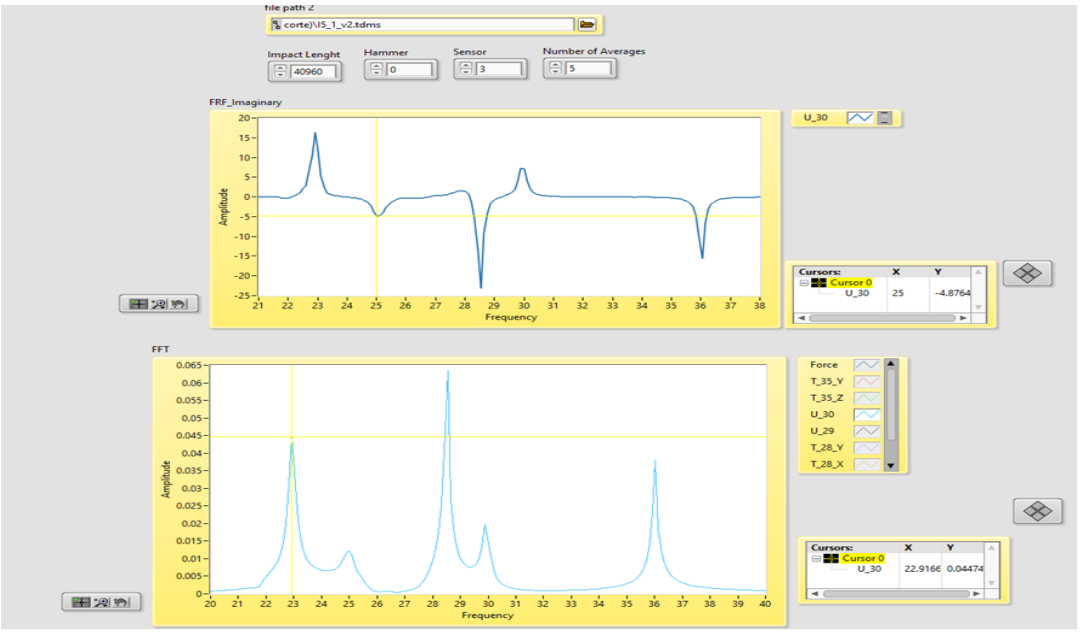

Figure 68: Frequencies and the amplitudes of the point I5_1

Firstly, we will try to identify the displacement of the points of the turbine at Fna'=21,88 Hz. By representing this time the amplitude of the 12 points of the edge of the blade, using the uniaxial sensor U30, situated on the first blade. The results obtained were the following shown in Figure 69 below, where we can see the values of amplitude for the 12 points of the corners of the blades for that natural frequency:

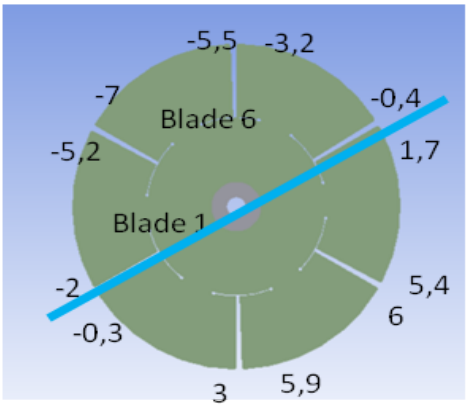

Figure 69: Mode shape of Fna'

To explain this previous figure we can see for example that the point I1_1 (point of the corner left of the blade 1) has an amplitude of -5.2. The point of the corner right (I1_2) has an amplitude of displacements of -2... and so on. We can see that this mode shape is still a 1ND mode shape. However, as happened before, it is not possible to say at all that this is the 1ND mode shape of the disk we are following. Maybe it is a bending of the turbine and the disk vibrates in a 1ND way in the part of the disk. We will have to check in the following mode shapes if it is possible to identify clearly this time the 1ND mode shape we are following.

Secondly, to identify the displacement of the points at $Fn_{b'}$=22,91 Hz, we will do the same as before, by using the same uniaxial sensor U30. Figure 70 below shows the tendency of displacement of the points of the edge of the blades, and the nodal line found for this frequency:

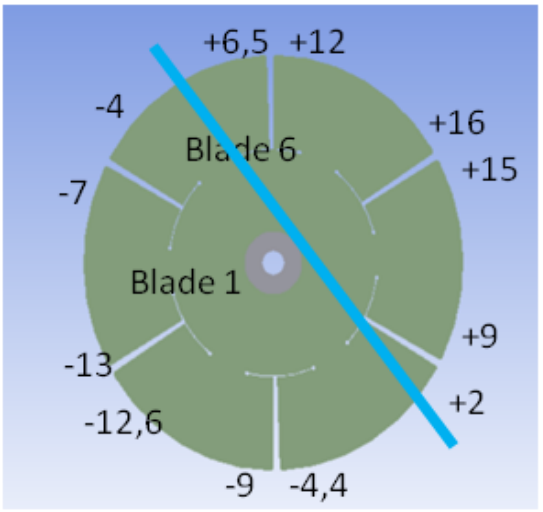

Figure 70: Mode shape of $Fn_{b'}$

To comment on the results obtained, it is clear that this frequency is the perpendicular to the previous found, and it totally matches with Ansys, as still in this simulation we can see the perpendicular 1ND mode shape (see Figure 67 on the top right). However, as we said before, it is too soon to say that this is the perpendicular to the 1ND we are following (even though it totally coincides with the Ansys). We will have to identify first if this is a vibration mode because of the movement of the axis.

Thirdly, we studied the $Fn_{c'}$=25,10 Hz with the sensor T_35_Z (the one of the third blade) and the results were clear in this case and there was no need to use the points of the corners of the blades. In the middle of the all the blades the displacements were negatives and practically the same, excepting the blades 3 and 6, that had a bigger negative displacement, which coincides totally with the mode shape 5 of the numerical simulation (the first of the bottom from the left of Figure 67). This mode shape was our previous 0NC which has changed slightly in this experimental mode shape. Therefore, the concept of 0NC mode shape from this point is lost, as now we don't have a symmetric displacement with respect to the center of the shaft. Below in Figure 71 we can see the displacements of the points studied of the blades for the $Fn_{c'}$ frequency.

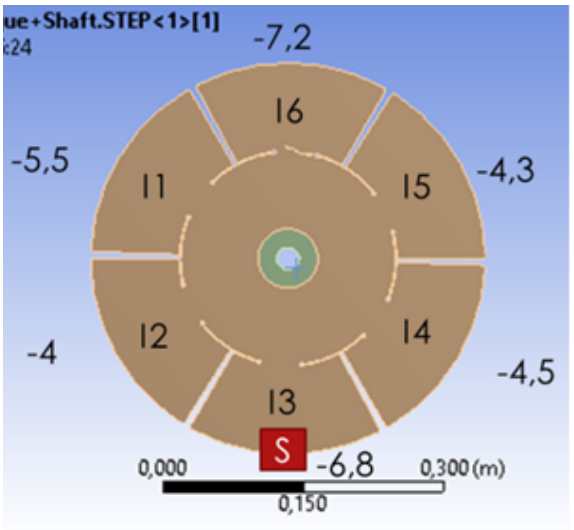

Figure 71: Mode shape of $Fn_{c'}$

Fourthly we studied the natural frequency Fnd'=26,66 Hz. This time we were expecting to see a 1ND mode shape as happened in the previous interval of study. Effectively, as we see in Figure 72 below, measuring with the uniaxial sensor of the first blade U30, a 1ND mode shape can be seen.

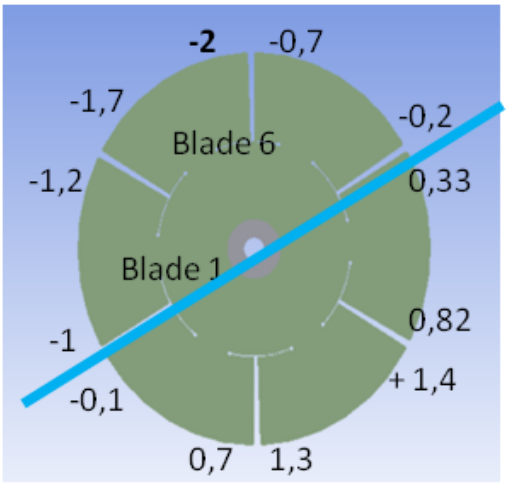

Figure 72: Mode shape of Fnd'

Figure 72 shows the amplitudes of the different points in the turbine measured. It is very significant that the mode shape seen is still a 1ND mode shape as predicted. Moreover, it is very significant also that the point I6_1 has an amplitude of displacement of -2, being this point the one that displaces the most in the disk. This fact could let us think that this mode shape of the Fnd' is the one we are following for the study of the evolution of the crack. However, while reading the results, we saw that the amplitudes of displacements of all the points were not significant at all compared to the other 1 ND mode shapes. Actually, if we see the previous Figure 69 we can see that the amplitudes of displacement of some points and for the same sansor U30 have a value of 7, which is almost three times bigger than the measured for Fnd'. This is a clue that this mode shape of Fnd' probably a 1ND of the turbine (disk+shaft) and not the one we are following from the disk. Actually, thanks to the impacts in the shaft, we can see if these frequencies (Fnd' and Fne') have a bigger amplitude of response than the impacts on the disk. Effectively in Figure 73 below we can see on the left part that the response of amplitudes of the turbine for the (Fnd'=26,66 Hz and Fne'=28 Hz) when hitting the shaft are bigger than the ones obtained when hitting the disk (right part), where there is almost no natural frequency or displacement response in the disk at that frequency.

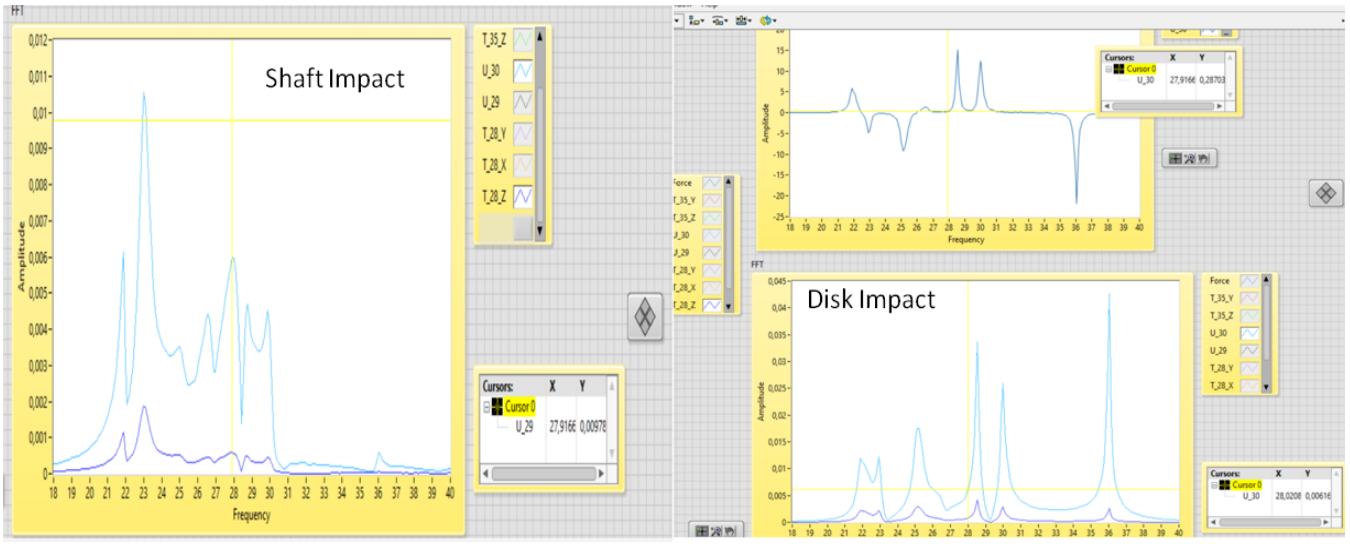

Figure 73: Response of frequencies by hitting in the shaft (left) and disk (right)

Thus, in this part of the project we could practically confirm that we have identified the 1ND mode shape we are following, which is the first mode shape studied corresponding to the Fna'. However, it will be necessary to analyze the next interval of study to confirm 100% our hypothesis.

After this crucial analysis, and once analyzed and identified our theoretical followed natural frequency, we proceeded to compare the other frequencies obtained to see if they really behave like Ansys predicted. The next step was to analyze the Fne'=27,91 Hz. On this occasion, we used the uniaxial sensor U30 situated in the first blade to analyze the mode shape.

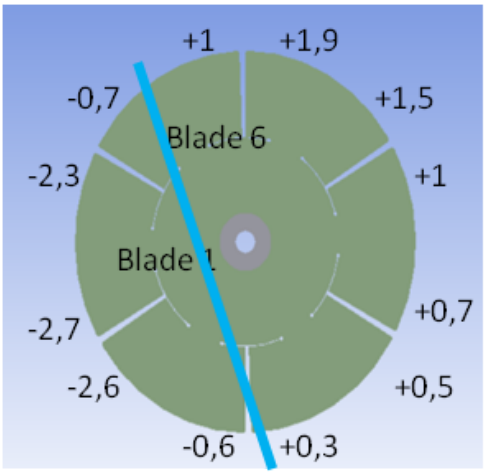

Figure 74: Mode shape of Fne'

As we can see in Figure 74, the result obtained was practically the same as the given in Ansys (see Figure 67). We have obtained a 1ND mode shape whose nodal line is approximately perpendicular to the previous mode shape. Moreover, as happened before, the amplitudes of response of the points of the disk are not as big as in the first two mode shapes, being the biggest amplitude of displacement in this case +1,9 in the I5_2. This fact gives more evidence to our idea that this frequency and the previous one are frequencies of the Shaft+Disk (all the structure).

Let's see now to finish this part of the project of appearance of the crack if the other mode shapes are equal, or at least similar in the numerical simulations and the experiment. Effectively, for this initial crack, all the rest of mode shapes coincided totally with the results in Ansys. We can see in Figure 75 the example of other two vibration modes (the two 2ND). The frequencies were Fnf' and Fng', and, as we can see, the amplitudes of displacement and the nodal lines of the 2ND mode shapes coincided with those obtained in Ansys.

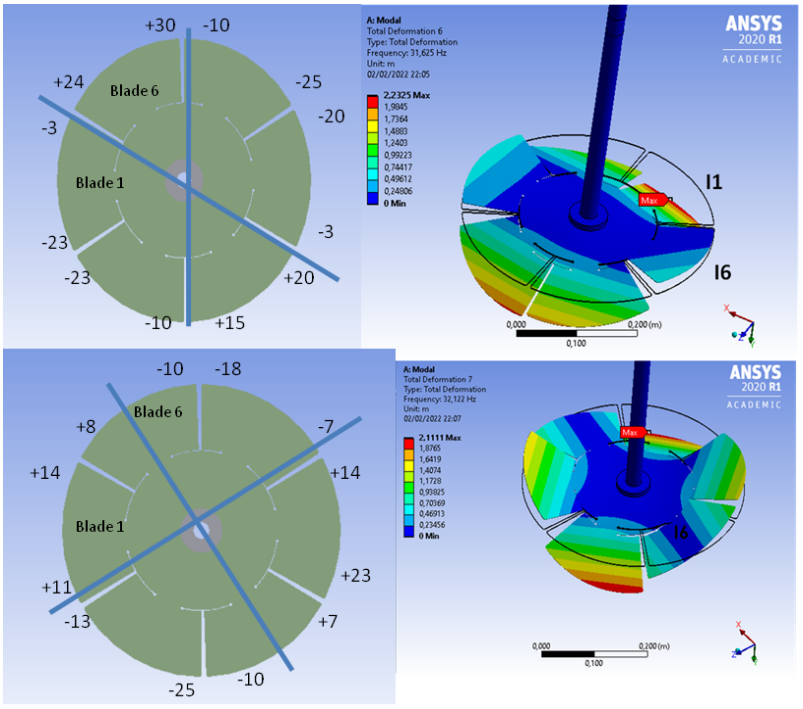

Figure 75: Sketch with the amplitudes and mode shapes of Fnf' and Fng'

From now on in different cuts and intervals of study of the crack, we will focus our attention on the firsts vibration modes, as, for instance, these previous two 2ND mode shape obtained are not very relevant for our study, but having identified them, we can confirm that the disk behave in all the range of frequency studied like Ansys predicted in with this crack length..

Finally, to see the difference between the experimental and numerical results, we did the Table 17 below to see and compare the differences between numerical models A and B and the experimental, although model B does not contribute at all to our study as the real one is the Model A.

Number	Experimental Mode shape	Experimental Fn[Hz]	Fn Model A [Hz]	Difference Experimental vs Model A	Fn Model B [Hz]	Difference Experimental vs Model B
1	(1ND)	21,88	-	-	-	-
2	(1ND)	22,91	-	-	-	-
3	(Initial 0NC)	25,10	30,48	21,43%	30,95	23,31%
4	(1ND)	26,66	-	-	-	-
5	(1ND)	28	-	-	-	-
6	(2ND)	28,60	31,62	10,56%	-	-
7	(2ND)	30,1	32,12	6,71%	-	-
8	(3ND)	36	37,14	3,17%	-	-

Table 17: Comparison numerical and experimental results with a crack of length equal to 25%Critical Length

The results that show this Table 17 are clear. From this point, the highest natural frequencies have an error of less than 11% in all cases, calling our attention the 3ND mode shape, which has an error of only 3,17%. Regarding the initial 0NC mode shape, the explanation of this big difference between models (21,43%) was done in the previous part of study (boundary conditions), so we will not explain it again.

Regarding the four 1ND mode shapes, although it is very likely that the first 2 obtained in the experiment corresponds to the ones of the disk (and therefore, the ones we are using to follow the crack), we will compare them with the Ansys results if the tendency in the turbine with a crack of length equal to 50% of the critical length continues, and our thoughts are proven in the following results of the displacements of the points in every mode shape.

From this point, and having seen a good relationship between models, let's move now to the part where the second crack is opened in the turbine. This next interval of study is quite interesting, and it could be determinant, as it could demonstrate the tendency followed by the turbine in the firsts two studies, so we could directly compare all the mode shapes between the experimental and the numerical simulations.

5.2.4 Experimental analysis with a Crack length equal to 50% of the critical length

Let's move now to study the turbine with a crack of length equal to the 50% of the critical length. The objective at this point of study is to check if the vibratory behaviour of the turbine is the same, or at least similar to the numerical results obtained in Ansys, including both natural frequencies and mode shapes. Moreover, we will try to analyze if our thoughts were right, as we should see in the first frequency a 1ND mode shape similar to the one obtained in Ansys, having in the broken blade higher displacements while the crack spreads.

The initial step was to take the disk to the manufacturing workshop and wait until they opened a crack of the mentioned length with the SolidWorks files given to the worker. Once the new crack was opened, we proceeded to install the disk in the test rig. Figure 76 shows the disk of the turbine cracked after opening the packaging.

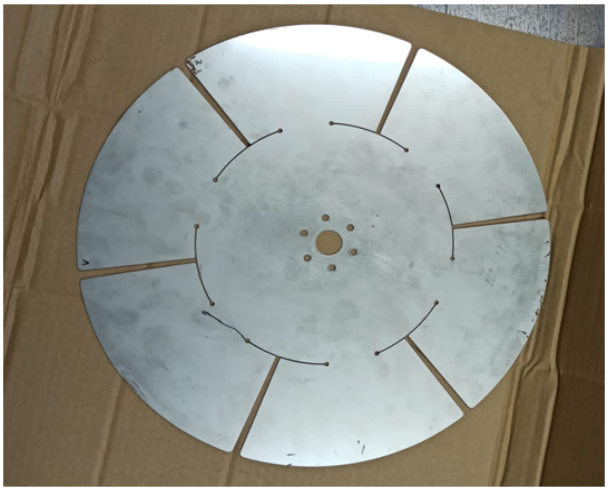

Figure 76: Turbine with a crack of length equal to 50% of the critical length

As we can see in the previous figure, the crack is not much longer than the previous one done in the disk (see Figure 63). Nevertheless, the results are expected to change just because of this tiny crack. After installing it, and configuring the computer, module and sensors like we did in the two previous interval of study, we proceeded to hit the same points of the previous interval (crack length equal to 25% of the critical length) for having an idea about the information of the amplitude of those points, as they were considered good points to hit for our study, having seen that the previous results were totally successful.

Like we did before, after having hit an amount of 120 times properly in the disk and 10 times in the axis, the results of frequencies obtained thanks to the Labview software using the uniaxial sensor U_29 were the following shown in Figure 77 below:

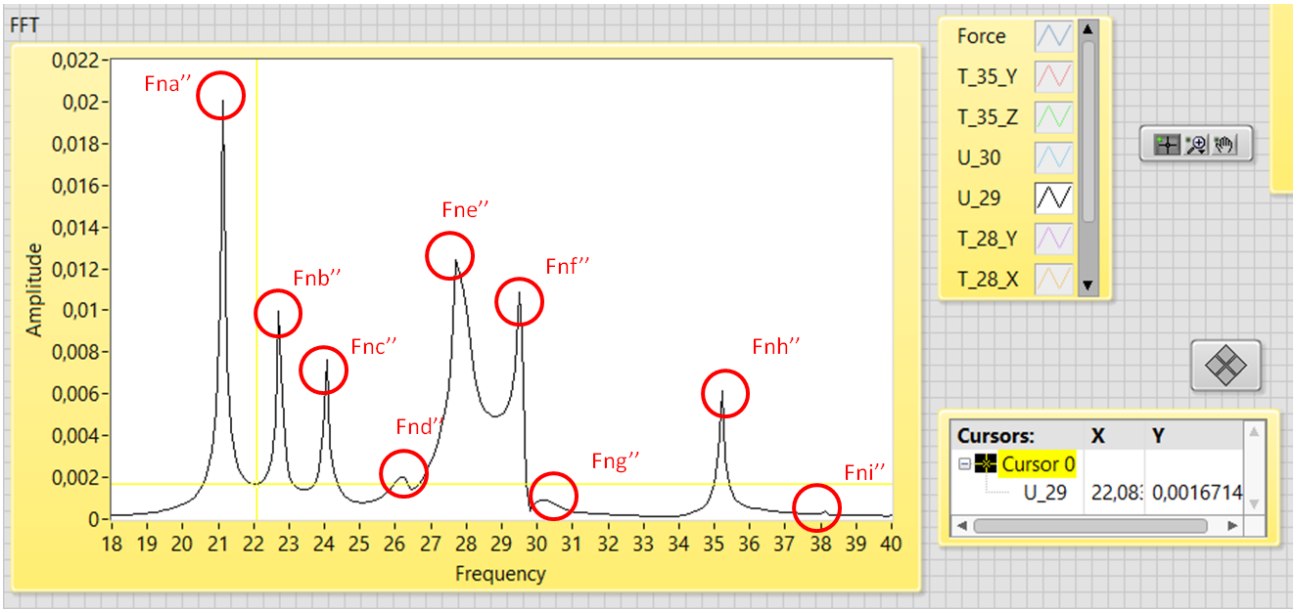

Figure 77: Natural frequencies seen in Labview with a crack of length equal to 50%Critical Length

The natural frequencies obtained, therefore, after moving the cursor through the interval of frequency response in the interval from 0-40 Hz of the Labview were the following shown in Table 18:

Result obtained	Natural frequency [Hz]	Comments
Fn$_{a}$”	21,14	It is likely to be the 1ND we are following
Fn$_{b}$”	22,71	
Fn$_{c}$”	24,06	This should the a variation of the initial 0NC
Fn$_{d}$”	26,14	This should be a frequency of the Shaft+Disk
Fn$_{e}$”	27,81	This should be a frequency of the Shaft+Disk
Fn$_{f}$”	29,58	
Fn$_{g}$”	30,32	
Fn$_{h}$”	35,21	
Fn$_{i}$”	38,12	

Table 18:Experimental results of the natural frequencies with a crack of length equal to 50%Critical Length

The first thing we noticed with respect to the previous part of the study is that in this case there were 9 natural frequencies in the range of 0-40Hz, one more than the previous experiments. This means that due to this tiny new crack opening, there has been for sure a change in the vibratory behavior of the turbine, as now it has found another dangerous way to vibrate in the range we are studying. In the previous analysis, after 40 Hz the closest frequency was approximately 60Hz, so it is not possible to see a reduction of 20 Hz of the vibration mode of that frequency. Therefore, we conclude that another hazardous vibration mode has appeared.

For comparing and analyzing the vibration modes, both numerical and experimental, as we did earlier, we added the shaft to the disk in the simulations, and proceeded to solve the system disk + shaft like we did before. The results of the mode shapes obtained in Ansys can be seen in Figure 78 below:

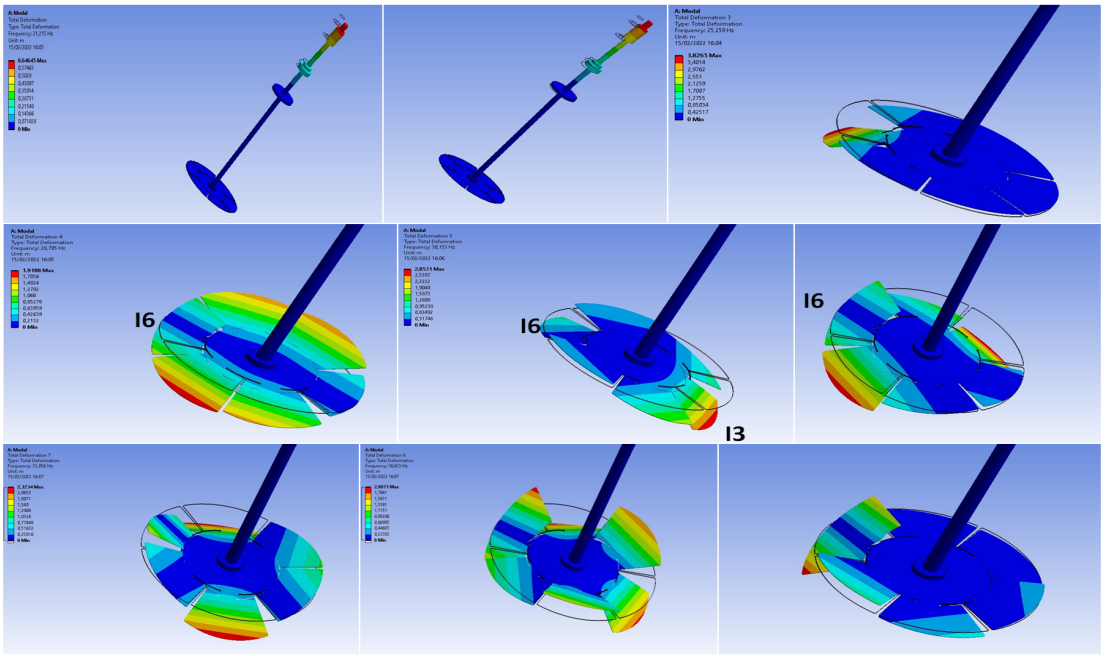

Figure 78: Numerical mode shapes obtained with a crack of length equal to 50%Critical Length

For having an idea of the natural frequencies obtained in this numerical simulation of the results shown in Figure 78 , below in Table 19 we can see the Ansys numerical values of those frequencies:

Result obtained	Natural frequency [Hz]	Observation
Fn1"	21,215	Shaf+Disk
Fn2"	21,216	Shaf+Disk
Fn3"	25,26	Mode shape we are following
Fn4"	28,80	
Fn5"	30,153	
Fn6"	31,49	
Fn7"	31,85	
Fn8"	36,613	3ND
Fn9"	38,65	Torsion of the damaged blade

Table 19: Numerical results of the natural frequencies with a crack of length equal to 50%Critical Length

The first conclusion we can get from here is that, at least, the amount of frequencies obtained in the range of study in the numerical simulation are the same as the experimental ones. This means that the frequency response is at least similar in both models. Nevertheless, having the same number of natural frequencies doesn't mean that the mode shapes had to be equal in both models, numerical and experimental.

To see if the experimental mode shapes still preserve the theoretical way obtained in Ansys in all the frequencies, we proceeded to analyse the amplitudes of the points excited to see if there is relation between the experimental and numerical models. Firstly, we proceeded directly to study the Fna" and Fnb". Regarding the **Fna"= 21,14 Hz** below we can see in Figure 79 the results of the displacements of the points experimentally:

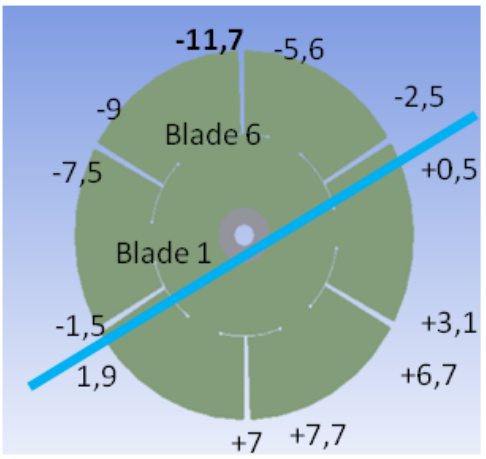

Figure 79: Mode shape of Fna"

As we can see, effectively, the disk vibrating at this frequency still preserves a 1ND mode shape, and we can confirm at this point of the experiment that we have obtained for sure the experimental natural frequency we have used in the first part of the project (Chapter 4) for studying the evolution of a crack in a turbine. We can say this because, as we can see in the figure, the mode shape coincides totally with the expected in Ansys for the 1ND we are following (see top right of Figure 78). The amplitude of the broken blade in Ansys is bigger than the others, having in the closest part to the crack the biggest displacements. The Ansys result totally matches with the experimental ones, as we have an amplitude of -11,7 in the point closer to the crack of the broken blade, almost doubling the maximum displacement obtained in the opposite corner of the disk (+6,7). The rest of the disk still preserves a 1ND mode shape (although it is represented totally in blue in Figure 78). If we zoom in on that figure, on the top right we will see that still one part of the turbine has positive displacement while the other half approximately is negative, having the highest displacement in the point I6_1. Therefore, we have identified clearly now the frequency and mode shape we are following. This will be useful for comparing it in future and previous experiments with the Ansys results.

Regarding the Fnb"= 22,71 Hz we should have the perpendicular 1ND mode shape to the previous one. It is still almost symmetrical without the influence of the crack. Effectively, in Figure 80 below we can see the mode shape that still preserves its shape as Ansys predicted (Figure 78, in the middle-left).

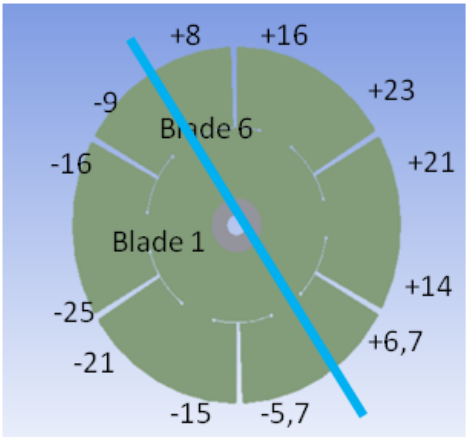

Figure 80: Mode shape of Fnb"

Centring our study in the following three natural frequencies the first thing that came to our mind was that watching the previous results, Fnc" should be the initial 0NC mode shape that in the previous Ansys result shown in the middle of Figure 78. It should become in a mode shape with the blades 3 and 6 with higher amplitudes and negatives, with all the rest having similar and negative values as well. Effectively, as we can see in Figure 81 below, in this case the mode shape obtained was similar to the predicted in Ansys, but there existed a big difference in the value of the frequency for the reason already explained in previous chapters (bearings and boundary conditions):

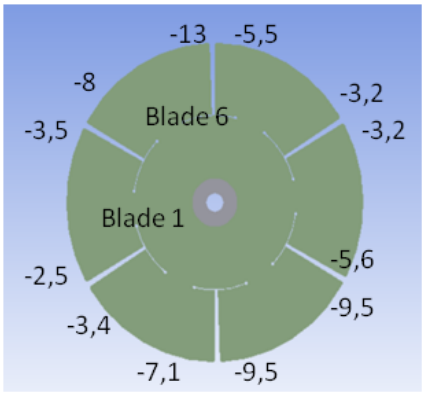

Figure 81: Mode shape of Fnc"

As we can see, to comment briefly on this result, the difference between the natural frequency of the experiment and the numerical simulation is quite big. However, in this case, the vibration modes of the experiment and the simulations are quite similar, as the maximum amplitudes effectively in both models are seen in the blades 3 and 6. The only difference is that for the numerical simulation, the maximum displacement can be seen in the blade 3, meanwhile in the experiment can be seen in the blade 6, the cracked one.

The following natural frequency Fnd"=26,14 Hz was supposed to be the initial a mode shape of the shaft+disk, as we have identified before the 1ND mode shape that was only of the disk. Below in Figure 82 we can see the experimental results of displacement of the points of the disk:

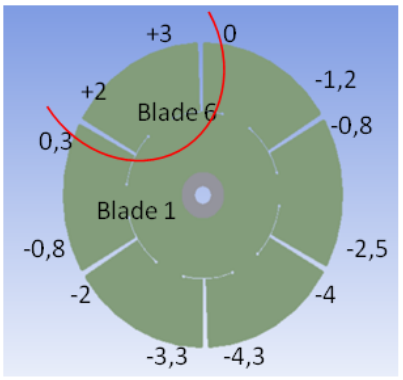

Figure 82: Mode shape of Fnd"

As we can see in Figure 82, the results obtained are quite different from the ones we have been obtaining. This is the first time that an initial 1ND mode shape drastically changes its mode shape. This result is actually brilliant for our study, as we have proved that this mode shape (which initially was a 1ND) is in fact a mode shape of the disk+shaft. As we can see, it is in contra phase just the blade 6 with respect to the rest of the disk, so we can confirm that the initial 1ND mode shape is lost and we can confirm that this vibration is of all the turbine and not just of the disk.

Finally, the following natural frequency Fne"=27,81 Hz was analyzed as well and confirmed our thoughts, as also this frequency lost the 1ND mode shape into a similar one to the previous Fnd" shown in Figure 82.

To end with this part of the study, we will compare the differences between the theoretical and experimental values of the natural frequencies. For doing so, it is necessary to compare the numerical model with the shaft added to the disk (initial Model A of the simulation) and the experimental natural frequencies we have obtained in the laboratory. The objective in this part is to see if the differences of the natural frequencies between models are not huge in the frequency response with a crack of length 50% of the critical length, and, consequently, try to analyze if the cracked turbine can be followed numerically without need to stop the production of electricity of the real model. If there is similarity between models also in terms of frequency, we could contribute to identify even better appearances and evolutions of cracks in turbines due to its frequency response. In Table 20 below we can see the comparison between models and its relative difference:

Result obtained	Experimental Natural frequency [Hz]	Numerical Natural frequency [Hz]	Difference [%]	Comment
1	**21,14**	**25,26**	**19,4%**	**1ND we are following**
2	22,71	28,8	26,80%	Perp. 1ND
3	24,06	30,153	25,32%	Initial 0NC
4	26,14	21,21	18,85%	Disk+Shaft
5	27,81	21,21	23,73%	Disk+Shaft
6	29,58	31,49	6,46%	Initial 2ND
7	30,32	31,85	5,05%	Initial 2ND
8	35,21	36,613	3,98%	3ND
9	38,12	38,65	1,39%	Torsion of the broken blade

Table 20: Comparison between models with a crack of length equal to 50%Critical Length

To comment on the results, it is necessary to start analyzing the differences in terms of frequency. As we can see in the table above, it seems clear that for the lowest frequencies of the turbine the differences between the values of the numerical and the experimental models are big, having values for example of 25% for the initial 0NC mode shape. However, although the numerical value of the frequencies are important and the differences are big, the way we are going to identify the crack is due to the mode shape and the displacement analysis, and the mode shapes analysis that we have done for these 3 initial frequencies totally matched between the numerical and experimental models as we have seen in the previous figures.

Another important thing is that there are 4 natural frequencies obtained that have a difference lower than 6,5%, which are the last 4 of the range of study. Having seen that in the first three analysis the higher frequencies n the range of study have similar values in terms of value of frequency and displacement of the points, we will do an extra chapter analyzing more in detail frequencies like the 3ND mode shape, and seeing if this can be one reference for studying variations in vibrations that appears in turbines due to the appearance of a crack.

Centering our analysis in the natural frequency we are following (shown in bold in the table), we can consider that in terms of value of frequency the difference is big (19,4%), although it is not the biggest of all of them. The frequency in this experiment should be followed not for comparing values between models, but by comparing the way that the disk vibrates. The difference in terms of values is important, but the fact that will identify the crack is the displacement of the points, and not the exact value of the frequency.

5.2.5 Experimental analysis with a Crack length equal to 75% of the critical length

The next step of this project was to analyze the behavior of the turbine with a crack of length equal to 75% of the critical length. To link concepts with the previous study, one of the objectives of this part will be to analyze if the natural frequency we said that would provoke the crack still preserves the mode shape expected and if the frequency has changed as expected in the numerical simulations. As this part of the study becomes hazardous for the turbine, as the crack is considerably long, we will try to see if with this crack length the behavior of the turbine is still linear by using the different sensors and comparing them. This part of the project, due to the crack length, becomes very unclear, as we have entered in the range that this disk could break suddenly, as it is supposedly in a zone of frequencies likely to break, which is the Zone 3 of the theory explained (see Figure 51 and the theory explained below that figure about the different zones of work with a crack in a machine).

As we did in the previous parts of the project, the first step was to take the disk to the manufacturing workshop and wait until they opened a crack of the mentioned length with the SolidWorks files given to the operator, and then, after using the laser machine, take it back again to the laboratory. Once the new crack was opened, we proceeded to install the diskit in the test rig. Figure 83 shows the disk cracked after opening the packaging.

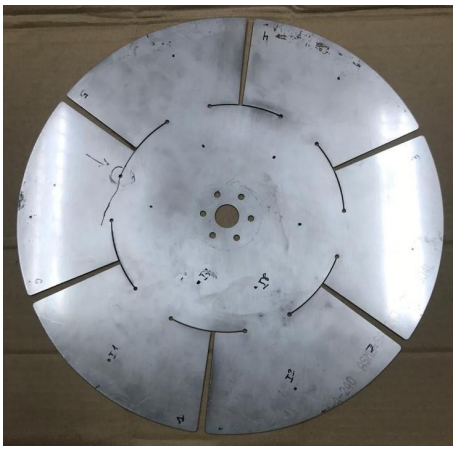

Figure 83: Turbine with a crack of length equal to 75% of the critical length

As we can see, the crack has become slightly bigger (compare it with Figure 76). Apparently, anyone should say that it is about to break just because of the length of the crack. Once I had all installed again in the test rig, I proceeded to take measures again by hitting the same points of the previous experiments. After having hit an amount of 120 times properly in the disk and 10 times in the axis, the results of frequencies obtained thanks to the Labview software using the Uniaxial sensor U_29 were the following shown in Figure 84 below:

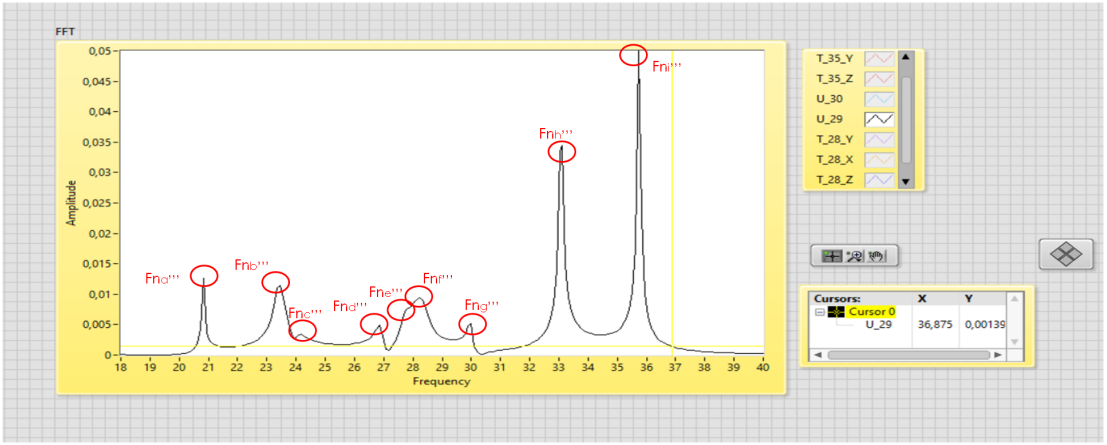

Figure 84: Natural frequencies seen in Labview with a crack of length equal to 75%Critical Length

The natural frequencies obtained, therefore, after moving the cursor through the interval of frequency response in the interval from 0-40 Hz of the Labview were the following shown in Table 21:

Result obtained	Natural frequency [Hz]	Observation
Fn_{a}'''	20,83	It is very likely to be the one we are following
Fn_{b}'''	23,33	It is likely the 1ND perpendicular to the one we are following
Fn_{c}'''	24,06	This should the a variation of the initial 0NC
Fn_{d}'''	26,88	This should be a frequency of the Shaft+Disk
Fn_{e}'''	27,81	This should be a frequency of the Shaft+Disk
Fn_{f}'''	28,23	
Fn_{g}'''	30	
Fn_{h}'''	33,02	
Fn_{i}'''	35,83	3ND

Table 21: Experimental results of the natural frequencies with a crack of length equal to 50%Critical Length

The first observation of this experiment done is that, despite the previous Figure 84 shown (where the results of the peaks of frequencies are clear), this time obtaining these natural frequencies was not as easy as the previous simulations. In many occasions, depending on the sensor used, the natural frequencies obtained were a little bit different between sensors (differences of 0,2Hz up to 0,3Hz), which is higher than the sampling range, and, depending on the point hitted, some new frequencies appeared while others didn't. Therefore, in this range of work, it is obvious that the structure is having a different behavior than before, as earlier, in previous experiments, responses of frequencies were clear and were always the same values independently of the point exited and sensor used. The explanation of this change in the behavior can be analyzed by the spread of the crack. As it continues growing, the symmetry of the turbine is losing slowly, and the longer the crack, the more difficult it is for the sensors to analyze and obtain the same response of frequency for the turbine. Anyway, for comparing the frequencies, a range or difference of 0,2 or 0,3 Hz for this crack length will not be very significant at all for following the first natural frequency. The importance will come from the mode shapes, but, as we have been seeing, if the mode shapes still preserve the numerical values of displacements of the points of the turbine it will be a total success.

For trying to compare the vibration modes obtained, both in numerical simulations and experiments, we added the shaft to the disk in the simulations in Ansys and proceeded to solve the system of the entire turbine (Disk+Shaft) like we did before. The results of the mode shapes obtained can be seen in Figure 85 below:

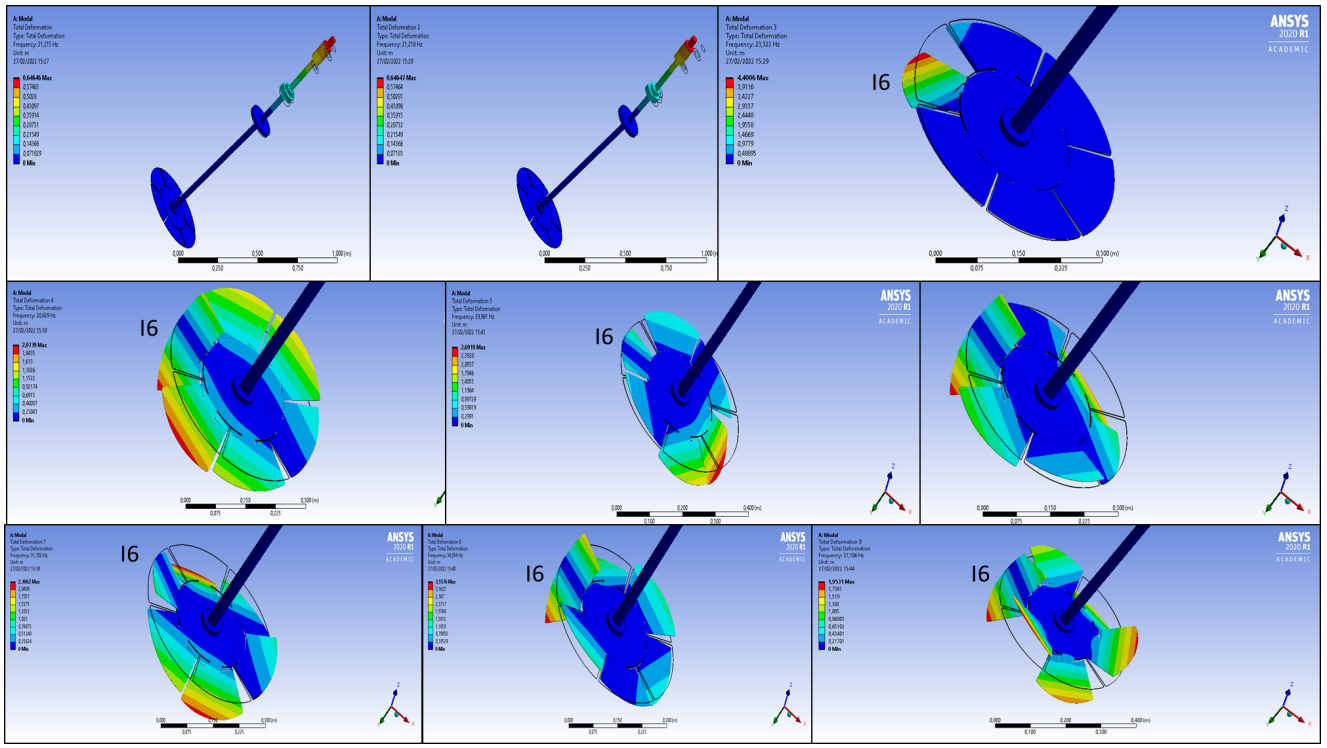

Figure 85: Numerical mode shapes obtained with a crack of length equal to 75%Critical Length

For having an idea of the numerical natural frequencies obtained, below in Table 22 we can see the Ansys results:

Result obtained	Natural frequency [Hz]	Observation
Fn1'''	21,215	Shaf+Disk
Fn2'''	21,218	Shaf+Disk
Fn3'''	**23,322**	**Mode shape we are following**
Fn4'''	28,629	-
Fn5'''	29,961	-
Fn6'''	31,056	-
Fn7'''	31,702	-
Fn8'''	34,854	-
Fn9'''	37,106	3ND+ Torsion of the broken blade

Table 22: Numerical results of the natural frequencies with a crack of length equal to 75%Critical Length

After doing this experiment, we can confirm the tendency we were having while the crack spread continues, as the amount of natural frequencies in the range studied are the same as Ansys. However, it is necessary as always to study the amplitude of different points in the disk to see if the experimental results match with the numericals one.

When I started the experiment, and after watching the second natural frequency it seemed weird at first, because in this simulation was the first time that a natural frequency increased after increasing the length of the crack. However, there was an explanation given by my director. In this interval, while the disk was in the manufacturing workshop, other experiments were carried out in the test rig, and there was a reconfiguration of the bearing and the mounts. Therefore, a little change in the boundary conditions was made. Anyway, it did not affect the experiment at all, as only some natural frequencies increased (and only a few tenths), for example, the perpendicular 1ND mode shape to the one we are following and the 3ND mode shape. Regarding this 3ND mode shape, we will talk and put more emphasis at the end of this work, as we have seen a clear tendency on it.

After this explanation, let's begin now the analysis of the amplitudes for the first natural frequencies. Firstly, we will try to identify the displacements of the points of the turbine at **$Fn_{a'''}$=20,83 Hz**. By representing this time the amplitudes of the 12 points of the edge of the blade, using the uniaxial sensor U30, situated on the first blade the results obtained were the following shown in Figure 86 below, where we can see the values of amplitude for the 12 points for that natural frequency:

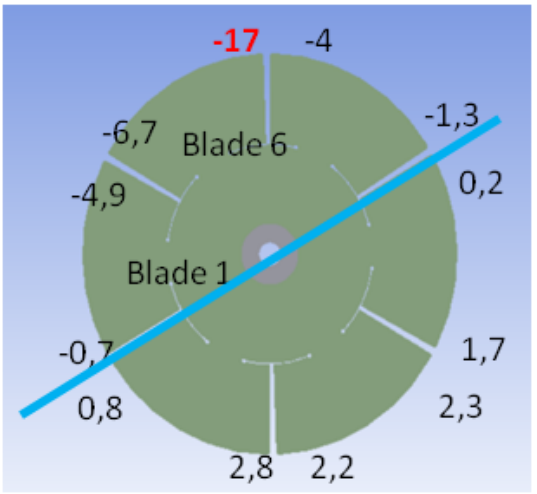

Figure 86: Mode shape of $Fn_{a'''}$

As we can see, there is a total match with the prediction of Ansys for this frequency (see Figure 85 on the top right). Yet a 1ND mode shape is shown, and also there is the existence of a point of extreme displacement, **-17** of amplitude highlighted in red, which is the point I6_1. This result totally coincides with the 1ND mode shape we are following. The rest of the points have very low displacement (specifically the points with positive displacement, as Ansys predicted) and the turbine still preserves a 1ND mode shape, but having a huge displacement in the broken blade. Therefore, we can say that this is a total success, as still with a 75% of crack the displacements of the turbine of both numerical and experimental models still match, and this is very useful for identifying the evolution of cracks in turbines and its possible failure and lost of efficiency due to the effect of fatigue.

Regarding the $Fn_{b'''}$= 23,33 Hz we should have the perpendicular 1ND mode shape to the previous one. As we said, the frequency increased a little bit due to the modified boundary conditions, but this should not affect the vibration mode of the turbine.The result should be an 1ND practically symmetrical as we have had in the previous results of the second frequency measured by the sensors. Effectively, in Figure 87 below we can see the vibration mode that still preserves its shape as Ansys predicted (Figure 85, in the middle-left):

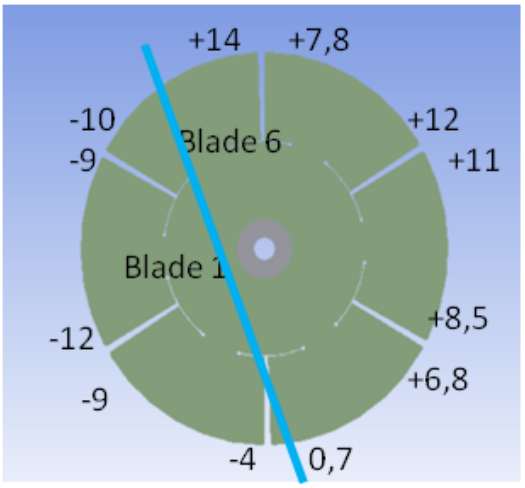

Figure 87: Mode shape of $Fn_{b'''}$

This second result is magnificent too, as the turbine also in the second vibration mode (the second most likely to fail due to fatigue if the first one doesn't) matches the behavior between numerical and experimental models. So far, the results of the displacements of the two first mode shapes have totally matched between models, so this can mean that these two initial frequencies can be followed until the 75% of a crack by sensors (in our case study, accelerometers).

Continuing with the experimental analysis, the next step was to analyze the $Fn_{c'''}$=24,06 Hz. We expected to see, as we have seen in the 3 previous simulations, the initial 0NC mode shape modified. However, in this experiment, the results were a little bit different. As we can see in Figure 88 below, and compared with the Ansys solution in the middle of Figure 85, for this crack length the mode shape does not match between models. It is the first time that in the turbine for the initial 0NC mode shape while suffering the effect of fatigue the numerical solution of displacements does not coincide with the experimental results. As we can see in Figure 88, there is one part of the turbine (just 2 blades) that are in contra phase with respect to the other blades. While in Ansys the blades that are in contra phase are the blades 2 and 3, in the experiment the blades are the 3 and 4. Moreover, those positive values are not big at all, as the maximum positive is +0,9 while the maximum negative is -4,8 (almost 5 times more). Ansys also estimated that the maximum displacement value is in the third blade, while in the experiment, the maximum displacement is in the broken blade number 6. Probably, due to the crack length the symmetry in the model is lost and the initial mode shape 0NC has been lost and has become in this. We will see the evolution of this mode shape in the following (and last) interval of study.

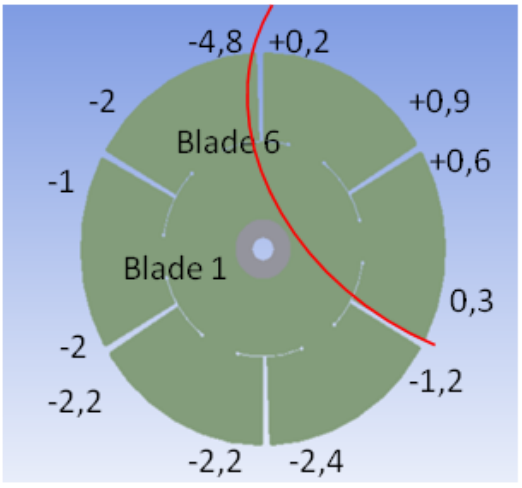

Figure 88: Mode shape of $Fn_{c'''}$

Finally, I proceeded to analyze experimentally the following natural frequencies obtained: Fnd'''=26,88 Hz and Fne'''= 27,81 Hz in the same part, as we have seen that this frequencies are not a 1ND to follow, but frequencies of the turbine (shaft+disk). After analyzing the results in Labview, using the Uniaxial sensor U30 situated in blade 1, I drawed the amplitudes of the points of the edge of the disk, and these amplitudes for the Fnd'''=26,88 Hz can be seen on the left part of Figure 89 below, and the results obtained for Fne'''= 27,81 Hz are on the right:

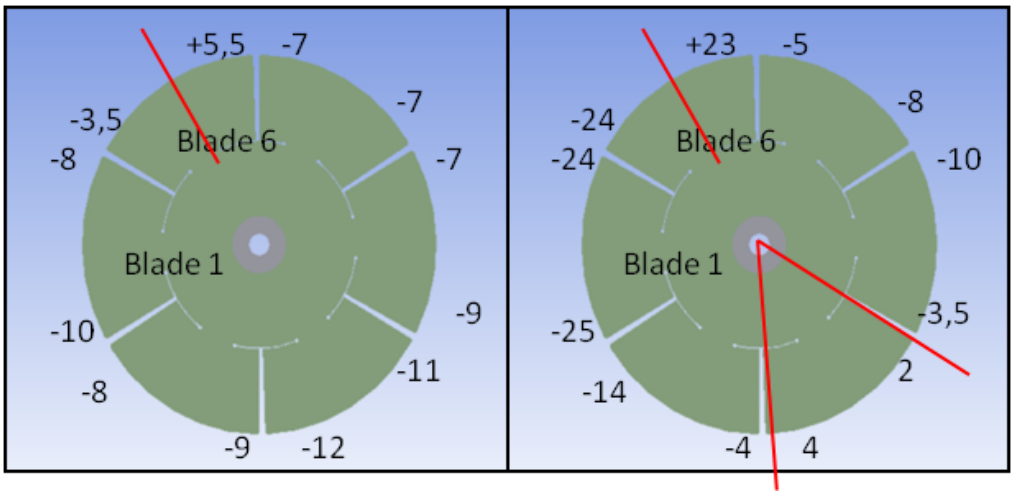

Figure 89: Mode shape of Fnd''' and Fne'''

With these results we can confirm what we set in the previous interval of study. These two frequencies definitely correspond to natural frequencies of the axis, as there is no match with the Ansys solutions for the 1ND we are following and with the perpendicular one too, that should still be a 1ND (see Figure 86). For instance, for the Fnd we can see that the mode shape is a torsion of the broken blade while the other points move down, which doesn't match with any Ansys result. Thus, we can say these two frequencies shown are natural frequencies of all the turbine, and not only of the disk.

To end with this part of the project with this crack length, we proceeded as in other parts to see numerically the differences between the values of the frequency between the numerical and experimental models. In Table 23 below we can see the comparison between the experimental and numerical models and its relative difference:

Result obtained	Experimental Natural frequency [Hz]	Numerical Natural frequency [Hz]	Difference [%]
1	**20,83**	**23,32**	**11,95%**
2	23,33	28,63	22,71%
3	24,06	29,96	24,52%
4	26,88	21,215	21%
5	27,81	21,218	23,69%
6	28,23	31,056	9,99%
7	30	31,702	5,67%
8	33,02	34,854	5,54%
9	35,83	37,106	3,56%

Table 23: Comparison between models with a crack of length equal to 75%Critical Length

To comment on the results, it is necessary to start analyzing the differences of the values in terms of frequency. As we can see in the table above, it seems clear that the average frequency response between the numerical and the experimental is not very similar, as, for instance, the initial frequencies of the axis have a difference of around 20% between models. However, the values of frequencies for the mode shapes with higher frequencies values presents good results, as, for example, the 3ND mode shape only has a difference of 3,56%, while the initials 2ND mode shapes have a difference of around 5%

Centering our analysis in the natural frequency we are following (shown in bold in the table), we can consider a good result having had this low difference, in comparison with the other low frequencies values mode shapes. Now the difference between models is 11,95%, which has been reduced from the previous interval of study. Seems, then, that the difference of frequency of the mode shape we are following is being reduced crack after crack. In the last chapter we will compare the models in terms of evolution of frequencies while the crack spreads and we will see the similarities between models in this aspect as well.

To end with this chapter, it would be great to set the objectives for the last experiment. Firstly, it will be necessary to see if the natural frequency we are following still preserves a value close to the one expected in Ansys. If so, and if the mode shape still preserves the theoretical one given in Ansys, we will have identified the vibratory response in all the lifespan of the turbine while the crack spreads, which would be a total success for the project, as we would be able to define and identify the evolution of a crack in a turbine. Secondly, we will analyze and compare the mode shapes, and we will see if there exists some similarity between the models. Finally, and as an extra chapter, we will focus our attention on the 3ND mode shape, as up to now, it is the mode shape that behaves exactly in both models numerical and experimental in all the phases of the. We will dedicate an extra chapter only to analyze and describe this mode shape and its evolution at the end of the project.

5.2.6 Experimental analysis with a crack length equal to the critical length

The next and final step of this project was to analyze the vibratory behavior of the turbine with a crack of length equal to the critical length. To link concepts with the previous study, one of the objectives of this part will be to analyze if the natural frequency we said that would provoke the crack still preserves the mode shape expected and if the frequency has changed as expected in the numerical simulations. This part of the study is still hazardous for the turbine, as the crack is considerably long (even more than the previous simulation), and as it has a length of 7,25 cm. We will try to see if with this crack length, the behavior of the turbine is still linear by using the different sensors and comparing them. This part of the project, due to the crack length, is even more unclear than the previous one, as we are totally in a range of work of the turbine where this disk could break suddenly, as it is supposedly in a zone of frequencies likely to break, the Zone 3 of the theory explained (see Figure 51 and the theory explained below that figure about the different zones of work with a crack in a machine).

As we did in the previous parts of the project, the first step was to take the disk to the manufacturing workshop and wait until they opened a crack of the mentioned length with the SolidWorks files given to the operator, and then, after using the laser machine, take it back again to the laboratory. Once the new crack was opened, we proceeded to install the diskit in the test rig. Figure 90 below shows the turbine cracked after opening the packaging.

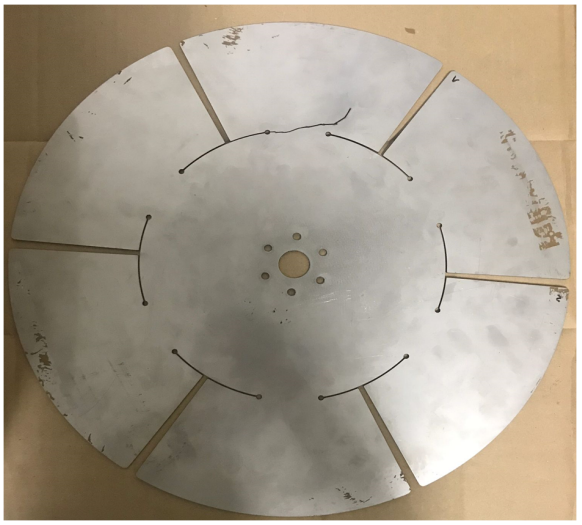

Figure 90: Turbine with a crack of length equal to the critical length

As we can see in the previous figure, the crack is much longer than the previous one done in the disk, as now the crack is 7,25cm long, while before, in the previous study, the length of the crack was 5,3 cm (now it is more than 2cm longer). After installing it, and configuring the computer, module and sensors like we did in the three previous interval of study, we proceeded to hit the same points of the previous interval for having an idea about the information of the amplitude of those points, as they were considered good points to hit for our study, as the previous results in all the experiments were totally successful.

Like we did before, after having hit an amount of 120 times properly in the disk and 10 times in the shaft, the results of frequencies obtained thanks to the Labview software using the triaxial sensor T_35_Z were the following shown in Figure 91 below:

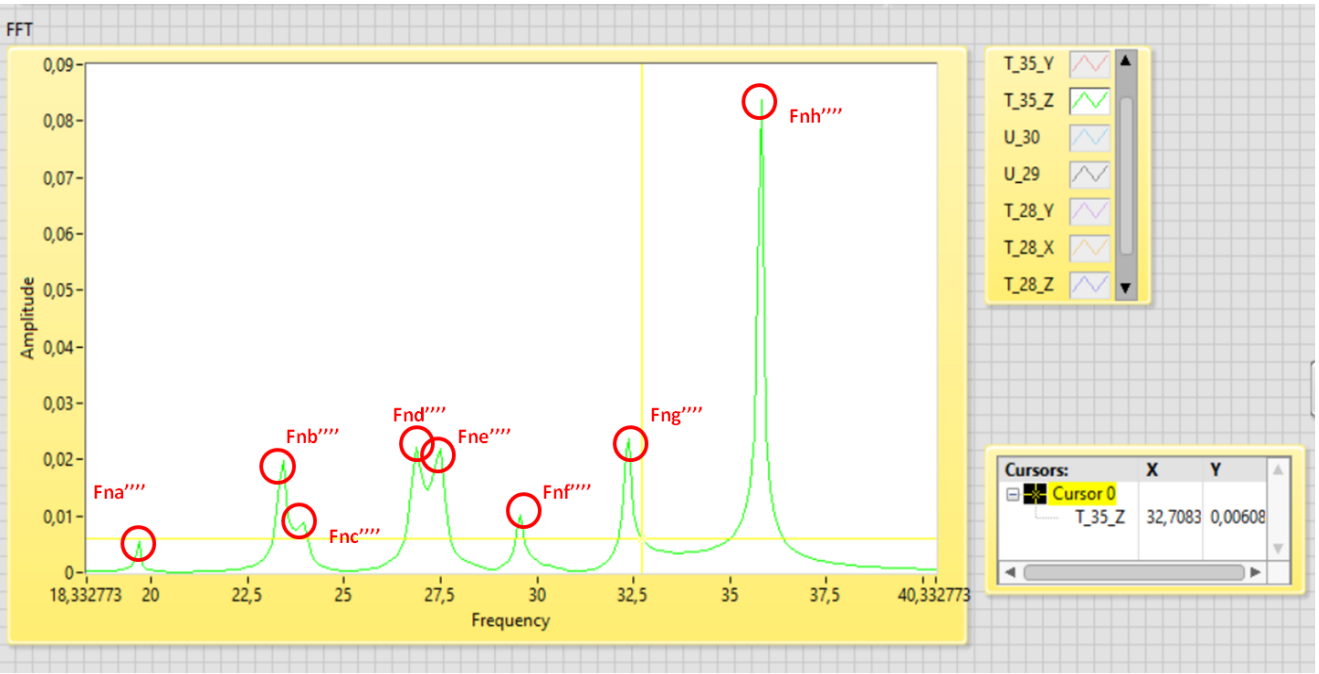

Figure 91: Natural frequencies seen in Labview with a crack of length equal to the Critical Length

The first thing we noticed in this experiment is that, unlike the previous one, the frequency responses were very clear and they were all the same for all the sensors. As we can see in the previous figure, the peaks of frequencies are clear and very differentiated from one another.

The natural frequencies obtained, therefore, after moving the cursor through the interval of frequency response in the interval from 0-40 Hz of the Labview were the following shown in Table 24:

Result obtained	Natural frequency [Hz]	Observation/Comment
$Fn_{a''''}$	19,68	It is very likely to be the one we are following
$Fn_{b''''}$	23,33	It is likely the 1ND perpendicular to the one we are following
$Fn_{c''''}$	23,95	This should the a variation of the initial 0NC
$Fn_{d''''}$	26,88	This should be a frequency of the Shaft+Disk
$Fn_{e''''}$	27,5	This should be a frequency of the Shaft+Disk
$Fn_{f''''}$	29,58	
$Fn_{g''''}$	32,40	
$Fn_{h''''}$	35,83	This should be the initial 3ND

Table 24: Experimental results of the natural frequencies with a crack of length equal to the Critical Length

At first view, the only big decrease in the frequency is done in the first mode shape, which makes sense as this is the one that must decrease simulation after simulation. In this last interval, the rest of the frequencies barely change. Moreover, unlike the previous experiment (crack length equal to 75% of the critical one) all the natural frequencies have decreased or remained practically equal, so we can confirm that the strange behavior we had in the previous chapter of slight increase of frequencies was due to the re-adjustment of the shaft.

In this last interval of study the most important part will be to identify clearly the mode shape that will provoke the failure (the initial 1ND that in this last part is $Fn_{a''''}$) and, if possible, see the difference between the real frequency failure and the numerical one given in Ansys. If the difference between mode shapes and frequencies in Ansys with respect to the measurements in the laboratory are small enough, we could say that it is possible to follow a crack in a turbine in all its lifespan in terms of frequency response and vibration modes.

For trying to compare the vibration modes obtained between the numerical simulation and the experiment, we added the shaft to the disk in the simulations and proceeded to solve the system of the entire turbine (Disk+Shaft) like we did before. The results of the mode shapes obtained in Ansys are shown in Figure 92 below:

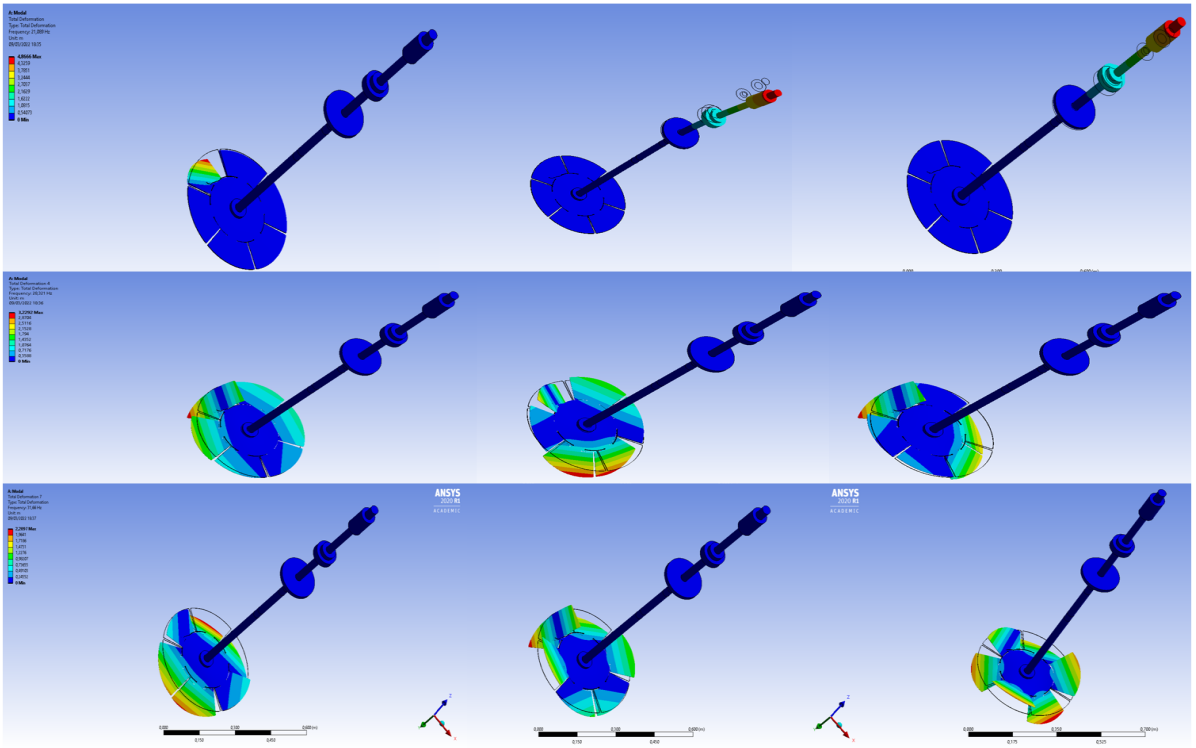

Figure 92:Numerical mode shapes obtained with a crack of length equal to the Critical Length

For having an idea of the numerical natural frequencies obtained, below in Table 25 we can see the Ansys results:

Result obtained	Natural frequency [Hz]	Observation
Fn_{1}'''	**21,09**	**Mode shape we are following**
Fn_{2}'''	21,21	Shaf+Disk
Fn_{3}'''	21,21	Shaf+Disk
Fn_{4}'''	28,32	
Fn_{5}'''	29,72	
Fn_{6}'''	30,52	
Fn_{7}'''	31,56	
Fn_{8}'''	33,75	
Fn_{9}'''	36,93	3ND +Torsion of the blade

Table 25: Numerical results of the natural frequencies with a crack of length equal to the Critical Length

As we can see in Figure 92, this time the lowest natural frequency corresponds to the initial 1ND that now has become a total displacement of the broken blade with a crack of critical length. The following two natural frequencies are the ones of the disk+shaft and the fourth one is the 1ND perpendicular to the first natural frequency, that still preserves practically its mode shape since the beginning of the project. Looking at Table 24, Table 25 and Figure 92 seems that there still exists a relation between the numerical simulation and the experiment. To confirm this, let's see now the results of the amplitudes of the points as always.

Firstly, we will try to identify the displacement of the points of the turbine vibrating at **Fn_{a}'''=19,68 Hz**. By representing the amplitudes of the 12 points of the edge of the blade, using the uniaxial sensor U30, situated on the first blade the results obtained were the following shown in Figure 93 below, where we can see the values of amplitude for the 12 points of the corners of the blades for that natural frequency:

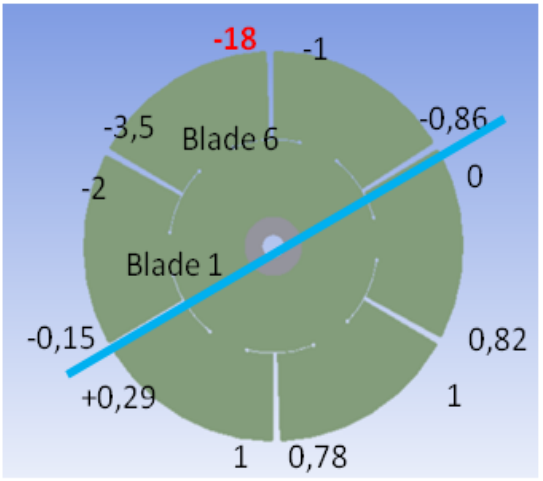

Figure 93: Mode shape of Fn_{a}''''

As we can see, there is a total match with the prediction of Ansys for this frequency (see Figure 92 on the top left). Now, a mode shape where practically all the disk is motionless, but the corner of the blade cracked, is shown, and the experimental analysis also shows one point of extreme displacement, with **-18** of amplitude highlighted in red, which is the point I6_1. This result obtained in the experiment totally matches with the initial 1ND mode shape we are following. The rest of the points have a very low displacement (specially, the points with positive displacement, as Ansys predicted), being +1 and +0,82 the maximums of the other side of the nodal line. This mode shape results in an almost unique vibration of the broken blade, and this is what Ansys showed in the simulations. Therefore, we can say that this result obtained is a total success, as we have followed the evolution of the crack during all the lifespan of the turbine we are using, and the mode shape expected in every simulation matched practically between both models, numerical and experimental.

Regarding the second experimental natural frequency, Fn_{b}''''= 22,71 Hz we should have in the results the perpendicular 1ND mode shape to the previous one mentioned Fn_{a}''''. It should be almost symmetrical without the influence of the long crack we already have. Effectively, in Figure 94 below we can see the mode shape that still preserves its shape as Ansys predicted (see Figure 92, in the middle-left). What we can see in this Figure 94 is not only a 1ND that separates two parts of the disk, but also a kind of torsion in the broken blade even with the nodal line crossing that blade, as the amplitudes of displacement of the points of the edge of the broken blade are respectively I6_1=+13,7 and I6_2=-13,5, what can be understood as an almost perfect torsion in that blade. Effectively, if we see the results in Ansys in Figure 92, in the middle-left we see that torsion too, even though for Ansys the negative value of displacement of I6_2 should be bigger than the positive value of I6_1. Finally, another important thing we could say is that the natural frequency with respect to the previous experiment has not changed, as Fn_{b}''''=Fn_{b}'''. In Ansys, for this last part of the study the frequency in the numerical simulation didn't change either, so this also is a point that both models have in common.

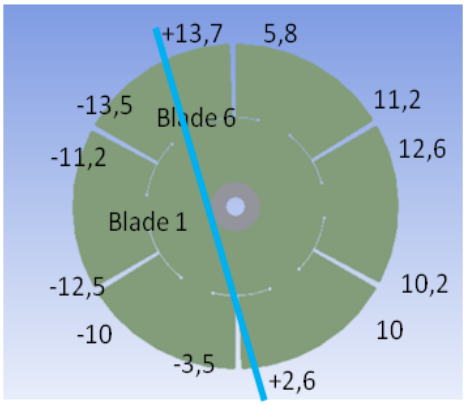

Figure 94: Mode shape of Fnb''''

Thirdly, we will show and discuss the results obtained from the Fnc''''=23,95 Hz. This time the value of the frequency of the initial 0NC mode shape has not practically changed, as before the result was Fnc''''=24,06 Hz and now Fnb''''=23,95 Hz. The mode shape expected did not match with Ansys, and was similar to the one obtained in the previous simulation. Figure 95 below shows the experimental results of the displacement of the points studied.

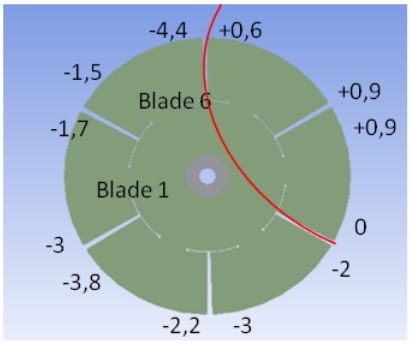

Figure 95: Mode shape of Fnc''''

Finally, I proceeded to analyze experimentally the following natural frequency obtained: Fnd''''=26,88 Hz and Fne''''= 27,5 Hz . The first thing I noticed was that Fnd'''' didn't change its value with this huge crack opened, meanwhile the Fne'''' did change only 3 tenths. This fact remarks the importance and singularities of a crack in a turbine, as we have seen that a big crack in a turbine may not affect some mode shapes. After analyzing the results in Labview, using the Uniaxial sensor U30 situated in blade 1, I drawed the amplitudes of the points of the edge of the disk, and these amplitudes for the Fnd''''=26,88 Hz can be seen on the left part of Figure 96 below, and the results obtained for Fne''''= 27,5 Hz are on the right:

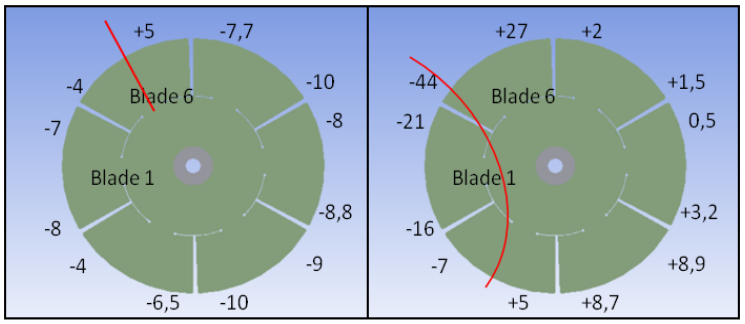

Figure 96 :Mode shape of Fnd'''' and Fne''''

To finish this last part of the project, we proceeded as we did in previous comparisons to see numerically the differences between the values of the frequency between the numerical and experimental models. In Table 26 below we can see the comparison between the experimental and numerical models and its relative difference:

Result obtained	Experimental Natural frequency [Hz]	Numerical Natural frequency [Hz]	Difference [%]
1	**19,68**	**21,09**	**7,16%**
2	23,33	28,32	21,38%
3	23,95	29,72	24,09%
4	26,88	21,21	21,09%
5	27,5	21,21	8,07%
6	29,58	30,52	3,18%
7	-	31,56	-
8	32,40	33,75	4,17%
9	35,83	36,93	3,07%

Table 26: Comparison between models with a crack of length equal to the Critical Length

The first thing we notice regarding this previous table is that it is the first time that Ansys gives one more natural frequency than the experiment. It is the first time that this happens, but it is understandable, as the turbine has reached a point where there is no symmetry, and the disk, due to the concepts we have followed, is about to break. At this point Ansys provides one more frequency of high value that does not affect our project in any case.

Regarding the first natural frequency, the one we are following, in terms of value, the difference between the numerical and the experimental model is **only 7,16%**. This means that at the point of fracture of the blade in the turbine it is possible numerically also to identify the frequency of failure approximately. We consider this result absolutely good for our project, as this mode shape is the most important one for us.

The following natural frequencies of the model (the perpendicular 1ND, the initial 0NC and the 2 natural frequencies of all the structure) present big differences between models in terms of values of frequencies, seen values of differences around 20%. Anyway, as the mode shape we are following is the first one (initial 1ND that has become now in a huge vibration of the broken blade), and the experimental mode shape, and also the value of frequencies are almost the same, it is almost irrelevant the other results at this point of the crack for our project.

Finally, as in the other parts of the project, the two initial 2ND mode shapes and the 3ND mode shapes have very low differences of frequencies between models. With respect to the 3ND, we will proceed later to analyze it deeply, as it has presented good results in terms of vibration mode and also in terms of value of the frequency. With all this, the experimental analysis of the turbine is over, and we will dedicate two more complementary chapters to see the evolution of some frequencies between intervals and, as we mentioned, study deeply the 3ND mode shape.

5.2.7 Evolution of vibratory behavior.

So far we have seen all the values of frequencies and mode shapes once every crack on the turbine was done. We have compared the different models stationary in each frame of crack. However, we have not seen the evolution of the frequencies or the evolution of the mode shapes because of the spread of the crack. In this chapter we will see the evolution of all the natural frequencies that the turbine suffers due to the effect of fatigue and we will see, for each frequency, how it evolves as the turbine worsens its efficiency because of the extension of the crack.

- **Transition of the experimental natural frequencies:**

First, Figure 97 shows the evolution of the frequencies (horizontal axis) and the amplitude of response (vertical axis) of the turbine used from the initial point (no crack) until the critical point (crack length equal to the critical length). The peaks of amplitudes of response correspond to the natural frequencies of the experimental turbine. The graph is divided in the four transitions of the crack. The impact used for comparing the frequencies was always the I12 (the one of the blade 6 that is next to the shaft) and the sensor used was the uniaxial U30. We have shown four different graphs in one that will provide clearer information about every transition.

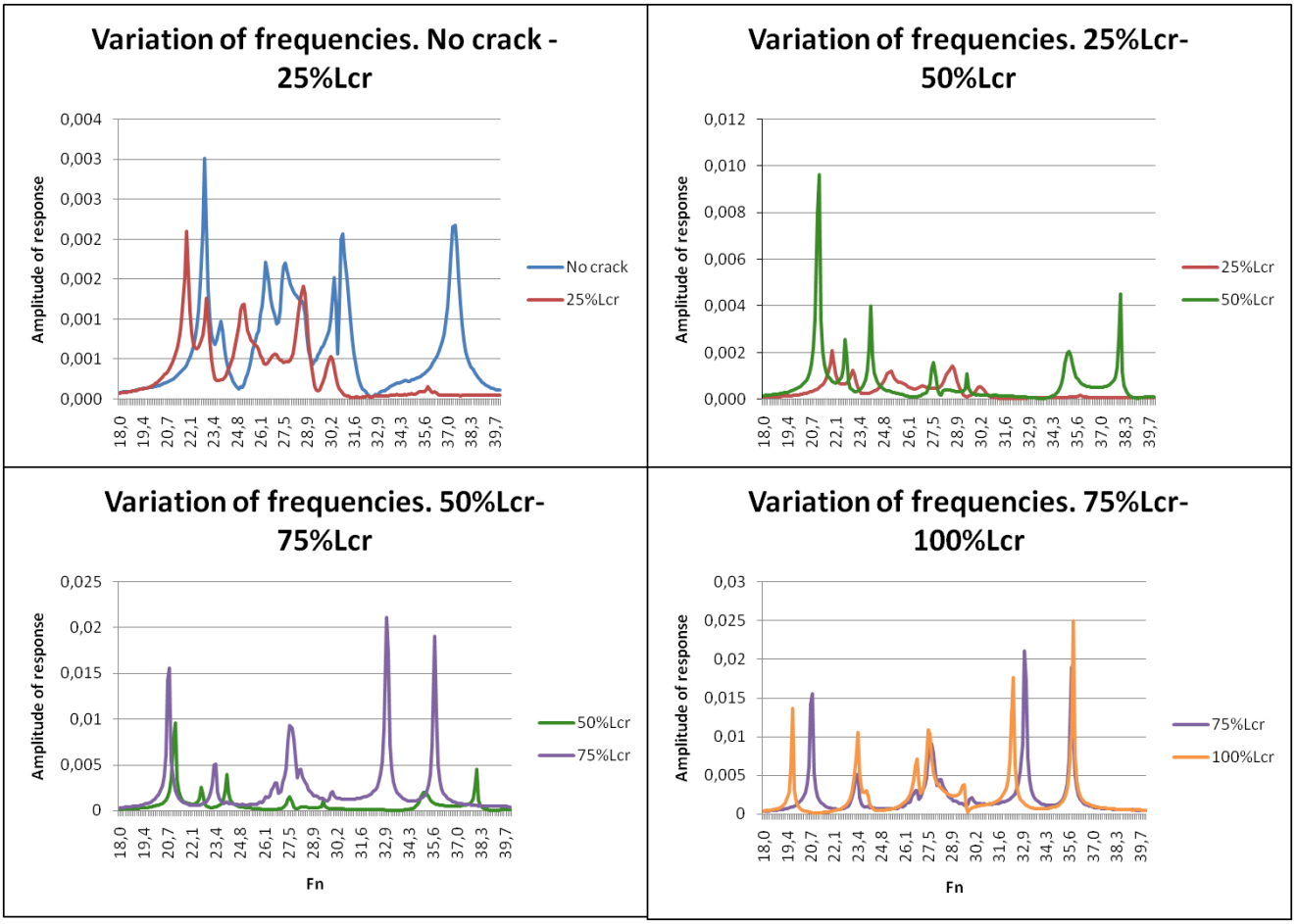

Figure 97: Evolution of response of the natural frequencies in each transition

As we can see, the transitions between all the models are more or less similar. Firstly, from No crack-25% of the critical length we can see that the lower frequencies value reduces their values a little bit in the transition, but having more or less the same amplitude of response in both models (see blue and red line of the graph in top-left of Figure 97). The 3ND mode shape, for the 25% of the critical length, does not have the same amplitude of response, but it actually exists as there is a tiny peak of response around 35,6 Hz.

In the top-right part of Figure 97 we can see the transition between the 25% of the critical length to 50% of the critical length. This transition is characterized by a new frequency response mentioned in the chapter 5.2.4 (see the green line that has another value of natural frequency at approximately 38,3 Hz). This transition actually is not the most clear, as the frequency responses are not the same, and some values remain close after the increase of the crack, but some others seem to have changed their frequency just because of that tiny crack. Moreover, the amplitude of response of the green line (50% of the critical length) is higher than the red line (turbine with a crack of length equal to 25% of the critical length).

Regarding the third transition (see the part of the bottom-left of Figure 97), we can see that the amplitudes of responses of frequencies are much higher in the crack of length equal to 75% of the critical one (see purple line) than the previous one (green line). This time, the values remain practically constant or even increase a little bit. This is due to the explanation given before of the re-adjustment of the axis. The torsion seen in the model with a crack of 50% of the critical length has gone, and now the last value of the frequency is the corresponding to the 3ND mode shape as happened in the first simulations.

Finally, in the last transition (bottom-right in Figure 97) we can highlight that the amplitudes of responses are practically the same, and, moreover, practically all the frequencies have the same value but the first one (the 1ND we are following that absolutely had to reduce its value) and one initial 2ND mode shape, with a frequency of 32,9 HZ approximately. The rest of the frequencies are practically overlapped, as they preserve their values and not only that, but also the amplitude of the response.

- **Comparison of the evolution of frequencies between models:**

Secondly, it is also important to see the evolution numerically of each initial natural frequency. The natural frequency that always suffers a decrease in its value will be the initial 1ND mode shape that we have been following for creating the crack. Effectively, as we said before, the first natural frequency of all the experiments (initially Fn_a and in the last experiment, Fn_a'''') is the one that suffers a big reduction of its value after all the transitions. In Figure 98 below we can see this frequency in tw graphs:

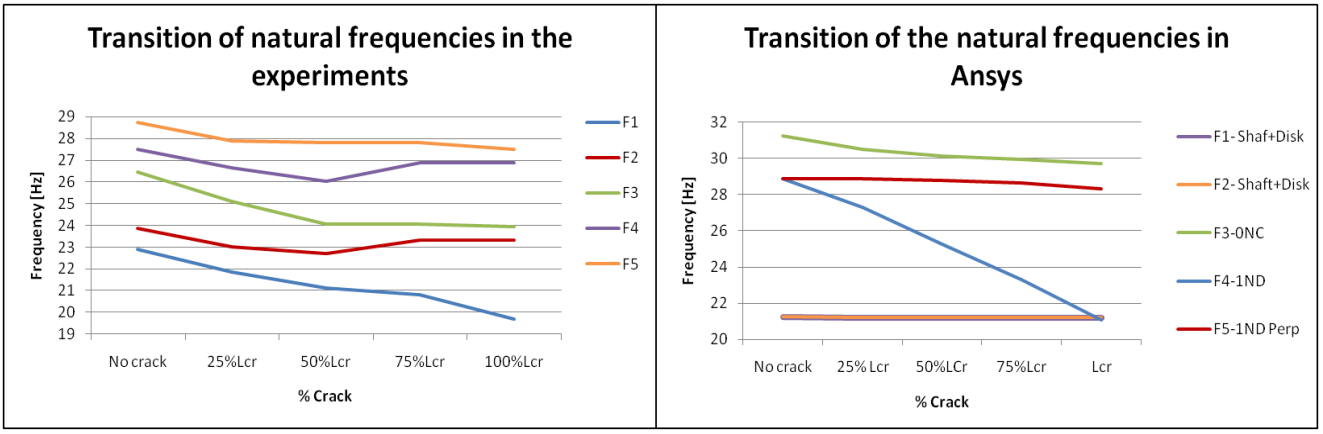

Figure 98: Transition of the natural frequencies in the experimental and numerical models

This Figure 98 shows as we said the evolution of all the natural frequencies of both experimental and numerical models. The evolution of the experimental frequencies is shown on the left, while the numerical evolution of the frequencies is shown on the right. They are relationated by their colors. This means that for example, the evolution of frequency of the initial 0NC mode shape that is in green in the graph on the right corresponds to the one in green in the left graph.

As we can see, all the frequencies between experimental and numerical models have approximately the same evolution. The initial 0NC in the experimental model decreases its frequency a little bit (around 1.5 Hz), and in

the numerical model there is a reduction of frequency due to the crack spread of 1.5 Hz too. For this mode shape, the green lines are practically parallels, as they decrease its frequency with a slope similar between intervals of study. The unique difference is the value of the frequency between models, but we have already talked about that and this part is done for comparing the shape of the evolution of the frequencies and not its value.

Another thing we can see is that the only frequency that suffers a big decrease in both models as the crack spreads is the initial 1ND (in blue in both graphs). In the experimental model, the reduction of frequency is about 3.5 Hz, while in the numerical model the frequency is reduced around 8 Hz. This is something to note, that the reduction of frequency because of the crack increment is bigger in the numerical model than in the experimental one. The rest of the frequencies practically don't change its frequency as the crack increases, as the biggest reduction of frequency in both models is 1 Hz as much.

The rest of the natural frequencies evolve similarly between models, as, for instance, the perpendicular 1ND to ours reduces a little bit the frequency in both models (1 Hz in both). The only difference is that in the natural frequencies of the entire turbine (disk+shaft) in the numerical model there is no reduction in the frequency. However in the experimental one we can see a reduction in both of them of maximum 1 Hz, but this reduction is not significant at all, as the reduction is very small (1 Hz or less) and, moreover, we are following the initial 1ND mode shape that is the farthest frequency from these two in value.

- **Comparison of Mode Shapes between models:**

Finally, let's see the evolution of the displacements of the points of the disk when it vibrates at a determined natural frequency. As in the first part of this project we explained the 3 first mode shapes (the initial followed 1ND, the perpendicular 1ND, and the initial 0NC), we will now see the transitions of them all cut after cut done in the disk in just one figure. This work will give us a better idea about the evolution of all the initial frequencies of the disk as the crack spreads.

Figure 99 shows the evolution of the 1ND we followed for doing the crack propagation. Figure 100 shows the 1ND perpendicular to the previous mentioned and, finally, Figure 101 shows the evolution of the initial 0NC mode shape in both numerical and experimental models:

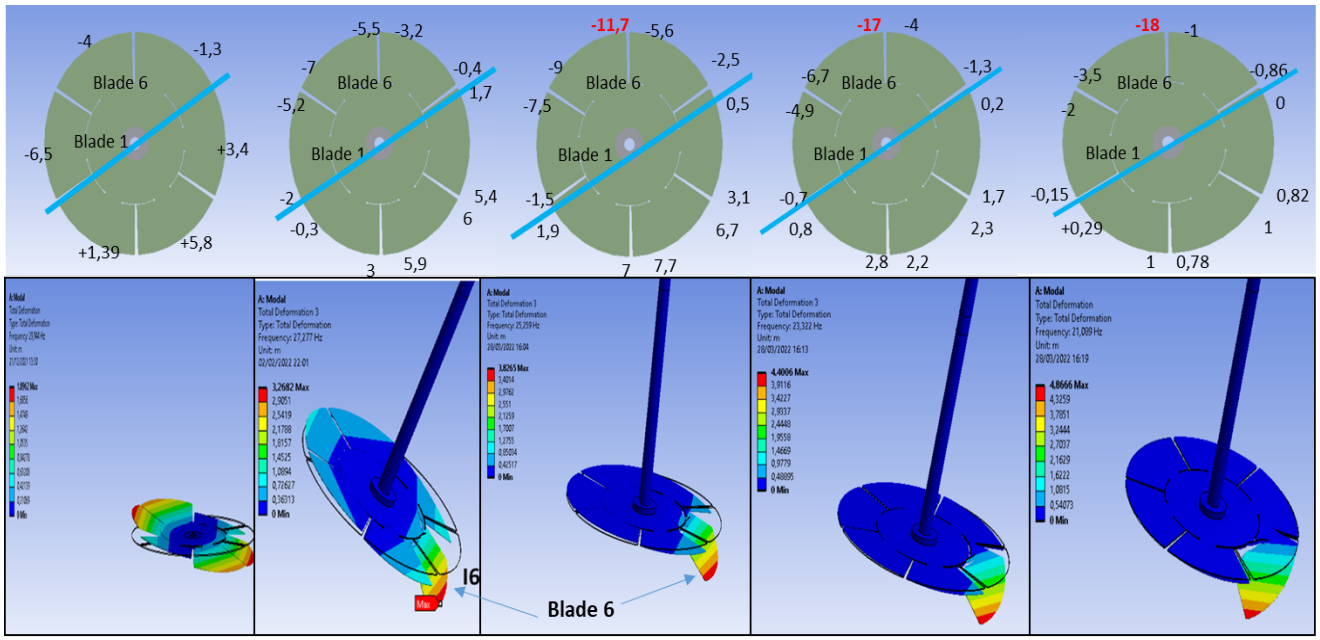

Figure 99: Comparison of the initial 1ND mode shape that provoked the crack between models

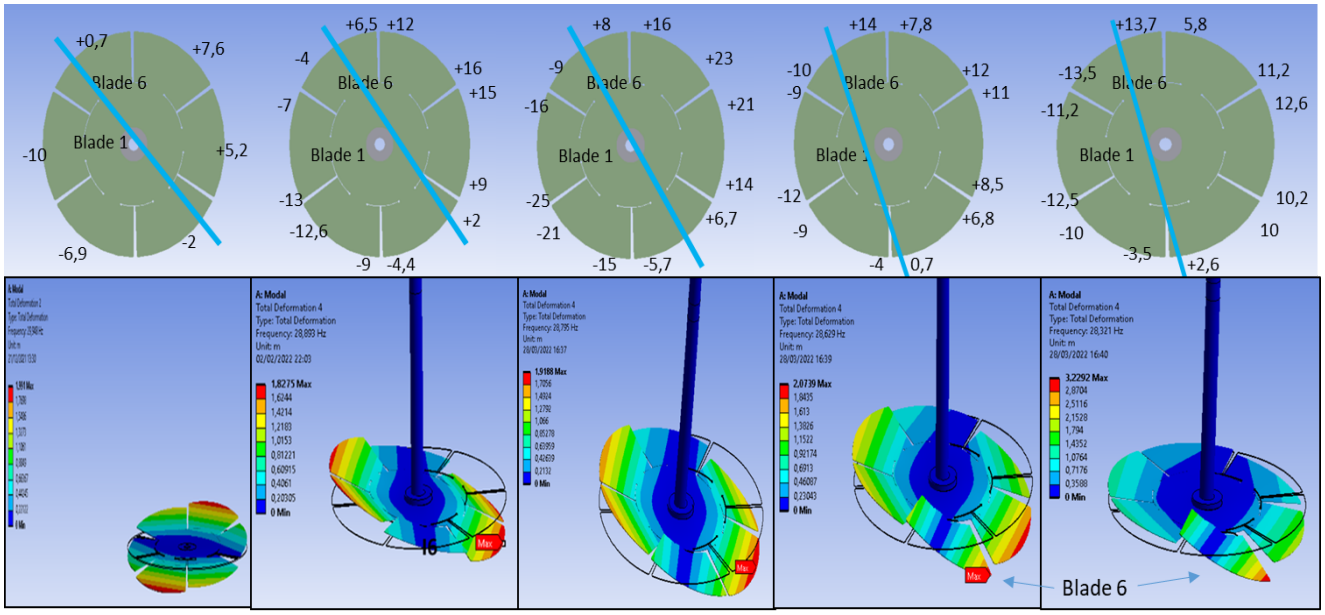

Figure 100: Comparison of the perpendicular 1ND mode shape between models

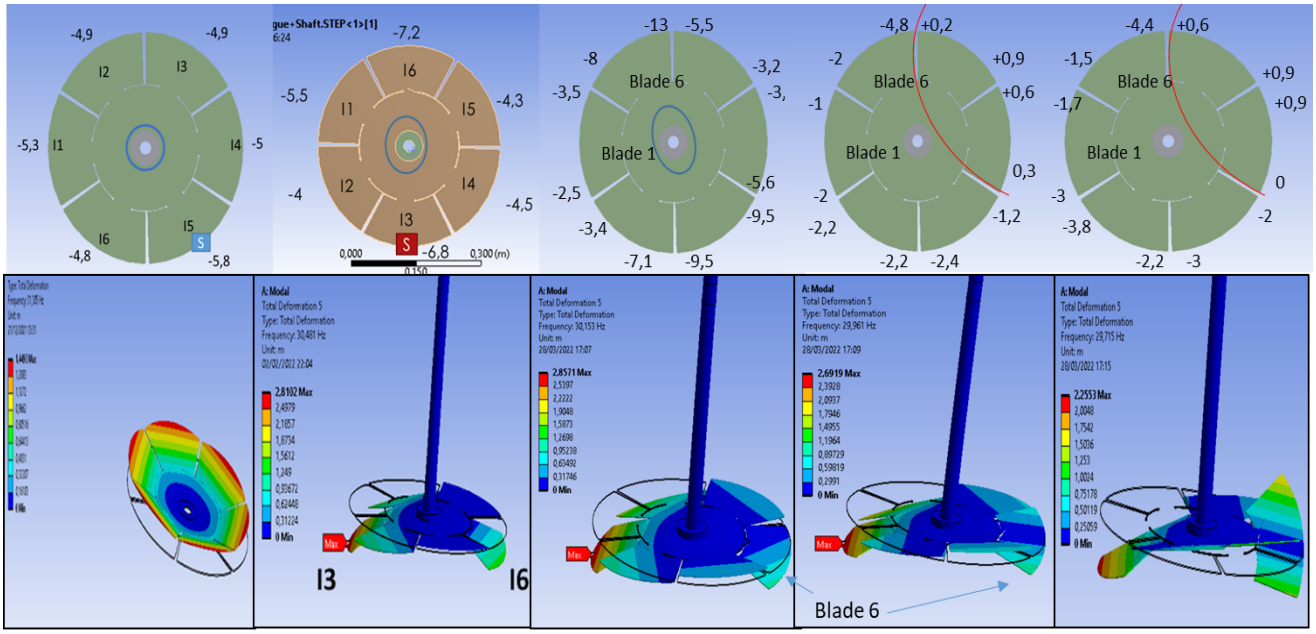

Figure 101: Comparison of the initial 0NC mode shape between models

To comment on the results again, we should highlight the practical coincidence of results we have obtained for the two 1ND mode shapes (the one we are following and its perpendicular) between the models. The experimental mode shape practically coincides with the numerical in each simulation for the 1ND followed for doing the crack, and also with its 1ND perpendicular. For higher length of cracks, moreover, the mode shape predicted by Ansys is even more precise, which is an astonishing result, because we thought initially that for long cracks (for example, cracks of more than 5cm in our turbine) Ansys would not be able to predict the modal behavior of the turbine for these frequencies. Nonetheless, it did predict quite precisely the vibratory behavior of the turbine with a long crack for these two mode shapes.

Regarding the initial 0NC mode shape, from the 75% of the crack the mode shape is lost and Ansys does not match with the reality of that experimental mode shape, but this is not important at all as the ones we have to focus our attention on are the two mode shapes with a lower frequency value, the 1ND explained.

5.2.8 The 3ND Mode Shape Analysis.

Finally, to end with this chapter of the analysis of the experiments and comparisons between models, during all the studies of the intervals that I have made, I saw another very interesting fact that could contribute to the improvement of the maintenance of the hydraulic turbines.

During all this work, I have been talking and focusing my attention on the firsts mode shapes that the Ansys and the experiments provided, as they were the most destructives and also they are the first founds in all simulations (approximately, between 19 Hz and 28 Hz). However, in the range from 0 to 40 Hz it has been interesting to analyze the last mode shape found, the 3ND mode shape, the one closer to a natural frequency of 40 Hz. This mode shape, as we mentioned, has the characteristic that has 3 nodal lines, and, therefore, as it has 3 nodal lines and the turbine has 6 blades, the consequence is that blade after blade of the turbine studied are in contra phase one with respect the other (this means that the amplitude of displacement of a blade n is positive, and the following blade n+1 is negative). Below in the right part of Figure 102 we can see the displacement analysis provided by Ansys for our model of turbine without any crack.

After analyzing all the experiments, we reached the conclusion that the 3ND mode shape has a specific characteristic, that is that the analysis of the frequency and the analysis of the mode shape of both numerical and experimental models practically match. Let's see the results hereinafter.

The first experiment was carried out without any crack in the disk. The results obtained for this mode shape provided by Labview and drawn by me, and the Ansys results can be seen below in two parts in Figure 102:

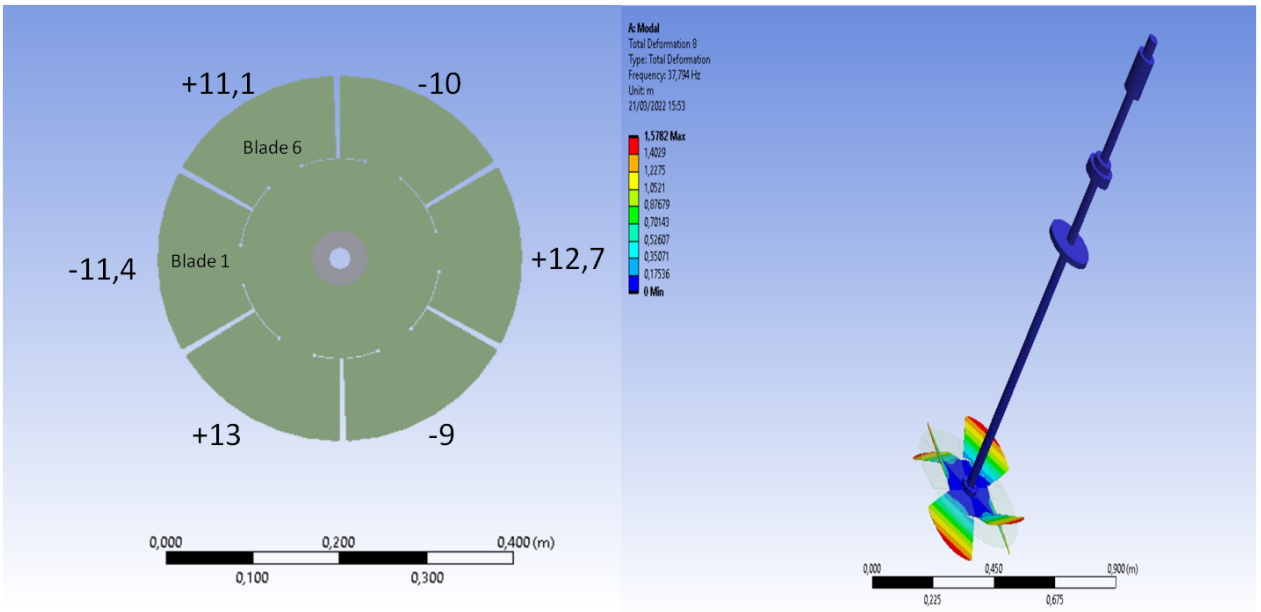

Figure 102: Experimental & Numerical results of displacements of the 3ND mode Shape without crack

As we can see, on the left of the figure there are the amplitudes of displacements of the blades obtained for this mode shape, while on the right part of the figure it is shown the numerical result of displacements obtained in Ansys. The first thing that can bee seen is that in the experimental analysis, the points of the edge of all the blades tend to move one in contraphase with respect to the previous one, as it is a 3ND mode shape. Moreover, the response of the amplitudes of displacements in the experiment are practically the same (From 9 to 13). These small differences can be explained by the fact that, depending on the blade, the point hitted was not in the exact position as in the previous blade. Anyway, the results are good enough to compare them with the numerical simulation (on the right part of the figure). As it is shown there, the maximum displacements for this mode shape are also more or less the same in all the blades, and coinciding in the edge of the blades, which totally matches with the experimental results obtained in the laboratory.

To compare the frequencies, in the numerical model we obtained for this mode shape a Fn=37,794 Hz and in the experimental analysis the natural frequency obtained was Fn=37,40 Hz. The difference between these two models was exactly 1%, which was an astonishing result in terms of comparison between models. Once we have seen the comparison between the experimental and the numerical models for this mode shape, we proceed to analyze the 3ND Mode shape for a turbine cracked with a crack of length equal to 25% of its critical length.

After opening the first crack and analyzing the cracked turbine in the laboratory, the results obtained for the last frequency of them all in the range of 0-40 Hz was, as it happened before, the 3ND mode shape. Figure 103 below shows the results of the displacements in the numerical simulation (on the right) and the amplitudes of displacement obtained in the laboratory in the zone of the corners of the edge of the blades:

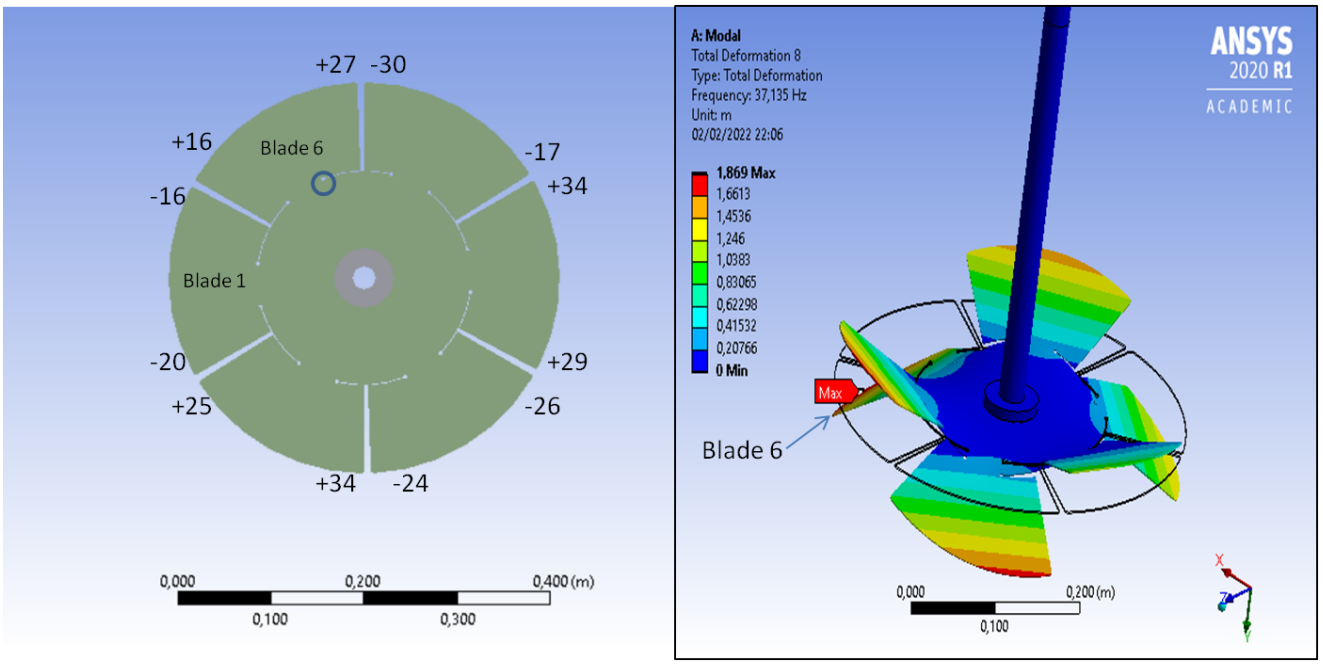

Figure 103: Experimental & Numerical results of displacements of the 3ND mode Shape with the first crack

As we can see in the figure, the cracked blade was the sixth blade, and the maximum displacement provided in the numerical analysis was in that blade also, but having a very similar value on the corner of the second blade, that also tends to displace in the same direction of the sixth blade. This result obtained in the numerical model was practically the same obtained in the experimental one, as the cracked blade has in the closest part to the crack a higher displacement (+27) and the second blade of the turbine has the biggest tendency of displacement (+34). The results of the 3ND mode shape with the crack of both models practically match, despite small differences due to the measurements performed.

With respect to the similarities in the frequencies of both models, Ansys estimated a natural frequency of Fn=37,13 Hz for this mode shape, and the obtained in the laboratory was Fn= 36 Hz. The difference between these two models was 3,14%, which was a little bit higher than the previous time, but also an incredible result in terms of similarity between frequencies of the models. Once we have seen the comparison between the experimental and the numerical models for this mode shape and this crack length, we proceed to analyze the 3ND Mode shape for a turbine cracked with a crack of length equal to 50% of its critical length.

After opening the second crack in the turbine, and analyzing the cracked turbine in the laboratory, this time the results obtained for the last frequency of them all in the range of 0-40Hz was not the 3ND mode shape. This time, a kind of torsion of the broken blade appeared only for this crack length (See Figure 78 on the bottom center). The natural frequency for this mode shape of torsion was 38,65 Hz. Anyway, the following lower frequency coincided totally with a 3ND mode shape, so it is the one we will explain in this part.

Centering our study in the 3ND mode shape, Figure 104 below shows the results of the displacements in the numerical simulation (on the right) and the amplitudes of displacement obtained in the corners of the blades in the laboratory (on the left):

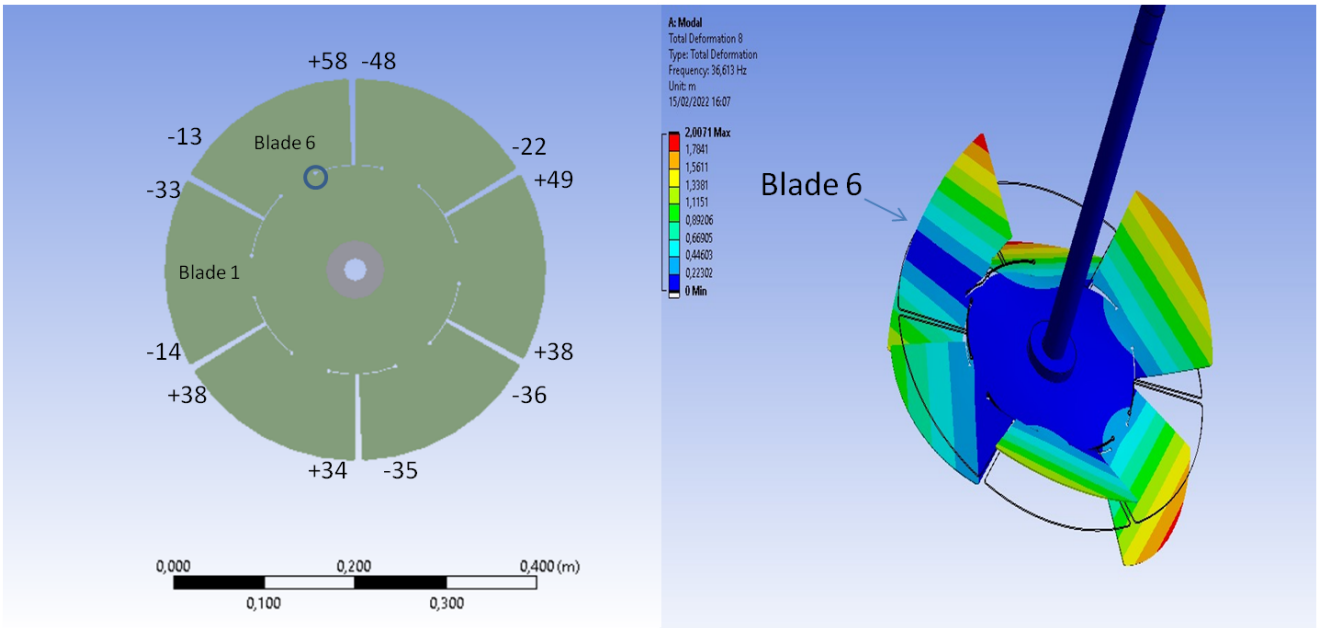

Figure 104: Experimental & Numerical results of displacements of the 3ND mode shape with the second crack

This time, as we can see in the numerical simulation, the mode shape was not exactly a 3ND, as we had in the beginning without crack. The broken blade in this simulation had its 2 corners in contraphase. When the cracked part of the broken blade tends to go up, the other part of the blade tends to displace in the reverse direction, and with lower amplitude. This behavior seen in Ansys was also seen in the experiment. For instance, in the cracked blade, the part closer to the crack has a positive and high tendency of displacement (+58), meanwhile the other part of the blade tends to go in the other direction with lower intensity (-13). Another thing that matches between the two models is that in the other 5 blades the alternative movement between blades continues, as one after another change the direction of displacements, having, for example, a high value of displacement (negative in this case) in the fifth blade in the experiment (-48) that coincides with a highlighted in red part of that blade also in the numerical simulation in that fifth blade. Another thing we can see is that the first blade does not tend to have big displacements in the closest points to the second blade (see the blue part), and this matches with the results obtained in the laboratory (-14 for that part of the blade 1). Therefore, with all this seen, we can say that the results of the 3ND mode shape with the crack of both models practically match, despite small differences due to the measurements done.

With respect to the similarities in the frequencies of both models, Ansys estimated a natural frequency of Fn=36,6 Hz for this mode shape, and the obtained in the laboratory was Fn= 35,21 Hz. The difference between these two frequencies was 3,94%, which was similar to the previous experiment analysis, and also good in terms of similarity between frequencies of the model. Once we have seen the comparison between the experimental and the numerical models for this mode shape and crack length, we proceed to analyze the 3ND mode shape for a turbine cracked with a crack of length equal to 75% of its critical length.

After opening the third crack in the manufacturing workshop, and after analyzing the cracked turbine in the laboratory, the results obtained for the last frequency of them all in the range of 0-40 Hz was the 3ND mode shape. Figure 105 below shows the results of the displacements in the numerical simulation (on the right) and the amplitudes of displacement obtained in the corners of the blades in the laboratory (on the left):

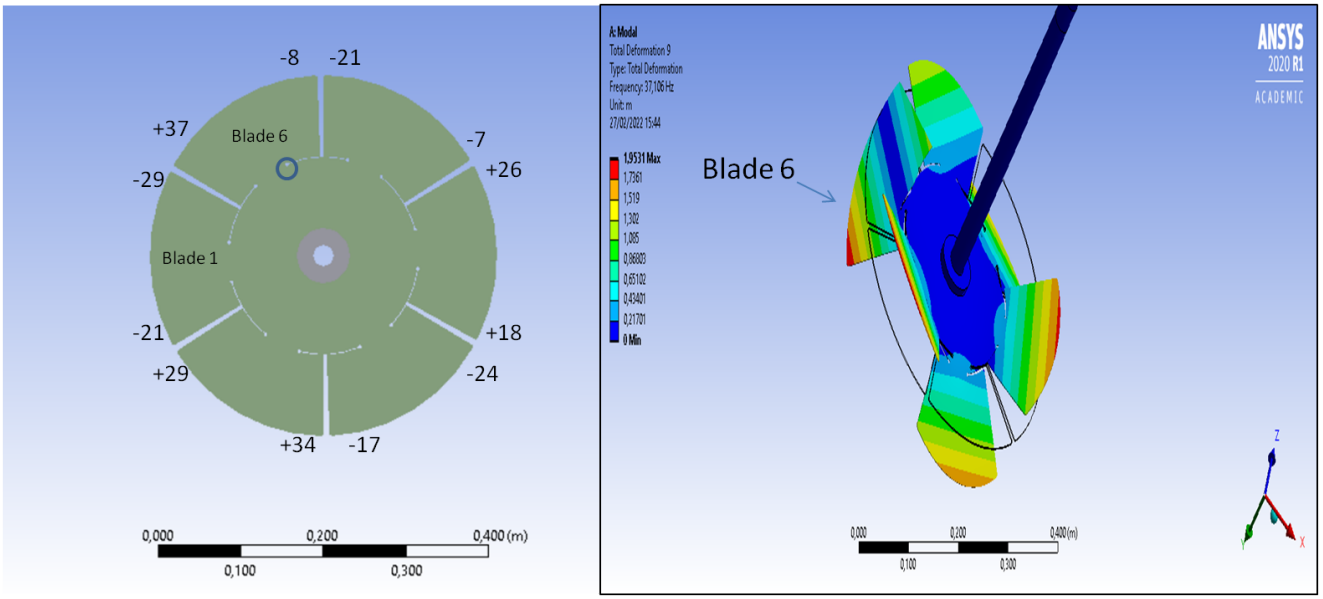

Figure 105: Experimental & Numerical results of displacements of the 3ND mode shape with the third crack

As we can see in the figure, the maximum displacement seen in the numerical analysis was in the sixth blade, but, this time (what is totally different from the previous simulation), the closest corner to the beginning of the crack on the blade (Point 6_1 in the experiment) has a lower amplitude of displacement than the other corner. The closest corner of the broken blade to the first blade has an amplitude of +37, the maximum measured in this experiment. The result obtained in the numerical model was exactly the same obtained in the experimental one, as the cracked blade has in the farthest part to the crack a higher displacement (+37) and the other part of the sixth blade had an estimated low amplitude in the numerical model, what coincides with the measured in the test rig (-8 of amplitude of that point). The other blades still present a 3ND mode shape, despite the non symmetrical model that the crack has provoked. Thus, the results of the 3ND mode shape with the crack length studied of both models totally match this time.

With respect to the similarities in the frequencies of both models, Ansys estimated a natural frequency of Fn=37,106 Hz for this mode shape, what is practically the same result obtained in the second experiment for this mode shape (Fn=37,13Hz) and the obtained in the laboratory was Fn= 35,21 Hz. The difference of frequencies between these two models was 3,56%, which was similar to the previous experiment analysis, and also good in terms of similarity between frequencies of the models. Once we have seen the comparison between the experimental and the numerical models for this mode shape and crack length, we proceed to analyze the 3ND mode shape for a turbine cracked with a crack of length equal to its critical length.

Finally, after opening the fourth and last crack in the manufacturing workshop, and after analyzing the cracked turbine in the laboratory, the results obtained for the last frequency of them all in the range of 0-40 Hz were, like the obtained in the firsts simulations, the 3ND mode shape. Figure 106 below shows the results of the displacements in the numerical simulation (on the right) and the amplitudes of displacement obtained in the laboratory (on the left):

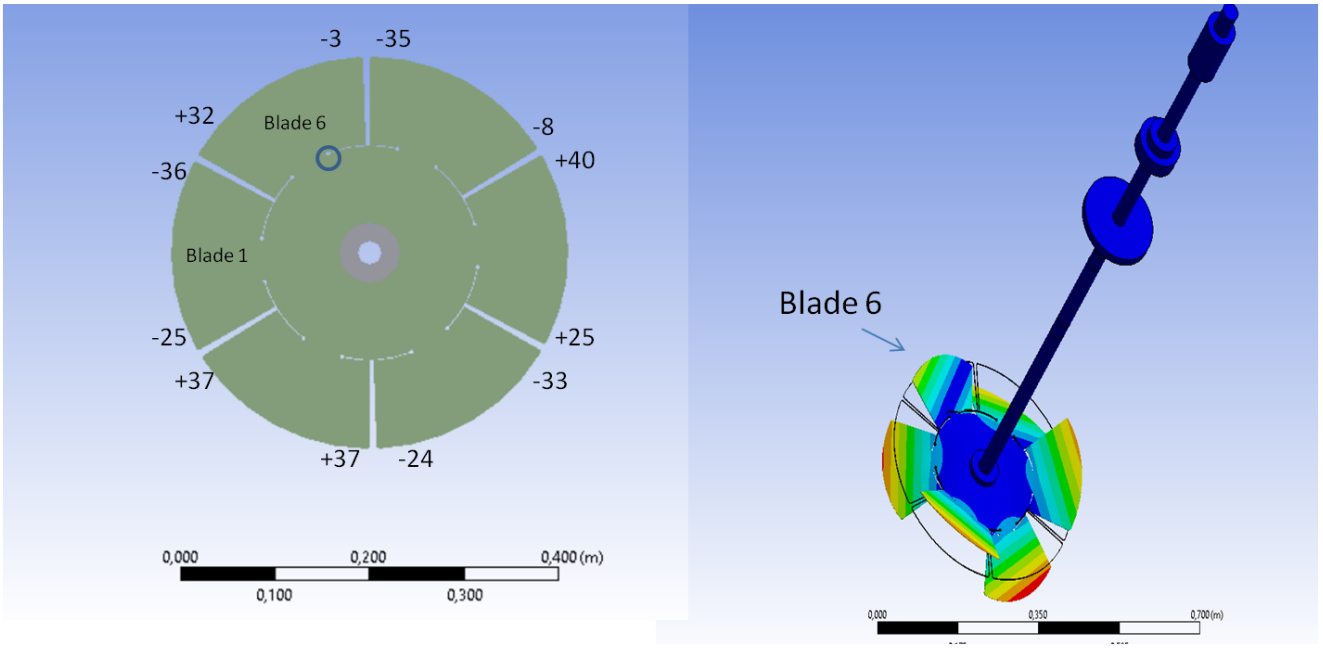

Figure 106: Experimental & Numerical results of displacements of the 3ND mode shape with the entire crack

This time, as we can see in the numerical simulation, the mode shape is not exactly a 3ND. The broken blade has its 2 corners in contraphase, but the closest corner to the crack has almost no displacement (see the part in blue in the numerical simulation). When the cracked part of the blade tends to go up, the other part of the blade tends to displace in the reverse direction with lower amplitude, being almost 0. This behavior is also seen in the experiment. For instance, in the cracked blade, the closest part to the crack has no practically displacement, and this can be seen in the experiment too, with an amplitude of displacement of that point at -3. Meanwhile, the other part of the broken blade is in contraphase with a higher amplitude, but it is not the biggest one as happened in the previous experiments. Another thing that matches between the two models is that in the other five blades the alternative movement of the blades continues, as one after another change the direction of displacements, having, for example, a high value of displacement (positive in this case) in the blade two of the experiment (+37) that coincides with a highlighted in red part of that blade also in the numerical simulation in that blade. The only difference is that in the third blade the amplitudes are not as big as predicted in Ansys, but they are really close. Therefore, with all these facts seen, we can say that the results of the 3ND mode shape with the crack of critical length in both models practically match, despite small differences due to the measurements performed or the antisymmetry of the model.

With respect to the similarities in the frequencies of both models, Ansys estimated a natural frequency of Fn=36,93 Hz for this mode shape, and the obtained in the laboratory was Fn= 35,83 Hz (both of them, were practically the same as in the previous experiment with the length of 75% of the critical length). The difference between these two models for this crack of critical length was 3%, which was similar too to the previous experiment analysis, and also good in terms of similarity between frequencies of the model.

Once we have seen and compared the experimental and the numerical models for this mode shape during all the spread of the crack (from 0 to 100%), we have seen the importance of following this mode shape to better predict how a fracture due to fatigue can appear because of a repetitive vibration of the first mode shape. To see the similarities between models in all the lifespan of the turbine, in Table 27 below we can see the differences of the frequencies (in Hertz) of the numerical and experimental analysis and its evolution while a crack spread due to the strains provoked by the first mode shape:

	No crack	25%Lcrit	50%Lcrit	75%Lcrit	100%Lcrit
Numerical simulation	37,794	37,13	36,613	37,106	36,93
Experiment	37,4	36	35,21	35,83	35,83
Difference between models	**1,05%**	**3,14%**	**3,98%**	**3,56%**	**3,07%**

Table 27: Natural frequency of the 3ND Mode shape in each model and its relative difference

As we can see, the maximum discrepancy between models in terms of frequency is only **3,98%**, for the 50%Lcrit. The results obtained, in terms of values of frequency, thus, are quite precise for this mode shape. Finally, the evolution of this 3ND mode shape in both numerical and experimental models can be seen below in Figure 107:

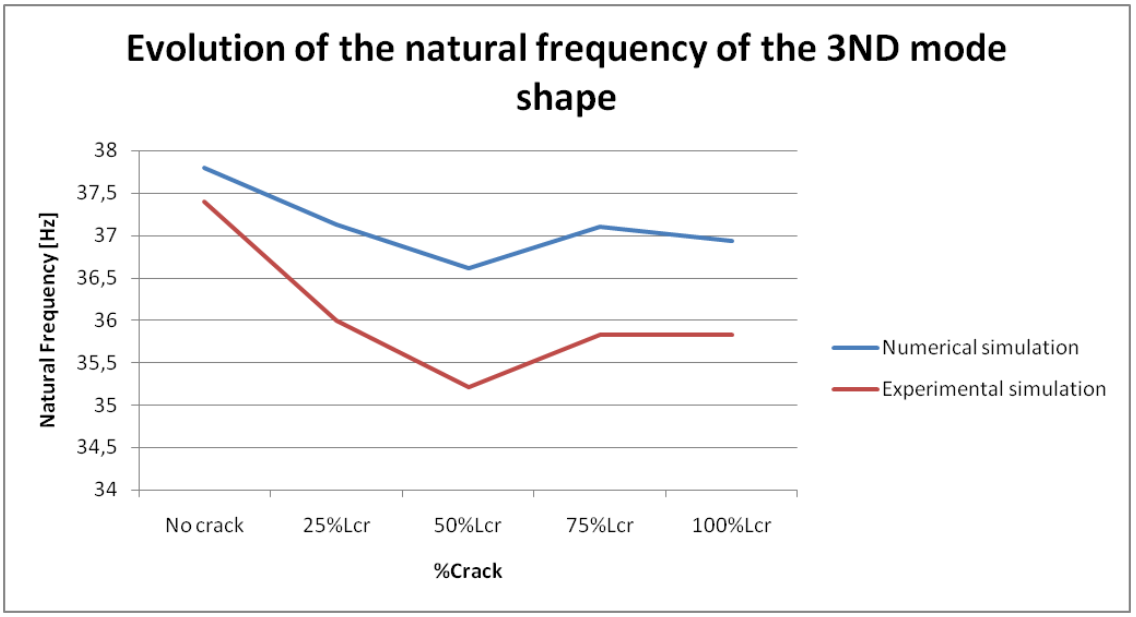

Figure 107: Evolution of the natural frequency of the 3ND mode shape in the different simulations

To sum up, putting an eye on the previous Figure 107 and the previous Table 27, we can confirm that this 3ND mode shape predicted in Ansys has the particularity that coincides totally with the real model of the laboratory, not only in terms of frequency, but also in terms of how it vibrates during all the lifespan of the turbine with a crack, and also in the way that the frequencies evolves as the crack spreads through the blade of the turbine.

5.3 Conclusions of the experimental modal analysis

The goal of this part of enlargement of the project was to compare if experimentally the values of a simplified Kaplan turbine when it suffers the effect of fatigue can be detected and followed, and if the vibratory behavior of our model of Kaplan turbine changes as the crack spreads in a blade. Having seen the different parts of the project and the results obtained, we can conclude that at least for the most hazardous natural frequencies of a simplified Kaplan turbine it is possible to follow and to predict when a crack achieves a determined length in a blade of the turbine, as the vibration modes were the same than the predicted in Ansys for each interval of study. Moreover, we have seen that despite some differences in the values of natural frequencies between models, the reduction of the natural frequencies because of the expansion of the crack in each mode shape we have analyzed is similar in both numerical and experimental models, as some vibration modes don't necessarily change their frequency if a crack appears or spreads through the blade of our simplification of Kaplan turbine.

Additionally, we have seen that there are some other mode shapes (not only the initial 1ND) that could be used as a reference in case the results in the beginning of the study for predictive maintenance of a turbine were doubtful. In our case, the 3ND mode shape had exactly the same behavior in terms of vibration mode and value of frequency in all the lifespan of the turbine, from the appearance of the crack until the failure because of the effect of fatigue. The maximum difference between models was just 4% when the crack was 4,5cm long.

Moreover, we have also discovered in our model of Kaplan turbine that for long cracks lengths (and therefore, for a critical situation of the turbine) the mode shapes that still preserve its theoretical vibration mode are the two initial 1ND mode shapes and the 3ND. What is more, we have also seen that the longer the crack, the more defined and clear are the results of the amplitudes of response of the natural frequencies, as the peaks of response in the frequency were bigger. For heavily used turbines, thus, it is highly recommendable to put an eye on these three mentioned mode shapes, as in our case they worked as expected in every numerical simulation, even with a long crack in the blade.

Regarding this last fact, it is also very interesting to mention that in the last interval of the study (from the 75% of the crack to the critical one), only the value of the natural frequency of the 1ND mode shape that we were following reduces more than only some tenths its value (approximately 1 Hz). This could be a good reference too to detect long cracks in a blade of the turbine, as if there is no change of frequency in the majority of the mode shapes after some decreases of frequency, it could mean that the turbine is about to fail because of the effect of fatigue.

Finally, we have also seen the importance of the boundary conditions and the environment of work of the experimental model, as if someone wants to analytically track the crack while it spreads, a minimum change on the configuration of the subjection of the axis of the turbine can slightly change the results obtained. We could say that the model of Kaplan turbine that we have used in this project is very sensitive to the environment where it works, as well as to the components that are related to it, such as bearings or transmission elements.

6. Conclusions of the project in global and future work

Regarding the conclusions we can obtain from our study, we should remember that the main objective of this project was to identify the effects of the appearance and expansion of cracks on the dynamic response of a hydraulic machine similar to a Kaplan turbine, and it has been a total success.

As we have seen, we have identified changes in the dynamic response of every single interval we have studied in the numerical simulation and also in the part of the experiment, even with small cracks done in the disk. For instance, the third interval of study had an increase of crack length of only 0.55cm, and a big change in the vibratory response was seen. What is more, during all the intervals, for the most destructives mode shapes, the vibration modes estimated by Ansys totally coincided with the experimental results obtained. Regarding the values of the natural frequencies, there was more discrepancy between the experimental model and the numerical one. Concretely, for the low value frequencies, we obtained the most similar value between the experimental model and the numerical simulation when the disk failed due to the effect of fatigue, with a difference in the first natural frequency of 7,16%. Other intervals had a higher discrepancy between models.

Anyway, if we consider that the vibratory response can be followed by the vibration mode (as we have done in this project), we can conclude that this project has proved that it is possible to follow the appearance and spread of a real crack provoked by the effect of fatigue in a simplified model of a Kaplan turbine.

Regarding the other complementary objectives mentioned in chapter 2, we reached the following conclusions:

- Knowing about the situation of the Kaplan turbines and their performance in today's society: Thanks to all the first part of research of the project, we have understood the importance of the Kaplan turbines in the society and how they work in order to produce clean energy to the society. We have seen the importance of having a good efficiency on them and how important they are to balance any electrical system. Moreover, we have seen their range of work, and we have introduced some equations that could estimate their efficiency and energy they could produce depending on the water flow they treat.

- Try to understand how the vibrations affect the integrity of a structure: In the chapters of research, we have seen theory about the vibrations in bodies and how due to a vibration it is produced in a body a displacement and, consequently, an acceleration that provokes strains in the structures. This part of the project was particularly interesting for us, as in all the courses we have done in the Master's we have not dealt with anything related to vibrations in structures or bodies, so it was a new concept for us to understand how important the vibrations are for the integrity of a structure. Moreover, with a practical approach, in the experimental analysis I have seen and analyzed how due to an appearance of a crack in a structure there exists a huge change in the vibratory response of the structure.

- Know how to apply simulation softwares like Ansys into reality: With the first part of the project (numerical simulation to identify a crack and its expansion) and putting it into practice in the second part (experiment over a simplified model of a Kaplan turbine) we have seen the importance of how Ansys can predict the vibratory behavior of a simplification of a Kaplan turbine, as we have had in the majority of the cases a really precise result between models. Moreover, this software (Ansys) is a key factor in our study, as it is the main tool to predict not only the appearance of the crack, but also its expansion, the way that the blades will vibrate at a certain natural frequency, and finally the mode shape expected for each natural frequency of the simplified turbine. Many results obtained comparing the numerical simulations and the experiments are quite similar, which is a total success.

- Learn how to measure different parameters of a real model in a laboratory: During all the time spent in the laboratory and all simulations I have done, I can conclude that this project has been totally useful to me to familiarize myself with all the instrumentation that could be used in a laboratory to experiment with a real structure, and also to analyze all the characteristic parameters that the structure could provide us by measuring on it with adequate sensors and software. From now on, it will be easier for me to work in a laboratory with some other structures that would require a modal analysis.

- Develop a methodology to carry out a project from its beginning, and know how to link a numerical model and a real model: While working on the project, the necessity of creating a methodology to follow and analyze the dynamic response of the simplified turbine was needed, as it was not clear at all from the beginning how to proceed to do the project. It was necessary planification and know when to measure in Ansys, when to do it in the real model, or even when to simplify parts of study. Results obtained show that the methodology we have followed is good, as results have been precise between models. In addition, some additional recommendations will be given at the end of this chapter to improve this complementary objective even more in future studies.

- Identify techniques and methods to improve the predictive maintenance in Kaplan turbines: Gathering all the previous conclusions obtained, we could say that using our method of comparing a numerical model with a real experiment in a laboratory, with the methodology we have used, could be useful in order to analyze the vibratory response of a hydraulic machine and know about the condition of the turbine. In our case, the techniques and methods used have provided some results that have given us an idea about the situation of a crack that our model of turbine is suffering because the effect of fatigue, and we think that these techniques we have used could be extrapolated to the studies of real models of the hydroelectric industry some day with future and complementary work.

Finally, we will share our point of view about what future work should be done from what we have done in this project to improve predictive maintenance even more with the techniques used for the hydraulic turbines.

- For trying to be as close as possible with reality, if time permits, it would be ideal to not simplify the model of Shaf+Disk into one that only simulates the disk, because some mode shapes are slightly different because of this fact. In our case, as time is limited, simulations of the turbine were carried out (mainly in the first part of the project) without taking into account possible influences of vibrations in the shaft for not having long time simulations, as only in the first part of the project, more than 50 simulations with a mesh of high resolution were carried out for example to identify the direction of the crack or to do some mesh analysis.

- Regarding future and complementary work, our recommendation is firstly to identify if the modal analysis could be carried out with the turbine rotating, and still working in air. If so, the solutions should not be quite different from our study, but this step is necessary to move the intention of this project to another level. The next level should be to do exactly the same experiment we have done, using both Ansys and a model of a Kaplan turbine, but this time with the turbine stopped and in water. If there is some influence because of the rotatory movement of the turbine when the measurement was done in air, there should be another additional step, that is to simulate the turbine working in water having the sensors in the own blades of the turbine, like we did. Finally, if the results are good enough, the ideal predictive maintenance procedure should be to have the sensors in the turbine casing to see if without necessity of measure the own turbine, just because of the vibration of all the structure, a new way to identify the appearance and expansions of cracks in turbines could be carried out without necessity to stop the electricity production.

7. Environmental impact

Concerning the environmental impact of the project, we will consider the consumption of energy of different parts of the project as responsible for the emissions of particles of CO_2 to the atmosphere. Moreover, the use of tools in the laboratory has an environmental impact too. These parts are detailed and explained below:

- To do the numerical analysis, 2 software were needed, and this software consumes energy, as the laptop of the department, or the computer of the university was used for doing the simulations. Moreover, the time spent to do the report of the project has been taken into account as well, considering my personal computer. Finally, the computer used in the laboratory for the experimental analysis has been considered too, although the time spent on it was very low with respect to the previous two. The average consumption of a computer working (depending on the model it can vary) is between 200W and 300W [27]. Moreover, an average of six 35W bulbs have been taken into account as electricity consumption of light for doing this project. According to the REE [28] (Spanish company that operates in the international electricity market as the main operator of the electricity network), the emissions of CO_2 per kwh consumed of electricity is 241 gCO_2/KWh in 2021. Once we have all this data, the estimated times of use of computers and total emissions of CO_2 is shown below in Table 28.

Device	Power [W]	Time used [h]	Energy consumed [kwh]	CO_2 Emissions [kg]
Personal computer	200	80	16	3,86
Computer of the laboratory (Labview)	250	15	3,75	0,90
Computer for the simulations (Ansys & SolidWorks)	300	160	48	11,57
Lights	210	600	126	30,37
Total [Kg CO_2]				**46,70**

Table 28: Calculations of Kg of CO_2 emitted in the project

- Moreover, to do the experimental analysis, some accelerometers and special wires were used, and these have a particular waste treatment for the EU rules [29], as once the lifespan of them ends, they must be treated as special waste, specifically, Waste from Electrical and Electronic Equipment (WEEE). Basically, this type of waste contains a complex mixture of materials, some of which are hazardous. These materials can cause major environmental and health problems if the discarded devices are not managed properly. Therefore, it is necessary to separate the hazardous materials. Moreover, modern electronics devices contain rare and expensive resources, which can be recycled and reused if the waste is effectively managed.

- Regarding the waste management of the cracked turbine, there is also legislation in the EU with respect to the treatment of waste of stainless steel[30]. In our case, all the object is made of stainless steel, and it needs to be separated and recycled, as there exists procedures for recycling stainless steel. The cracked turbine will be sent to an external company that will recycle the steel following the rule mentioned.

8. Budget

To analyse the economic impact of the project, we will focus this part of the study to the total cost of it. For doing so, we have to focus our attention on the duration of the project, and the amortization of all the instruments used in the period of study. There are different parts that imply a cost for the project.

- **Labour costs:**
  For the labour cost, we will consider that the total amount of hours dedicated to the project have been around 600 hours, as it is an estimation of working every day of the project an average of 2,5 hours. Considering also that the salary for a technical engineer is 15€ per hour, the total labour cost is therefore 9000€. Moreover, it was necessary to have the support of, at least, one supervisor in the project, which makes the labour cost increase. Considering that the supervision of the project was one tenth of the total time of the project (60 hours), and a salary per hour is 20 €/h, the cost of the supervisor of the project was 1200€.

- **Licenses costs:**
  Regarding the license cost, three non-free software with license have been used in the project. Firstly, SolidWorks, which has a total cost of license of 3.400€ per year. Secondly, Ansys, which has a total cost of license of 4.000$ per year (3.527€ per year). Finally, Labview, which has a total cost of license of 3.111€ per year. The total cost (due to the amortization in this project) will be calculated in a final table in this chapter.

- **Material costs:**
  Regarding the material cost, it is necessary to take into account some parts of the project. First, the most important one, the cost of the simplified turbine and the different cracks provoked in the manufacturing workshop. The cost of the disk and shaft was 1.210€, and the cost of the 4 cracks opened was 145€. Secondly, the cost of the instrumentation sensors, modules and chassis. The cost of the 2 uniaxial sensors was 662€, and the cost of the 2 Triaxial sensors was 1736€. The NI-9231 module has a total cost of 3465€. The hammer had a total cost of 2637€, as it is special and has an integrated sensor as well. The compact chassis cDAQ-9185 has a total cost of 1569€. Finally, I will consider the use of a unique laptop (although I used three), because with only one this project could have been carried out. The total cost of the laptop (the personal one) is 1079€.

- **Energetic costs:**
  Regarding the energetic cost, lights were used during 600 hours of the project, and the power consumed of the laptops is explained in Table 28 above. Therefore, having an average value of 0,29€/kwh and having consumed 193,75 kwh for this project, the total cost is 56,16€ in energy, which is negligible with respect to the other costs as we can see.

- **Other costs:**
  Other costs could be associated with the project as well in terms of additional requirements like transport or office material. For the transport, we will consider a total cost of 160€ (around 80 displacements) counting the trips to the university and to the manufacturing workshop. For the office material, we will consider a total cost of 80€ that includes dossiers, USBs, pens, and other material.

All these costs are the ones that have been involved in the project. Nevertheless, it doesn't mean that, for example, the compact chassis cDAQ-9185 is only going to be used in this project. Hence, it is necessary to calculate the amortization of all the costs mentioned above to the project. We will consider a lifespan of 8 years for all the instrumentation, and taking into account that the project takes 8 months, the results of the total cost associated with the project can be seen below in Table 29:

Type of cost	Item	Total cost [€]	Contribution to the Project [€]
Labour Costs	Technical engineer	9000€	9000€
	Supervisor	1200€	1200€
License Costs	Ansys	3527€	2531,33€
	SolidWorks	3400€	2266,66€
	Labview	3111€	2074€
Material Costs	Turbine	1210€	1210€
	Manufacturing processes	145€	145€
	4 Accelerometers	4796€	399,66€
	Hammer	2637€	219,75€
	NI-9231 module	3645€	303,75€
	cDAQ-9185 chassis	1569€	130,75€
	Laptop	1079€	89,92€
Energetic Costs	Electricity	56,16€	56,16€
Other Costs	Transport	160€	160€
	Office material	80€	80€
Total cost without fees			**19.866,98€**
VAT (21%)			4.172,06€
Total Cost			**24.039,05€**

Table 29: Total cost associated to the project

9. Project Plan

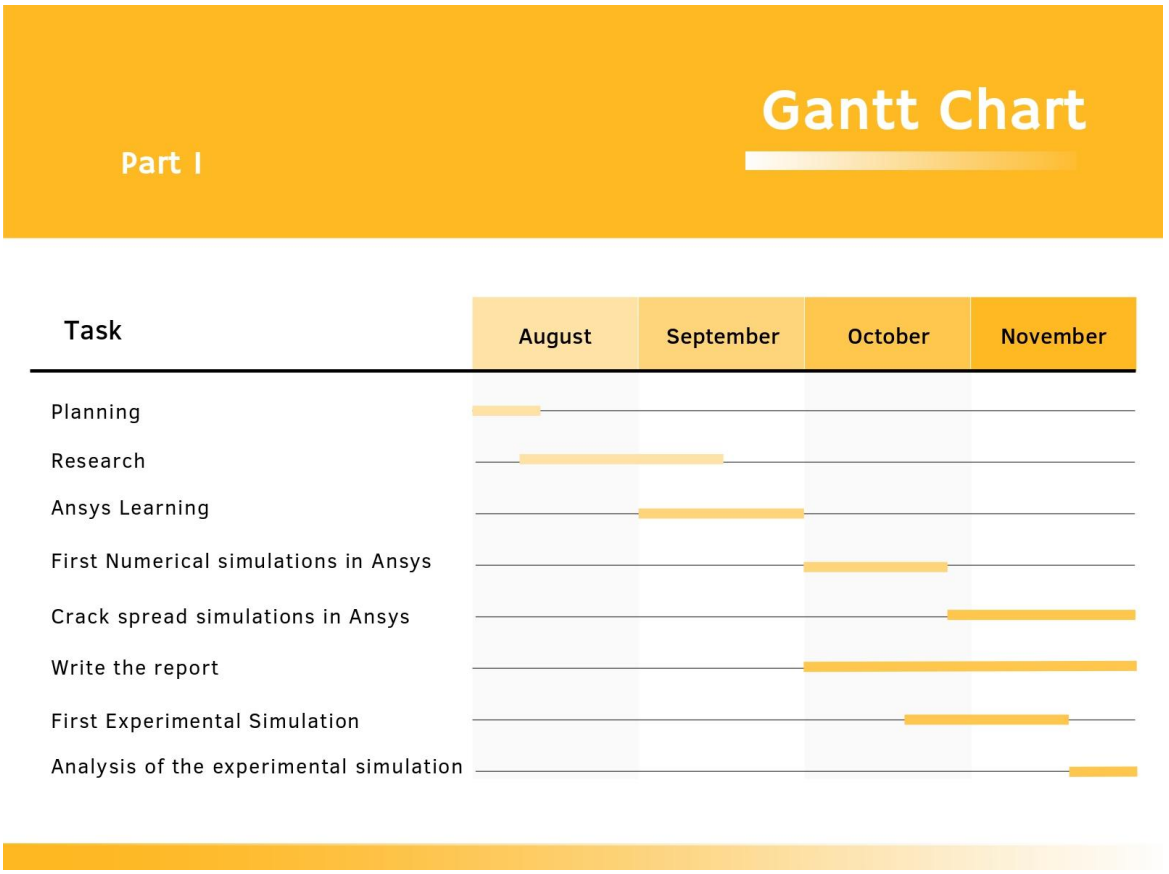

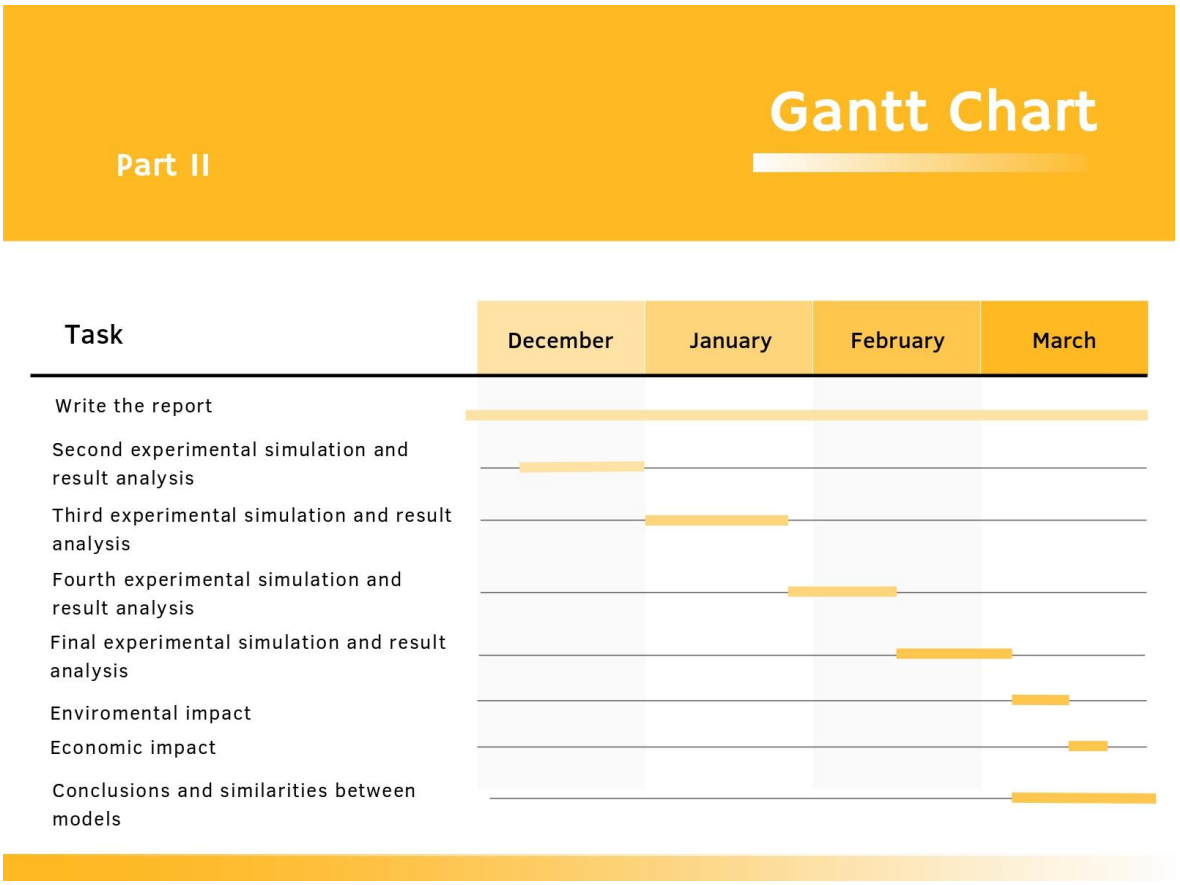

ETSEIB

Acknowledgment

I would like to start this chapter by thanking my family for its support during all these years in the UPC. They have always helped me when I needed it and they have always been by my side even in the most difficult moments. I will always be grateful to them due to this magnificent chance they gave me. Thanks also to my girlfriend, who has been living with me these years and has helped me a lot in all aspects of my life, personally and professionally.

Special thanks also to the manager of this project, Xavier Escaler, who has always been there once things were not as good as expected, and has always followed up my work week after week. Of course, many thanks to the teammates of the department of fluid mechanics, Rafel Roig and Xavier Sanchez. Without them this project would have been much more difficult, and I would have had many difficulties using all the tools of both the laboratory and the informatic software. I really appreciate how kind they were with me and how implicated they were with my project.

I would like to mention as well the contribution of Xavier Ayneto, who has supported this project with information about fatigue and other tools and knowledge, guiding us in different steps of the project.

Finally, I would like to deeply thank every single person in the ETSEIB I have found during these 8 years of education. Friends, teachers, other personal… etc. I have lived and learned many things that I am sure I would not have learned in other places. Thanks to all of them, because from them all I have learned, at least, one thing that I think will make me a better person.

Annex 1: Drawing of the turbine to study

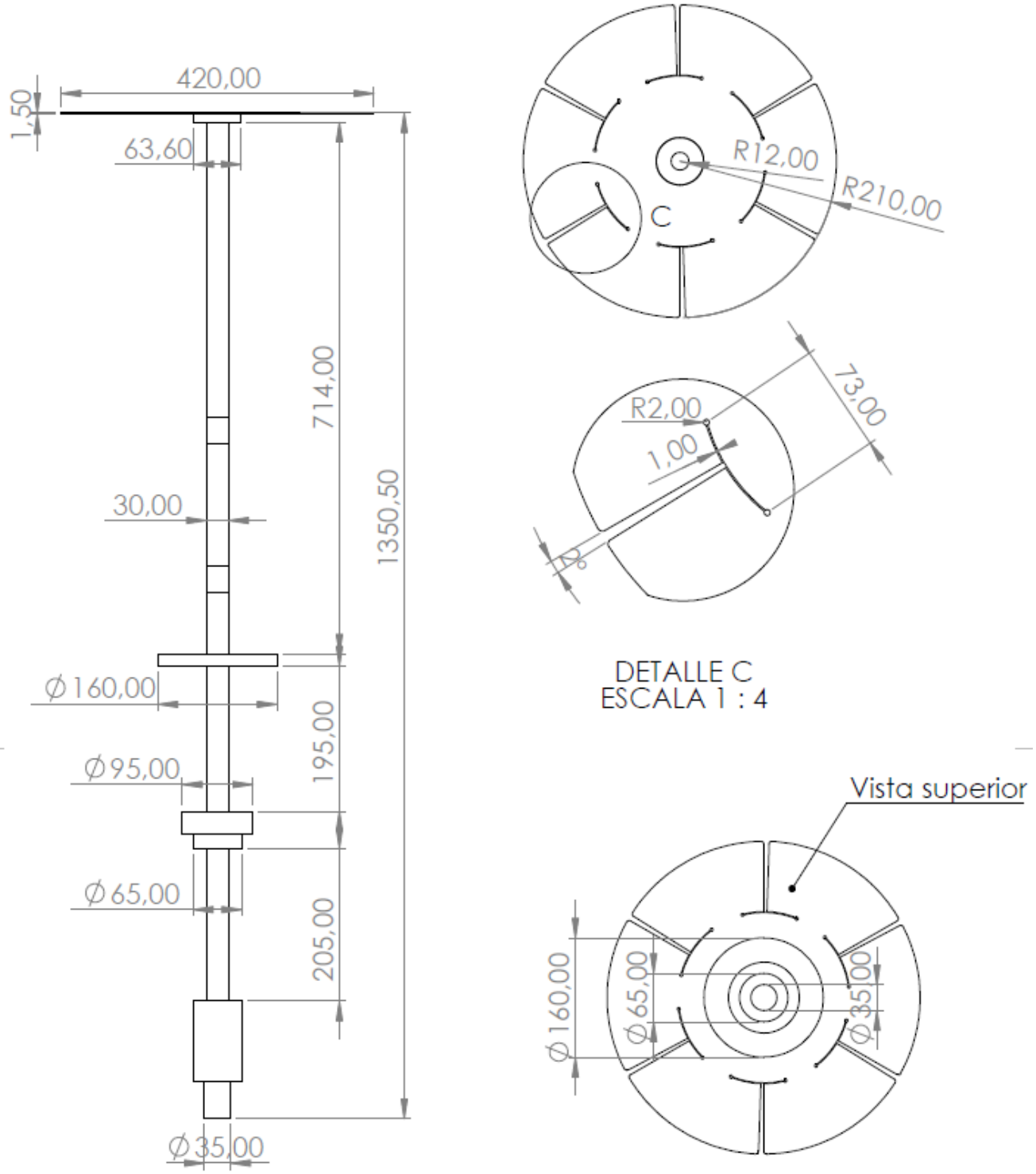

Annex 2: Drawing of the disk after the failure due to fatigue

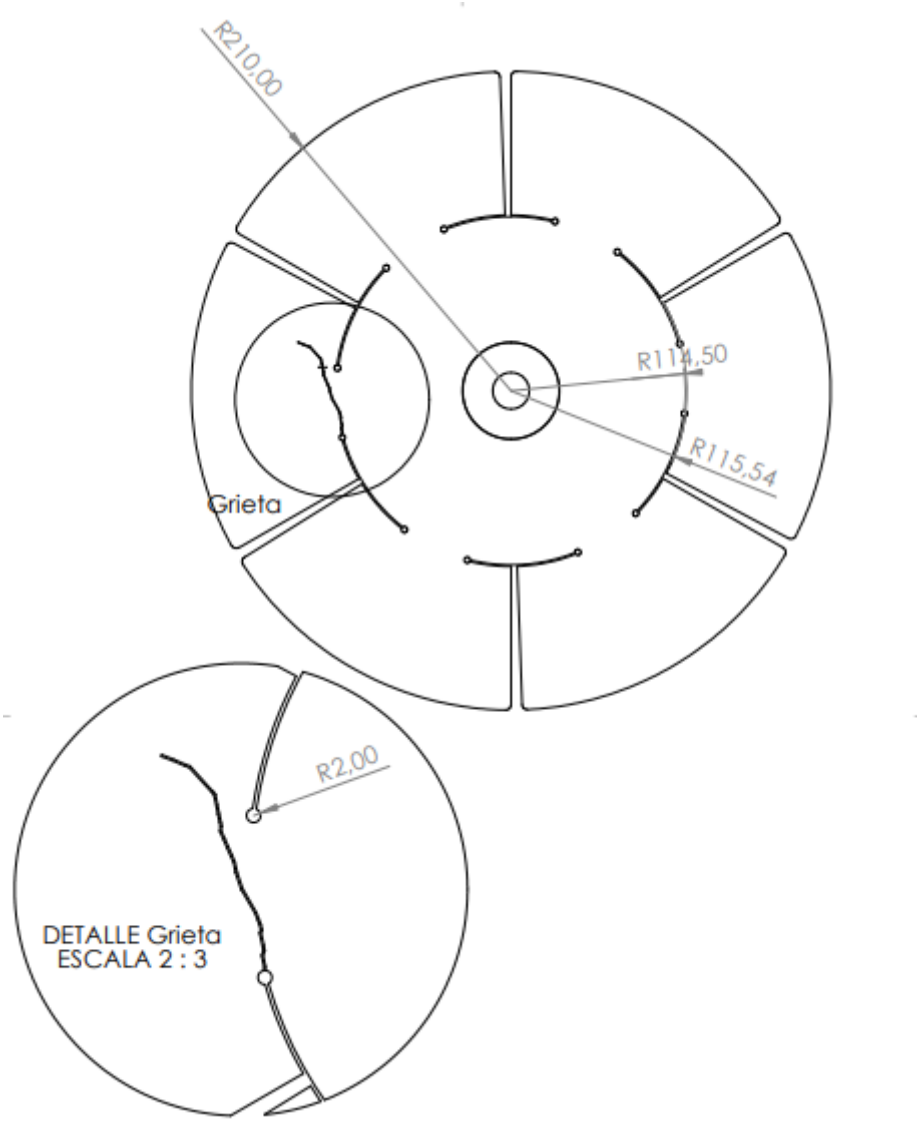

Bibliography

[1] https://www.nationalgeographic.org/encyclopedia/hydroelectric-energy/

[2] https://www.nationalgeographic.org/photo/800px-water-cycle/

[3] https://www.iea.org/

[4] https://ourworldindata.org/

[5] https://ruahaenergy.com/hydro/hydro-overview/

[6] https://www.researchgate.net/figure/Schematic-of-pumped-storage-hydropower-system_fig4_318469208

[7] https://simple.wikipedia.org/wiki/Base_load_power_plant

[8] https://www.rikuden.co.jp/sp/eng_shika/need.html

[9] Blas Zamora y Antonio Viedma. Máquinas Hidráulicas, teoría y problemas. Universidad Politécnica de Cartagena.Rai ediciones. Consulted on 05/10/2021

[10] (PDF) Turbinas-hidraulicas | Yerko Garcia Vargas - Academia.edu. Consulted on 06/10/2021

[11]https://en.wikipedia.org/wiki/Water_turbine

[12]https://gunt.de/index.php?option=com_gunt&task=gunt.list.category&category_id=756&product_id=846&lang=en

[13]https://www.areatecnologia.com/mecanismos/turbinas-hidraulicas.html

[14]https://www.mechanicalbooster.com/2016/10/pelton-turbine-working-main-parts-application-with-diagram.html

[15]https://www.ltu.se/cms_fs/1.4069!/turbineselection.pdf. Consulted on 13/10/2021

[16]Pedro Fernández Díez. Turbinas hidráulicas. Departamento de ingeniería eléctrica y energética. Universidad de Cantabria. Consulted on 15/10/2021

[17] Notes of Hydraulic Machines subject. Consulted on 17/10/2021

[18]Pedro Fernández Díez. Turbinas hidráulicas. Departamento de ingeniería eléctrica y energética. Universidad de Cantabria. Consulted on 21/10/2021

[19] Hydro turbine failure mechanisms: An overview. Ugyen Dorji and Reza Ghomashchi. School of Mechanical Engineering, The University of Adelaide, Australia Consulted on 25/10/2021

[20] Glen White.Introducción al análisis de vibraciones.Azima Dli,Boston. Consulted on 18/09/2021

[21]https://www.spaceagecontrol.com/calcsinm.htm

[22] http://ocw.upm.es/pluginfile.php/1321/mod_label/intro/VIBRACIONESMECANICAS%281%29.pdf

[23] Notes of Machines Technology subject. Consulted on 06/11/2021

[24] Failure investigation of a Kaplan turbine blade. Center for Industrial Diagnostics and Fluid Dynamics (CDIF), Polytechnic University of Catalonia (UPC), Av. Diagonal, 647, ETSEIB, 08028. Barcelona, Spain.Consulted on 08/11/2021

[25] http://vlabs.iitkgp.ernet.in/vlabs/vlab17/web/note3.html

[26]Experimental and numerical investigation on the influence of a large crack on the modal behaviour of a Kaplan turbine blade. Ming Zhang, David Valentina,∗, Carme Valero, Alexandre Presas,Mònica Egusquiza, Eduard Egusquiza. UPC.

[27]https://chcenergia.es/blog/cuanto-consume-un-ordenador-o-pc/#:~:text=Cuanta%20electricidad%20consume%20un%20ordenador&text=Y%20es%20que%20al%20igual,en%208%20horas%20de%20trabajo.

[28]https://canviclimatic.gencat.cat/es/actua/factors_demissio_associats_a_lenergia/#:~:text=El%20mix%20de%20la%20red%20el%C3%A9ctrica%20espa%C3%B1ola%20publicado%20por%20la,25%20kg%20CO2%2FkWh.

[29]https://ec.europa.eu/environment/topics/waste-and-recycling/waste-electrical-and-electronic-equipment-weee_es

[30] https://ec.europa.eu/trade/import-and-export-rules/export-from-eu/waste-shipment/